UCL SCHOOL OF PHARMACY
BRUNSWICK SQUARE

Engineering Nanoparticle Agglomerates as Dry Powders for Pulmonary Drug Delivery

Maria S. Malamatari

Thesis submitted in accordance with the requirements of UCL for the degree of Doctor of Philosophy

July 2016

UCL SCHOOL OF PHARMACY
29-39 Brunswick Square
London WC1N 1AX

DECLARATION

This thesis describes research conducted in the UCL School of Pharmacy from May 2013 to July 2016, under the supervision of Prof. Kevin M.G. Taylor, Emer. Prof. Graham Buckton and Dr Satyanarayna Somavarapu.

I, Maria Malamatari confirm that the research described in this thesis is original and that any parts of the work that have been conducted by collaboration are clearly indicated. I also certify that I have written all the text herein. Where information has been derived from other sources, I confirm that this has been indicated in this thesis.

Signature: ---------- **Date:** ----------

To Dad
for being
"the breath of life"

ABSTRACT

Background: Controlled agglomeration of nanoparticles to micrometer-sized composites (i.e. nanoparticle agglomerates) has been suggested as a particle-engineering approach to combine the advantages of nanoparticles with the aerodynamics of microparticles for pulmonary drug delivery. The aim of this thesis was to engineer nanoparticle agglomerates with properties suitable for inhaler formulation, for drugs with different physicochemical properties.

Methods: Nanoparticle agglomerates of three model drugs, namely indometacin, ibuprofen and theophylline, were prepared by coupling wet milling and spray drying. In the case of indometacin and ibuprofen, matrix formers (i.e. mannitol and L-leucine) were added to the aqueous nanosuspensions of the drugs prior to spray drying while for theophylline wet milling was carried out in isopropanol in the presence of mannitol. Nanoparticle agglomerates were characterised with respect to their particle size, morphology, solid state, redispersibility and dissolution, while their in-vitro aerosolisation performance was determined using the next generation impactor. A full factorial design and the fast screening impactor were employed in the case of ibuprofen nanoparticle agglomerates while computational modelling was used to investigate interactions between the crystals of theophylline and mannitol.

Results: Nanosupensions of indometacin and ibuprofen stabilised with various polymers/surfactants were successfully prepared by wet milling and were further spray dried. Incorporation of matrix formers before spray drying resulted in nanoparticle agglomerates with improved redispersibility (ability to reform nanoparticles upon hydration), dissolution and higher fine particle fractions compared to those without matrix formers. In the case of theophylline, mannitol acted as a co-milling agent facilitating the size reduction of the drug's needle-like crystals. Increasing the amount of mannitol led to the formation of smaller, more spherical and porous particles with enhanced aerosolisation performance. For each drug, the nanoparticle agglomerates produced retained the crystallinity of the starting materials ensuring the long-term physical stability of the formulations upon storage.

Conclusions: Combining wet milling and spray drying can be used as an industrially feasible particle-engineering platform for dry powders for

inhalation. By careful selection of formulation and process parameters, this platform can be applied to a range of drugs with different physicochemical properties.

ACKNOWLEDGEMENTS

First of all, I would like to express my gratitude to my supervisors Emer. Prof. Graham Buckton, Prof. Kevin M.G. Taylor and Dr Satyanarayana Somavarapu for their scientific guidance and constant encouragement throughout this PhD. I am especially grateful to Prof. Kevin M.G. Taylor for for his research vision and also for his valuable suggestions and corrections which improved the present thesis.

EPSRC Centre of Doctoral Training (CDT) in Targeted Therapeutics and Formulation Sciences is acknowledged for the financial funding of my research (EP/I01375X/1). Through the CDT programme, I had the opportunity to meet many people from both academia and industry and receive training on developing both my research and interpersonal skills.

I wish to express my warm thanks to Prof. Steve Brocchini and Prof. Simon Gaisford for their constant support and our excellent collaboration in the context of the CDT. Special thanks also to Prof. Abdul Basit for welcoming me in the School and kindly hosting me in his lab when I firstly arrived for my Erasmus placement in 2012. The support and help from him and his amazing group was continuous throughout my PhD.

Thank you to Mr Mark Bloxham who kindly hosted me during my industrial placement in GlaxoSmithKline giving me access to the cutting-edge laboratory facilities of the GSK Medicines Research Centre in Stevenage and Ware. I have also the pleasure to acknowledge other scientists from GSK: Ms Wendy Knight, Dr Toma Chitu, Dr Peter Hamilton, Mr Ian Kemp and Mr Eugene Meenan. Without their help with many techniques and our discussions, the learning curve would have been very much steeper.

Back to Greece: Thanks to Assoc. Prof. Kyriakos Kachrimanis of Aristotle University of Thessaloniki for carrying out the computational modelling and for his advice on design of experiments; and to Assoc. Prof. Dimitrios Fatouros and Mr Georgios Eleftheriadis at the same University for the determination of surface area and pore volume of the engineered particles of theophylline.

I would also like to express my appreciation to all the staff at the UCL School of Pharmacy. Especially to Mr David McCarthy for his help with electron

microscopy, Ms Isabel Gonçalves and Mr John Frost for their technical assistance, Ms Catherine Baumber and Mr Victor Diran for their administrative assistance.

I am extremely grateful to all my colleagues at the Department of Pharmaceutics for providing an excellent environment of collaboration and for their friendship. I also wish to extend my sincere thanks to my friends from Goodenough College for all the experiences and the laughs we had together.

Last but definitely not least, I am truly indebted to my parents, Zetta and Stavros, and my brother Christos for their generous love, caring nature, encourangement and inspiration throughout my life. Without their support and faith in me, I couldn't have made it!

TABLE OF CONTENTS

LIST OF TABLES

LIST OF FIGURES

LIST OF ABBREVIATIONS

AIM: Abbreviated impactor concept

API: Active pharmaceutical ingredient

BCS: Biopharmaceutics classification system

BET: Brunauer-Emmett-Teller

COPD: Chronic obstructive pulmonary disease

DE: Dissolution efficiency

DLS: Dynamic light scattering

DLVO theory: Derjaguin- Landau- Verwey- Overbeek theory

DoE: Design of experiments

DSC: Differential scanning calorimetry

DPI: Dry powder inhaler

F127: Poloxamer 407 (Pluronic F127)

F68: Poloxamer188 (Pluronic F68)

FPD: Fine particle dose

FPF: Fine particle fraction

FSI: Fast screening impactor

FT-IR: Fourier transform infrared spectroscopy

GSD: Geometric standard deviation

HPC: Hydroxypropylcellulose

HPLC: High pressure liquid chromatography

HPMC: Hydroxypropylmethylcellulose (Hypromellose)

IBU: Ibuprofen

IND: Indometacin

L64: Poloxamer 184 (Pluronic L64)

MAN: Mannitol

MDT: Mean dissolution time

MF: Matrix former

MMAD: Mass median aerodynamic diameter

MOC: Micro-orifice collector

NCE: New chemical entity

NGI: Next generation impactor

PI: Polydispersity index

pMDI: pressurised metered-dose inhaler

PSD: Particle size distribution

PVP: Polyvinylpyrrolidone (Povidone)

QbD: Quality by design

RDI: Redispersibility index

RT: Room temperature

SEM: Scanning electron microscopy

SLS: Sodium lauryl sulfate

TEM: Transmission electron microscopy

THEO: Theophylline

TPGS: D-α-tocopherol polyethylene glycol succinate 1000

UV: Ultraviolet

XRPD: X-ray powder diffraction

CHAPTER 1

GENERAL INTRODUCTION

1. GENERAL INTRODUCTION

Drug delivery to the lungs is an effective way of targeting inhaled therapeutic aerosols for the treatment of respiratory diseases such as asthma, chronic obstructive pulmonary disease (COPD) and cystic fibrosis. In comparison with oral or parenteral administration, pulmonary drug delivery results in a rapid onset of action as the drug is delivered to its site of action. For example, inhalation is the preferred route of administration of salbutamol which is a short-acting β-agonist used in the treatment of asthma and COPD. According to Du et al. (2002), peak plasma levels were found to be achieved considerably earlier for inhaled salbutamol (Ventolin® Inhaler, single dose: 12 × 100 μg, t_{max}: 0.22 h) compared to oral administration (oral aqueous solution 1.2 mg/100 mL, t_{max}: 1.8 h). The rapid onset of action of inhaled salbutamol can be attributed to its absorption via numerous lung blood vessels, while when the drug was orally administered it had to pass through more biological barriers before entering the systemic circulation. Additionally, pulmonary drug delivery enables local delivery of higher drug concentration at the lung tissue while concentrations elsewhere are kept at a minimum. In this way, a maximum therapeutic effect can be achieved by administering lower inhaled doses compared to those required for systemic administration and as a result side effects can be minimised. Moreover, the lungs possess a relatively large surface area for drug absorption, lower metabolic activity compared to the liver and the gastrointestinal tract, abundance of capillaries and thin air-blood barrier. Therefore, the lungs are considered an ideal portal of entry for the systemic drug delivery of small molecules but also therapeutic biopharmaceuticals as peptides (e.g. insulin), proteins and vaccines (Zeng et al., 2001; Patton et al., 2004; Taylor, 2013).

1.1. The human respiratory tract

The respiratory tract is the anatomic part of the human body that is mainly involved in the oxygenation of the blood and the removal of carbon dioxide from the body. Apart from the gaseous exchange between the inhaled air, the blood and the cells, it is responsible for the homeostatic maintenance of the blood pH by adjusting the rate of removal of the acid-forming carbon dioxide but also for the provision of vocal expression.

The respiratory tract starts at the nose and terminates deep in the lungs at an alveolar sac. There are several ways for the classification of the different

regions of the respiratory tract. Commonly, it is divided into the upper and lower respiratory tract. The upper respiratory tract comprises the nose, nasal cavity, throat, pharynx and larynx while the lower respiratory tract consists of the trachea, bronchi, bronchioles and the alveoli. Another classification is to divide the respiratory tract into the following three regions: nasopharyngeal, tracheobronchial and alveolar. More specifically, the nasopharyngeal region comprises the airways of the head from the nose to the larynx and is often referred to as the extrathoracic airways. The tracheobronchial region starts at the larynx and extends via the trachea, bronchi, bronchioles and ends at the terminal bronchioles and its main function is air-conduction. The alveolar region is the gas-exchange compartment comprising the respiratory bronchioles, alveolar ducts and alveoli (Taylor and Kellaway, 2001).

In 1963, Edward Weibel proposed a morphometric model of the human lung with the main aim to develop a quantitative description of the pulmonary anatomy and the correlation of anatomy with physiology (Weibel, 1963). The Weibel-A model divides the lungs into 24 compartments, each compartment corresponding to a generation of the model. It assumes that each generation of the airways branches symmetrically into two equivalent generations and it is the most widely used model for the investigation of particle deposition in the human lung. According to this model, the tracheobronchial region comprises generation 0 (trachea) to 16 (terminal bronchioles) while the alveolar region includes generations 17 to 23 (Fig. 1.1).

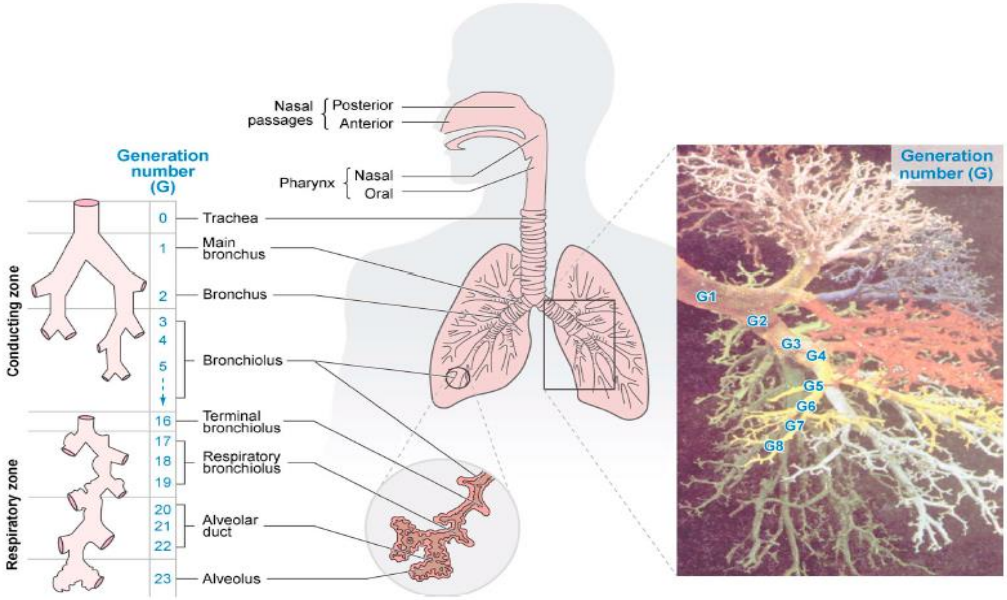

Figure 1.1 Schematic of the human respiratory tract and morphometric model of the conducting and respiratory zone according to the Weibel-A model (Kleinstreuer and Zhang, 2010)

1.2. Inhalation aerosols and particle aerodynamic diameter

With the exceptions of medical gases and administration by pulmonary instillation, a drug must be presented as an aerosol in order to be delivered to the lungs. In physical pharmacy, an aerosol is defined as a colloidal dirspersion of liquids or solids in gases, having sufficiently small size to exhibit considerable stability as a suspension (Taylor, 2013). Typically, aerosol particles range in diameter from about 10^{-9} to 10^{-4} m and the unit of micrometre (1 μm = 10^{-6} m) is used to describe their particle size (Zeng et al., 2001).

The most important physical property of an aerosol for inhalation is its particle size. This property is the main parameter, which defines the site of deposition of aerosol drugs within the respiratory tract and it is usually described by the aerodynamic diameter of the particles. The aerodynamic diameter is defined as the diameter of a sphere of unit density that has the same terminal settling velocity as the particle under consideration. It depends on the airflow (particle Reynolds number, *Re*) and the particulate properties including the geometric size, shape and density of the particle. At Stokes flow regime of $Re < 0.1$, the aerodynamic diameter of a particle (d_a) can be calculated using Eq. 1.1:

$$d_\alpha = d_v * \sqrt{\frac{\rho}{\chi \rho_0}} \quad . \quad . \quad . \quad \text{Equation 1.1}$$

where d_v is the volume-equivalent diameter, ρ is the particle density, ρ_0 is the unit density (i.e. 1 g cm^{-3}) and χ is the dynamic shape factor. The dynamic shape factor is defined as the ratio of the drag force on a particle to the drag force on the particle volume-equivalent sphere at the same velocity. For a spherical particle, the dynamic shape is defined as 1 (Chow et al., 2007).

Most therapeutic aerosols are polydisperse consisting of a wide range of particle sizes. The particle size distribution is described by the geometric standard deviation (GSD), when size is log-normally distributed. A GSD of 1 indicates a monodisperse aerosol while a GSD > 1.2 indicates a polydispersed aerosol (Traini, 2013).

1.3. Particle deposition in the respiratory tract

Deposition occurs when an inhaled particle does not follow airflow streamlines and it comes into contact with a respiratory surface from which it does not rebound or resuspend. Particles that remain airborne and do not deposit throughout the respiratory cycle are exhaled. The main mechanisms responsible for particle deposition in the respiratory tract include inertial impaction, gravitational sedimentation, Brownian diffusion and to a lesser extent interception, and electrostatic precipitation (Fig. 1.2).

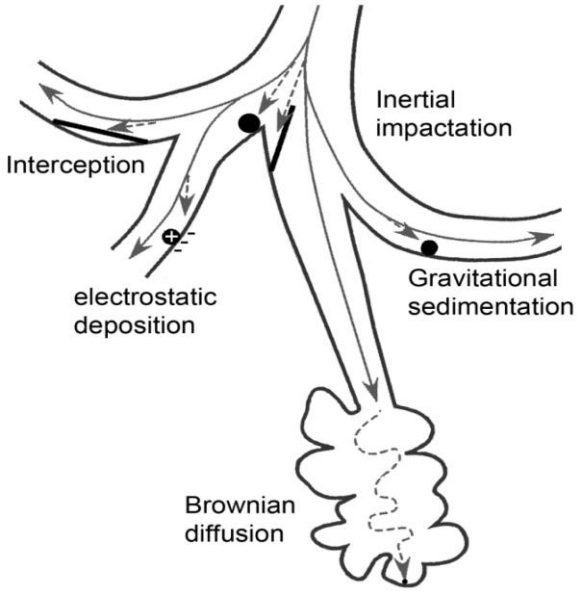

Figure 1.2 Particle deposition in the airways (Fröhlich and Salar-Behzadi, 2014).

1.3.1. Inertial impaction

Inertial impaction is the predominant mechanism of particle deposition in the respiratory tract. Inertia is the tendency of a moving particle to resist acceleration. Inertial impaction occurs at the bifurcations of the respiratory tract when the airflow changes direction and the particles within the airstream follow their original trajectory instead of adjusting to the airflow.

For a particle travelling in an airway, Stokes' number (*Stk*) is a dimensionless number used to predict impaction driven deposition (Eq. 1.2).

$$Stk = \frac{\rho_p * d^2 * V}{18\eta * R} \quad . \quad . \quad . \quad \text{Equation 1.2}$$

where ρ_p is the particle density, d is the particle diameter, V is the air velocity, η is the air viscosity and R is the airway radius. The Stokes' number shows that the probability of a particle to deposit due to inertial impaction is directly proportional to the particle density, the square of particle diameter and the air velocity whereas it is inversely proportional to the airway radius. Inertial impaction is a velocity-dependent mechanism and causes most of the particles larger than 5 μm and particularly greater than 10 μm to deposit in the upper respiratory tract and the large conducting airways (Asgharian and Anjilvel, 1994).

1.3.2. Gravitational sedimentation

Gravitational sedimentation refers to the settling of the particles under the action of the gravity. The terminal settling velocity (V_t) of particles settling under gravity is given by Stokes' law (Eq. 1.3).

$$V_t = \frac{(\rho_p - \rho_a) * d^2 * g}{18\eta * R} \quad . \quad . \quad . \quad \text{Equation 1.3}$$

where ρ_a is the density of the air and g is the gravitational constant. Stoke's law is valid for unit density particles with diameter between 1 to 40 μm and if laminar flow within the airways is assumed. According to Eq. 1.3, the gravitational sedimentation of a respirable particle is dependent on its size and density. Gravitational sedimentation is a time-dependent process and deposition by this mechanism increases with increasing residence time of a particle in the airways and alveoli (e.g. during slow, steady breathing or breath-holding). It is an important deposition mechanism for particles in the size range 0.5-3 μm, in the small airways and alveoli (Taylor, 2013).

1.3.3. Brownian diffusion

Deposition by Brownian diffusion results from the random motions of the particles caused by their collisions with gas molecules. This motion transports particles from high to low concentrations causing the movement of particles from the aerosol cloud to the airways' walls. The rate of Brownian diffusion (D) is given by Stokes-Einstein equation (Eq. 1.4).

$$D = \frac{K_B * T}{3\pi * \eta * d} \quad . \quad . \quad . \quad \text{Equation 1.4}$$

where K_B is the Boltzmann constant and T is the absolute temperature. Unlike deposition by inertial impaction and gravitational sedimentation, which increase with increasing particle size (Eq. 1.2 and 1.3), deposition by Brownian diffusion is inversely proportional to the particle diameter. This means that deposition by Brownian diffusion increases with decreasing particle size and becomes the predominant mechanism for particles smaller than 0.5 μm in the deep lungs (Fig.1.3, Zeng et al.,2001; Taylor, 2013).

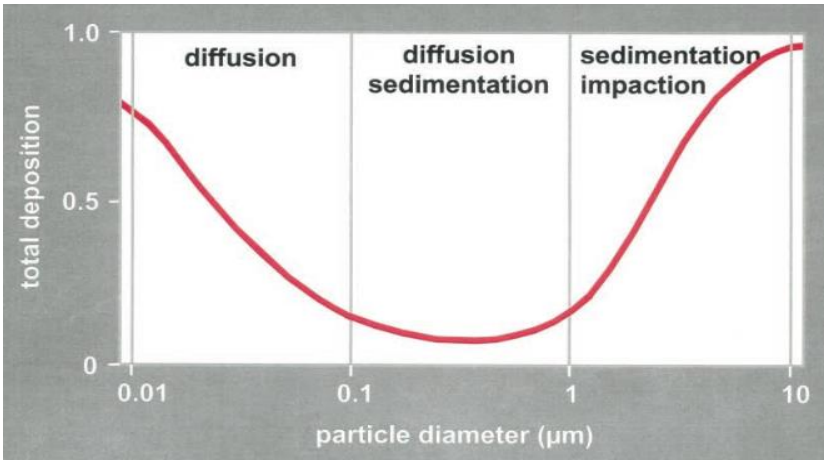

Figure 1.3 Total deposition of unit-density spheres in the human respiratory tract inhaled orally at rest (Heyder, 2004).

1.3.4. Interception

Interception occurs when a distal end of a particle comes into contact with the airway wall despite the fact that its centre of mass remains within the streamlines of the gas phase. Although negligible for spherical particles, interception can play an important role regarding the deposition of elongated particles with small aerodynamic diameter (Johnson and Martonen, 1994).

1.3.5. Electrostatic precipitation

During aerosolisation, particles may become electrostatically charged. Deposition of charged particles by electrostatic precipitation can occur either through the induction of an opposing charge on the airways' surface and subsequent electrostatic attraction of via the repulsion between particles of the same charge directing them towards the airway walls (Melandri et al., 1983).

1.4. Delivery devices

There are currently three main types of aerosol delivery systems commercially available: nebulisers, pressurized metered-dose inhalers (pMDIs) and dry powder inhalers (DPIs). The characteristics of these three types of devices will be described below. Particular emphasis will be placed on DPIs as the formulations prepared in this thesis have been developed for this type of device. At this point, it should be highlighted that in recent years, the technological innovations in device engineering and formulation science have significantly improved the performance of all types of inhalers. Factors such as the drug and formulation properties, the device and the patient are all of paramount importance and should be addressed in order to achieve optimum delivery to the lungs (Fig.1.4).

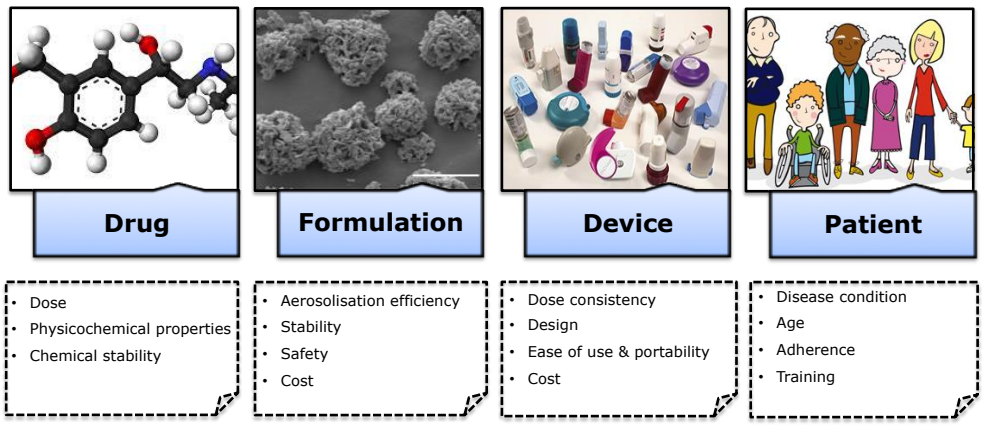

Figure 1.4 Factors that can influence optimal aerosol drug delivery from inhaler devices.

1.4.1. Nebulisers

A nebuliser is a device for converting an aqueous solution or suspension into an aerosol for inhalation. The aqueous solution or suspension is contained inside nebules. The nebule content is dispensed into the reservoir chamber via a jet, ultrasonic or vibrating-mesh nebuliser device. Jet nebulisers operate under the Bernouilli's principle using compressed gas (air or oxygen) passing through a Venturi nozzle. The smaller respirable droplets generated during the atomisation are carried on the airstream out of the nebuliser and via either a mouthpiece or face mask into the airways of the patient, while the larger non-respirable droplets impact on built-in baffles returning to the reservoir for renebulisation. In ultrasonic nebulisers the energy of

atomisation comes from a piezoelectric crystal, which vibrates at a high frequency (1-3 MHz). Modification to ultrasonic nebulisers resulted in the development of the recently introduced vibrating-mesh nebulisers, which employ plates with multiple apertures through which liquids are extruded to generate aerosols (Taylor, 2013).

Nebulisers have sometimes been used for the delivery of drugs that cannot be formulated into pMDIs or DPIs. They are able to deliver high drug doses to the lungs, which is especially useful for the pulmonary administration of antibiotics (e.g. tobramycin) to patients with cystic fibrosis. Nebulisers can be used at any age and for any disease severity as they are simple and intuitive devices and the drug can be inhaled during tidal breathing through a mouthpiece or facemask. Moreover, as long as there are no physicochemical compatibility issues, it is possible to mix more than one medications in the nebulisers and thus co-administer them simultaneously (Kamin et al., 2006).

Regarding the disadvantages of nebulisers, prolonged treatment time is required to deliver an adequate dose. Jet nebulisers also require a source of compressed air, which together with the need for equipment maintenance and cleaning for infection control increase the running cost and have limited their use to the treatment of hospitalised or non-ambulatory patients. Despite the fact that ultrasonic nebulisers are compact and portable, the rise in temperature during their operation may cause degradation of thermolabile drugs. The droplets produced by ultrasonic nebulisers have often a higher aerodynamic diameter compared to jet nebulisers explaining why they tend to be less widely used. The recently introduced vibrating-mesh nebulisers manage to overcome many of the aforementioned limitations as they generate aerosols with high fine particle fractions (FPF), have very small residual volumes (i.e. the volume of solution left in a nebuliser chamber once nebulisation has ceased) and treatment times compared to jet and ultrasonic nebulisers (Geller, 2005; Alhaddad et al., 2015).

1.4.2. Pressurised metered-dose inhalers (pMDIs)

Pressurised metered-dose inhalers (pMDIs) were introduced by Riker Laboratories (now 3M Health Care), which in the mid-1950s set out to develop formulations of bronchodilators in pressurised containers with multi-dose capability and reproducible dosing characteristics. In pMDIs, drug is either dissolved or dispersed in a liquid propellant or a mixture of propellants

together with other excipients including co-solvents, solubilising and lubricating agents, which are contained in a pressurised canister with a metering valve. Upon actuation of the metering valve, a predetermined dose is released as a spray. Upon exiting the canister, the formulation expands which is followed by rapid evaporation of the volatile propellant. It is the latent heat of evaporation of the volatile propellant that provides the energy of atomisation resulting in the breaking-up of the liquid into a fine spray of droplets (Newman, 2005; Taylor, 2013).

The main advantages of pMDIs are their small size, portability, disposability and relatively low cost. Many doses (up to 200) are available in the canister and dose delivery is reproducible. Moreover, they are quick to use as a dose can be delivered in a few seconds, unlike nebulisers, which typically take a few minutes. The propellant liquid offers inert conditions and the content of the canister are protected from moisture, oxidative and microbiological contamination. The aforementioned advantages explain why the pMDIs have been the device of choice for the outpatient treatment of asthma and COPD (Newman, 2005; Geller, 2005).

Over the years, a number of drawbacks related to the use of pMDIs have been identified (Newman, 2005; Geller, 2005). Most pMDIs only deliver 10-20% of the stated emitted dose to the lungs, even with a good inhaler technique. The main reason for that is the high droplet exit velocity, which leads to extensive impaction in the oropharyngeal region. Moreover, as drug delivery from pMDIs is highly dependent on patient's inhaler technique, misuse of pMDIs and especially the difficulty of many patients to coordinate actuation with inhalation further reduces the amount of the drug that reaches the site of action (Fink and Rubin, 2005). Also, some patients suffer from the so-called "cold-freon" effect in which the arrival of cold propellant spray on the back of the throat causes patients to stop inhaling or to inhale by the nose. The use of a spacer between the pMDI and the patient can reduce the problem of oropharyngeal deposition and the importance of actuation/inhalation coordination. Spacer devices fitted with a facemask have been usually employed with a pMDI for administering aerosol inhalation to young children. An alternative approach is the use of breath-actuated pMDIs which do not release drug until inspiration occurs, and in this way they can overcome the coordination problem of conventional pMDIs.

Another drawback is associated with the propellants used in pMDIs. The traditionally used chlorofluorocarbons (CFCs) are considered environmentally harmful as they have been linked with the depletion of the stratospheric ozone layer and they contribute to global warming. In accordance with the Montreal Protocol of 1987, CFCs have been replaced by the non-ozone depleting, non-flammable hydrofluoroalkenes (HFA-134a, HFA-227). However, the replacement of CFCs with HFAs presented major formulation problems as the two types of propellants exhibit different physicochemical properties (e.g. polarity, vapour pressure, density etc.). Further replacement of HFAs may be required in the future, as these gases have been found to contribute to global warming (Leach, 2005).

1.4.3. Dry powder inhalers (DPIs)

Dry powder inhalers (DPIs) are devices by which a dry powder formulation of a drug is delivered for local or systemic effect via the lungs. Their market is estimated to reach over USD 31.5 billion in 2018, while they have been identified as the most lucrative market segment of the asthma and COPD devices market by 2020 (Dhabale, 2014). The main advantages and disadvantages of DPIs are presented in Table 1.1. Based on their design, DPI devices can be classified into three categories (Fig.1.5).

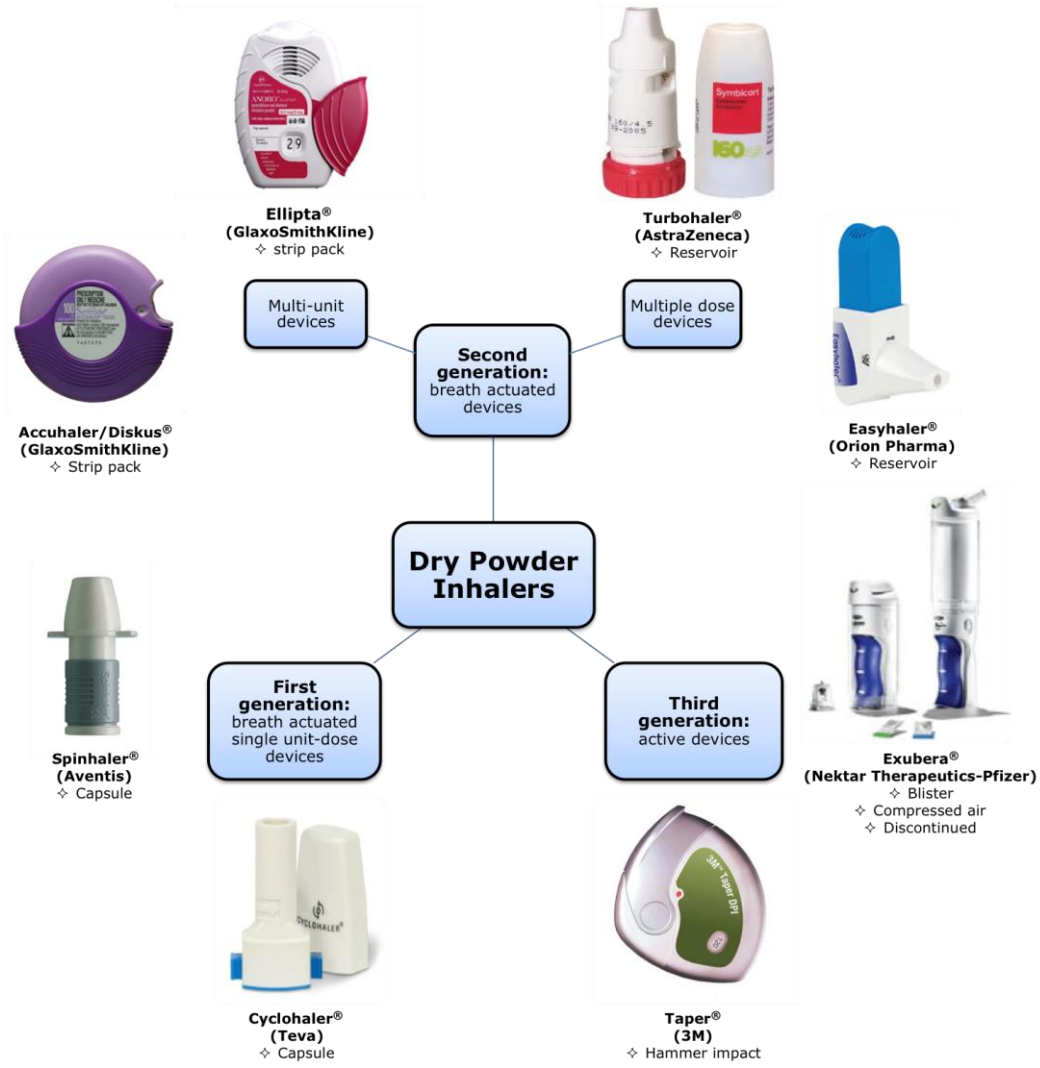

Figure 1.5 Different types of dry powder inhalers.

Table 1.1. Advantages and disadvantages of dry powder inhalers (Chrystyn and Price, 2009; Taylor, 2013).

Advantages of DPIs	Disadvantages of DPIs
• Breath-actuated and so no need for patient coordination required	• Some need to be shaken prior to use
• Enhanced physicochemical stability as the formulation is in the solid state	• Dose preparation errors can be critical mistakes
• Ability to deliver high drug payloads to the lungs	• Attention required to orientation of the inhaler during dose preparation and before inhalation
• No propellant	• Flow-dependent dose emission
• Most have dose counters	• Need for a fast acceleration rate at the start of the inhalation
• Short treatment time	• Poor quality or no dose emitted if inhalation is too slow
• Small and portable	• Uncertainty of dose emission during acute exacerbations
	• Can result in high oropharyngeal deposition
	• More expensive than pMDIs
	• Need to be stored in a cool and dry place

The first-generation DPIs were breath-actuated single unit-dose devices. A powder-containing capsule is loaded into the device holder prior to use of the device, the capsule is opened within the device and the powder is inhaled. The spent capsule is discarded after use. The Spinhaler® (Rhône-Poulenc Rorer, now Aventis), the first DPI device developed for the delivery of sodium cromoglicate, belongs in this category. The drug formulation is prefilled into a capsule and loaded into the device on top of a propeller. Two pins pierce the walls of the capsule when the patient actuates the device by sliding a cam. Once the capsule has been broken, the patient inhales through the device causing the propeller to turn and vibrate dispersing the powder into the inspired airstream (Chrystyn, 2007). Although, the Spinhaler® is discontinued, various other single unit-dose devices are currently on the market such as the HandiHaler® (Boehringer-Ingelheim/Pfizer) and the

Aerolizer® (Novartis) which is similar to the Cyclohaler® (Teva). The Aerolizer® employs four pins located on each side to pierce a capsule. Upon inhalation, the powder is deaggregated by a spinning motion via turbulence generated by a plastic grid (Coates et al., 2004). Hard gelatin or hydroxypropylmethylcellulose (HPMC) capsules have been used for this type of DPIs. Although hard gelatin capsules have been the standard for more than 40 years in dry powder inhalation, HPMC capsules are currently used in the majority of the newly developed medicinal products. HPMC capsules contain less water than the gelatin capsules and thus are more suitable for moisture sensitive formulations (Jones, 2003). Moreover, HPMC capsules are less prone to triboelectrification during spinning and their tendency to fragment at extremely low relative humidity when pierced is less compared to the gelatin capsules (Birchall et al., 2008). In this way, the risk of inhalation of capsule fragments and poor capsule emptying is reduced.

Single unit-dose inhalers are considered inconvenient to use as many steps (i.e. take capsule, load into the device, pierce) are required prior to their use. Carrying out all these steps may not be easy for a patient who is undergoing an asthma attack or for elderly patients who may lack the manual dexterity to accomplish all the required maneuvers (Chrystyn, 2007). However, it would be wrong to conclude that their use will be discontinued in the future, as they are attractive devices especially in emerging economies due to their low cost and ease of manufacturing. According to Harris (2016), the development of capsule-based DPIs that use capsules with size larger than size 3 and the introduction of an opening rather than piercing mechanism that would minimise the risk for creation of fragments, are two fields for innovation in the future.

The second-generation DPIs can be further divided into two categories: the multiple dose and the multi-unit devices. The multiple dose DPI devices measure the dose from a powder reservoir, and consequently they are also known as reservoir systems. The multi-unit dose DPI devices disperse individual doses, which are premetered into blisters or disks by the manufacturer.

The Turbohaler® (AstraZeneca) was the first representative of the multiple dose DPIs to enter the market and is employed for the administration of β_2-agonists (formoterol, terbutaline) and the corticosteroid budesonide separately and in combination. In the Turbohaler®, the drug is formulated as

a pellet of a soft aggregate of micronised drug particles with or without additional lactose excipient. Other reservoir devices have been developed and entered the market including the Clickhaler® (Innovata Biomed), the Easyhaler® (Orion Pharma), the Novolizer® (ASTA Medica, now Viatris GmbH) and the Pulvinal® (Chiesi). These devices try to minimise the flow-dependent dose emission that occurs with the Turbohaler®. More specifically, the dose emission from the Easyhaler® was found to be relatively consistent regardless of the inspiration rate (Palander et al., 2000). Based on the fairly consistent dose emission irrespective of the inhalation technique used by patients of all groups and the increased patient preference the Easyhaler® closely meets the criteria for an 'ideal inhaler' (Chrystyn, 2006). It should be noted that attention has to be given to the protection of the formulation from moisture when reservoir devices are used. In the case of Turbohaler® this is achieved by including a desiccant, while the Easyhaler® has a protective case and the hopper is designed so as it is impossible for the patient to blow into it. Moreover, it is often important to hold the reservoir devices in a vertical position during operation as some of these devices rely on gravity to fill the metering dose cup.

To address issues related with multiple and consistent dose-to-dose delivery, multi-unit devices were developed. Multi-unit DPIs include Diskhaler® and Accuhaler/Diskus® both developed by GlaxoSmithKline. The Diskhaler® employs individual doses contained within blisters (4 or 8 blisters) on a disk. Upon actuation, a needle pierces the upper and lower surfaces of a blister and as the patient inhales, the contents of the blister are dispersed in the airstream. The drug particles are detached from the carrier particles and a fraction is delivered to the lungs. On repriming the device, the disk rotates to expose the next blister to the piercing needle (Chrystyn, 2007). The Diskhaler® has now been withdrawn from the market, but in the past it was used for the delivery of drugs such as salbutamol, salmeterol, beclometasone, fluticasone propionate and the antiviral drug zanamivir. Accuhaler/Diskus® was marketed in the late 1990s as an improvement of the Diskhaler®, as it has the advantage of holding additional doses. It contains 60 doses (one-month therapy assuming one 'puff' twice daily dosage) in a double-foil strip. Advair/Seretide Diskus® which contains fluticasone propionate and salmeterol xinafoate, occupied 5th place on the list of best-selling medicines for 2013, indicating its wide acceptance among patients and physicians (US. Pharmaceutical Sales - Q4 2013, 2014). The recently

developed Ellipta® (GlaxoSmithKline) is a multi-unit device which can hold sufficient medication for one month (30 doses). It delivers the fixed combination of the inhaled corticosteroid fluticasone furoate and the long-acting β_2-agonist vilanterol as a once-daily inhaled maintenance therapy for asthma and COPD. The Ellipta® has a three-step operation procedure: 'open the cover', 'inhale the dose' and 'close the cover' and it was designed to be easily operated by patients of all ages including the elderly. In a recent study, Svedsater et al. (2013) found that Ellipta® was associated with high patient satisfaction and was preferred to other inhalers (i.e. Diskus® and pMDIs) based on interviews of participants with asthma and COPD. Ergonomic design, mouthpiece fit, dose counter visibility and ease of interpretation emerged as frequently cited drivers of preference for the Ellipta®.

The third-generation DPIs are also known as active devices as they employ electrical or mechanichal energy (compressed gas, battery-driven impellers, vibrating piezoelectric crystals) to disperse the drug powder (Islam and Gladki, 2008). While the efficiency of the passive, breath-actuated devices (first and second-generation DPIs) depends on the patient's inspiratory force, the active devices, due to the presence of an energy source, enable respiratory force-independent dosing precision and reproducible aerosol production (Crowder et al., 2001; Islam and Gladki, 2008). The Exubera® (Nektar Therapeutics/Pfizer) was the first approved active DPI using compressed air for the pulmonary drug delivery of insulin. While the Exubera® was expected to revolutionise the treatment of diabetes and increase patient's adherence, the device was withdrawn by Pfizer in the end of 2007 after it was on the market for only a year, due to the very poor sales numbers. Detailed commentaries on the reasons of the withdrawal of Exubera® and the future of inhaled insulin have been provided by Mack (2007) and Heinemann (2008).

In-vitro studies have demonstrated that active DPIs can produce aerosols with fine particle fractions (i.e. the fraction of emitted dose less than a stated size, usually 5 μm) of 50-70% (Islam and Clearly, 2012). Moreover, while passive devices are commonly used for local respiratory delivery, the active devices can play a future role in the delivery of drugs for systemic action, which need to deposit more deeply into the lungs.

1.4.3.1. Device resistance

A passive DPI depends on the patient's inspiratory flow rate for the required energy to disperse the powder. The internal resistance of a DPI is a consequence of its design, and contains elements of flow restriction to increase the kinetic energy of the airflow through the device during an inhalation. More specifically, during inhalation from a DPI, the patient's inspiratory effort with the resistance of the device creates turbulent energy, which is measured as pressure drop (ΔP in cmH_2O) that causes the dispersion of the powder (Eq.1.5, Clark and Hollingworth, 1993).

$$\sqrt{\Delta P} = Q * R_D \quad . \quad . \quad . \quad \text{Equation 1.5}$$

where Q is the volumetric flow rate in L min^{-1} and R_D is the device resistance. The resistance of devices can be classified from low (e.g. Aerolizer®) to medium/low (e.g. Accuhaler/Diskus®, Ellipta®) to medium/high (Turbohaler®) and then to high (e.g. HandiHaler®) (Demoly et al., 2014). According to Eq. 1.5, airflow is inversely proportional to device resistance indicating that high-resistance devices require low flow to create the required pressure drop.

Most inhalers deliver fine particle fractions between 20 and 30% of the label claim between 2 and 4 KPa pressure drop. A common misconception is that high resistance DPIs require a high flow rate or considerable inspiratory effort in order to be operated correctly limiting the prescription of these inhalers to patients with COPD (Hoppentocht et al., 2014). However, studies have shown that it is easier to achieve such pressure drop when using high-resistance inhalers than low-resistance inhalers and that patients were able to achieve the required pressure drop even during exacerbations of asthma and COPD (Börgstrom, 2001). Moreover, the high flow rates associated with low-resistant inhalers lead to the impaction of drug particles in the oropharynx, which is at the cost of central and peripheral lung deposition.

1.4.3.2. Dry powder inhaler formulations

Drug particles should exhibit an aerodynamic diameter between 1 and 5 μm so as to be delivered to the lungs (Heyder et al., 1986). Such fine drug particles exhibit a high surface free energy. In an attempt to minimise their surface energy, the particles have the tendency to stick together (cohesion)

or to any surfaces they encounter (adhesion). Moreover, such fine particles tend to suffer from poor flowability and aerosolisation performance as they are retained in the device when used alone.

The most commonly applied approach in order to address the above challenges is to blend the fine drug particles with an inert carrier consisting of coarser particles usually in the size range of 40-150 μm. During blending, the micronised drug particles adhere to the surfaces of the carrier particles forming adhesive mixtures (Fig.1.6). The carrier particles act as a diluent (a typical drug-to-carrier ratio is 1:67.5) but also as a flowability enhancer leading to a more reproducible dose metering.

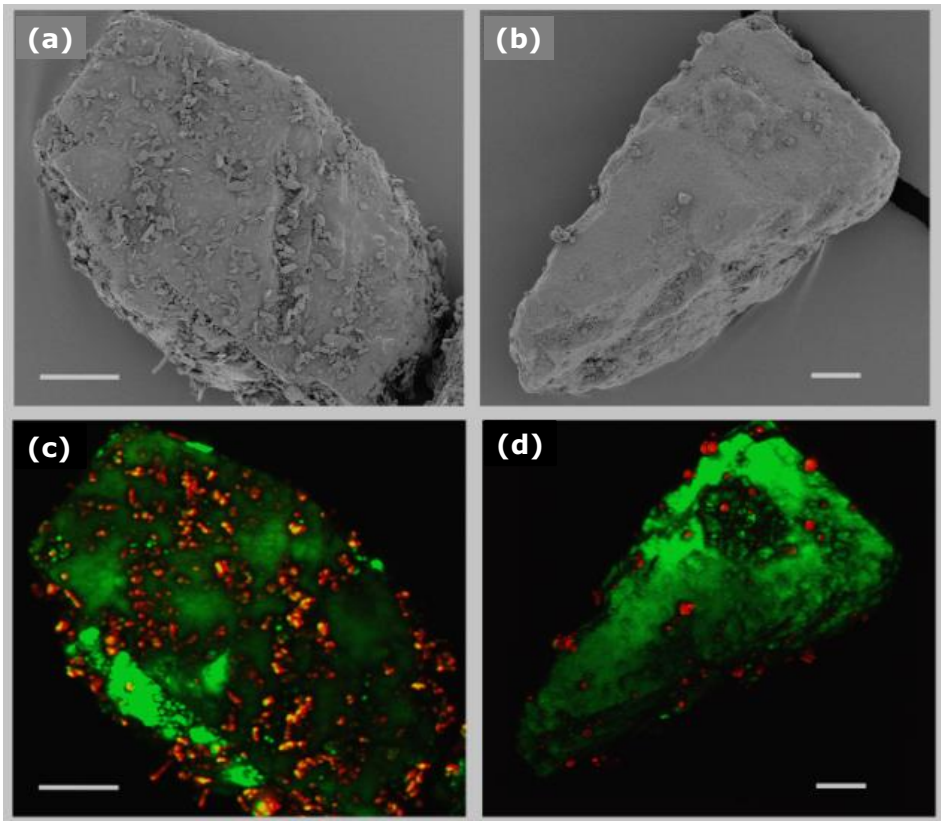

Figure 1.6 (a,b) Scanning electron microscopy and (c,d) coherent anti-Stokes scattering microscopy images of adhesive mixtures of salmeterol xinafoate (red) and lactose carrier (green) after 0.5 (left) and 600 minutes of mixing (right). Scale bars represent 20 μm (Fussell et al., 2014).

The dispersion of adhesive mixtures upon inhalation may be regarded as a three-step process including: fluidisation of the powder in the airstream, detachment of primary or agglomerated drug particles and break-up of detached agglomerates into primary particles (Grasmeijer et al., 2015). The

particles that exhibit an aerodynamic diameter in the range of 1-5 μm will be deposited in the lungs while larger particles will be impact in the mouth and the back of the throat where they are swallowed (Fig.1.7). The degree of dispersion achieved depends on the cohesive/adhesive forces and the separation forces generated by the kinetic energy of the inhaled airstream. The balance between adhesive and cohesive forces should be adjusted to ensure sufficient adhesion between carrier particles and drug so as the adhesive mixture to be stable during handling and filling but also sufficient detachment during aerosolisation.

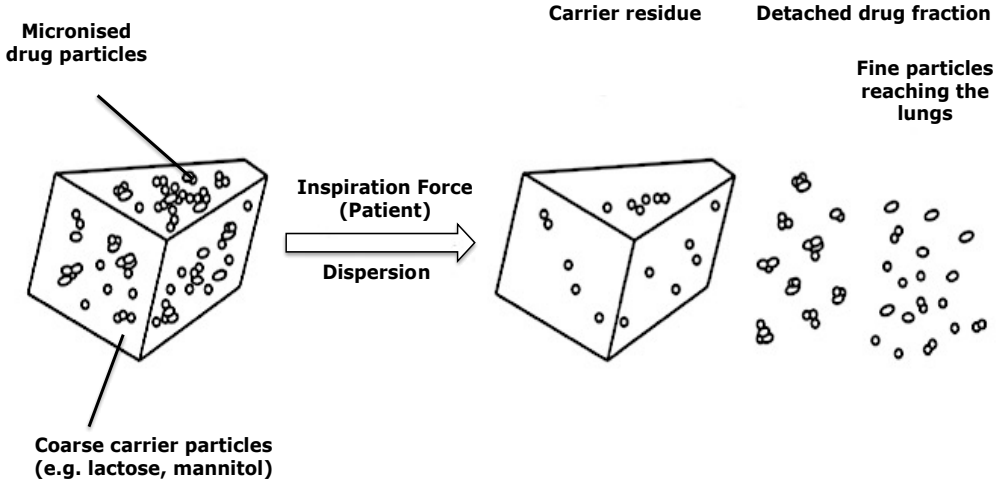

Figure 1.7 Schematic diagram of adhesive mixtures for DPIs. The formulation consists of micronised drug particles adhered on the surface of large carrier particles. Upon inhalation, drug particles detach from the surface of large carriers and deposit in the lungs. The carrier particles impact at the back of the throat.

Lactose is the most widely used carrier in DPIs with various inhalation grades of different physicochemical properties available on the market. Apart from lactose, a wide range of other generally regarded as safe (GRAS) excipients have been studied as carrier for DPIs including D-mannitol, trehalose dihydrate, sorbitol, erythritol and D-raffinose. Mannitol, a reducing sugar which is less hygroscopic than lactose, has been proposed as the most promising alternative carrier to lactose in DPIs (Steckel and Bonzen, 2004; Rahimpour et al., 2014).

Many studies have investigated the effect of parameters that can influence the aerosolisation performance of adhesive mixtures including the effect of carrier particles size distribution, fine excipient particles, carrier surface roughness, drug content, and the physicochemical properties of carrier and drug. However, general conclusions regarding the effects of these variables

cannot be drawn as inconsistent findings have been reported in the literature. The inconsistency of the findings can be attributed to the complex interplay among the properties of starting materials, the mixing process and the dispersion performance (Grasmeijer et al., 2015).

Over the last three decades, particle engineering for pulmonary drug delivery has focused on the design of carrier-free particles (i.e. particles free of carrier) for DPIs. Engineering of carrier-free particles has the potential to overcome the problems associated with the presence of carrier (most commonly lactose) (Healy et al., 2014). In this way, issues of blend uniformity can be avoided but also it is possible to deliver high drug payloads to the lungs, which is especially useful in the case of antibiotics. Spheroids (soft agglomerates) prepared by spheronisation of micronised particles are used with the Turbohaler® device where they are loaded as spheroids and they break up into individual particles upon inhalation. With a diameter around 0.5 mm, the spheroids exhibit enhanced flowability compared to micronised drug and they do not suffer from electrostatic charging during handling and operation. However, a high variability in the emitted dose has been identified as the main limitation of the spheroids (Pilcer and Amighi, 2010) .

1.5. Particle engineering for pulmonary drug delivery

In attempts to enhance efficiency of delivery from DPIs, various techniques have been used to engineer respirable drug particles. These include micronisation, crystallisation, spray drying, freeze drying, spray-freeze drying, supercritical fluid technology and antisolvent technology (Murnane et al., 2014). From the aforementioned techniques, spray drying will be considered in depth, as it was one of the key techniques used in the context of this thesis.

1.5.1. Spray drying

Spray drying is a well-established technique, having been used for many years in a variety of fields. It was first applied in the dairy and detergents industries in the 1920s, and its popularity increased as it was used in the manufacture of instant coffee. Today, dry milk powder, instant soups, coffee, detergents and dyes are examples of spray-dried products used in everyday

life. However, it remains an active field of research and innovation as particle engineering becomes more sophisticated.

Spray drying is a widely used technique for the formation of pharmaceutical particles with size ranging from the nanometre to the micrometre scale. The main advantages of spray drying for the production of inhalation particles are the ability to manipulate and thus control particle size distribution, shape and density as well as flowability and dispersibility of the powders (Van Oort and Sacchetti, 1996).

Spray drying is a one-step manufacturing process where a liquid feed (solution, coarse or ultrafine suspension or an emulsion) is converted to a dried particulate form (Fig.1.8). The main principles behind spray drying are the atomisation of a liquid feed into fine droplets and evaporation of the solvent (aqueous or organic) by means of a hot drying gas. For the atomisation of the liquid feed a nozzle is used to form droplets in a range of 5-200 μm. For aqueous feeds with less than 20% of organic solvent, spray drying is carried out in the open mode where the drying gas (e.g. compressed air) is exhausted in the atmosphere. For concentrations greater than 20% organic solvent in the feed, spray drying should be carried out in the closed mode, so as to reduce the risk of flammability and explosion when organic solvents are heated in the presence of oxygen. In the closed mode, the heated inert gas (e.g. nitrogen) is recirculated and an inert loop (condenser) is used to convert organic vapours to liquid (Kleinhans et al., 2007).

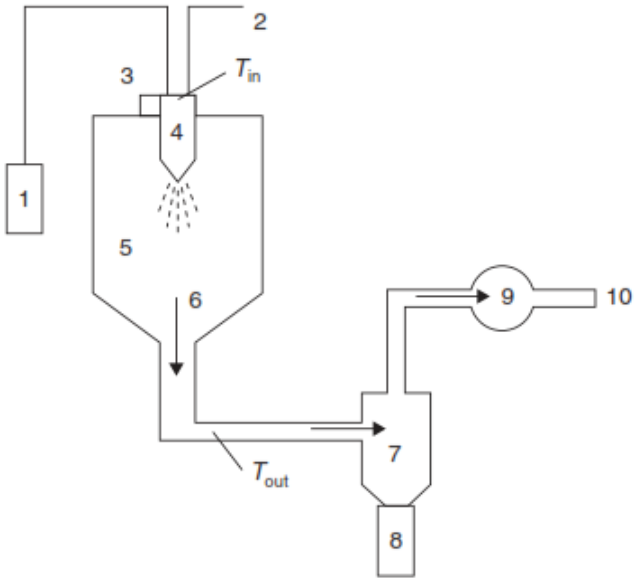

Figure 1.8 Schematic representation of spray dryer instrumentation. 1: Feeding liquid, 2: Drying gas flow, 3: Heater for drying gas, 4: Nozzle, 5: Drying chamber, 6: Dried product and process gas flow, 7: Cyclone, 8: Collection vessel, 9: Aspirator and 10: Exhaust gas, (Peltonen et al. 2010).

The spray drying process consists of a sequence of four steps (Masters, 1991):

- Preparation of the liquid feed.
- Atomization of the feed into a spray through a nozzle and contact with the hot drying gas
- Evaporation of liquid and particle shape formation and drying
- Separation of the dried product from the drying gas.

Preparation of the liquid feed: The prepared liquid feed must be pumpable, homogenised and free from impurities. It can be a solution, suspension or emulsion made up from a solvent or a mixture of solvents and the substance to spray dry. It is reported that increasing the concentration of solids in the liquid feed leads to the formation of larger particles and an increase in the effective particle density (i.e. the mass of a particle divided by its volume including both open and close pores) (Van Oort and Sacchetti, 1996; Elversson and Millqvist-Fureby, 2005).

Atomisation: This is the process whereby the liquid feed is broken up into a collection of droplets. There are many different types of atomizers available

(two-fluid or pneumatic, hydraulic pressure, rotary disk atomizer and ultrasonic nozzles), with the two-fluid or pneumatic nozzles being the most common choice in the spray driers used in the pharmaceutical industry (Fig. 1.9). This can be explained by the fact that they are suitable for smaller scale plants and also they produce smaller sized droplets compared to other types of atomisers. In this case, atomisation occurs by rapid expansion of the spray gas, which is mixed with the liquid feed either within the nozzle body (internal mixing) or at its tip (external mixing). More specifically, the liquid feed is pumped at relatively low flow rates and at the discharge orifice is impinged by a gas under pressure. As the velocity of the gas is much higher than the velocity of the liquid at the orifice, the relative velocity provides the work required to create the large surface area of the spray. For a given nozzle, the flow rate of the liquid and the gas pressure are the factors controlling the particle size distribution of the generated droplets (Van Oort and Sacchetti, 1996).

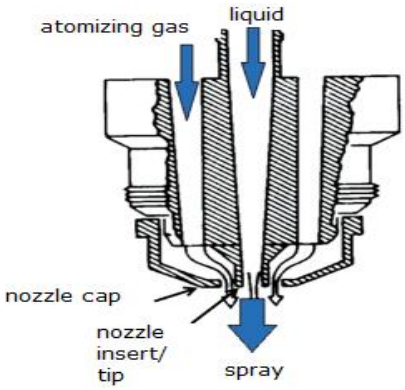

Figure 1.9 Two - fluid (pneumatic) nozzle with external mixing (Kemp et al., 2013).

Drying: The drying of the droplets to solid particles by contact with heated gas inside the drying chamber is essentially the step of solvent removal. The evaporation of solvent during the droplet drying is described as a coupled heat and mass transfer phenomenon, with the difference between the vapour pressure of solvent and the partial pressure in the gas phase being the driving force of the drying.

Separation: The final step of spray-drying is the separation of the spray-dried particles from the drying gas. Although the primary separation of the dried particles from the drying gas takes place at the base of the drying chamber, the use of a cyclone is the most commonly used separation technique for the recovery of the finer particles from the drying gas. In the cyclone (Fig. 1.10),

centrifugal forces are applied to the spray-dried particles, which are collected in a bottom vessel.

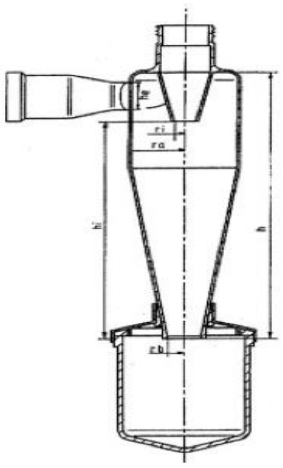

Figure 1.10 Design of the standard Büchi cyclone (Maury et al., 2005).

1.5.1.1. Selection of spray-drying process parameters

The process parameters and their influence on the end product obtained by spray drying have been extensively studied with both experimental techniques (e.g. the droplet chain and the mono-dispersed spray dryer) but also with analytical and numerical models (Vehring, 2008).

From all these studies, it is evident that spray drying is a method with a high interdependency between the process and formulation variables and the characteristics of the final product.

In the past, the selection of spray drying process parameters was based on 'one-factor-at-a-time' studies. These 'trial and error' procedures illustrated that process parameters (namely inlet temperature, feed flow rate, gas spray flow and aspirator flow) combined with formulation parameters (e.g. concentration of the liquid feed), influence the product characteristics such as the particle size, moisture content and the process yield.

Recently, the optimisation of spray-drying parameters is carried out by using the Quality by Design (QbD) concept characterised as a holistic approach for the formulation development (ICH Q8). QbD combines both designing and developing formulations and procedures which ensure predefined characteristics in the final product, while emphasises the demand of regulatory authorities to pharmaceutical industries to acquire a more

comprehensive insight into their manufacturing processes (Maltensen et al., 2008; Lebrun et al., 2012).

1.5.1.2. Particle formation by spray drying

According to Vehring (2008) there are two dimensionless parameters, which were found to influence and explain particle formation by spray drying. The first is the Peclet number (*Pe*) which is the ratio of evaporation rate (*k*) to the diffusion coefficient (D_i) of a solute i (Eq.1.6) and the second parameter is the initial saturation of excipients:

$$Pe = \frac{k}{8D_i} \quad . \quad . \quad . \quad \text{Equation 1.6}$$

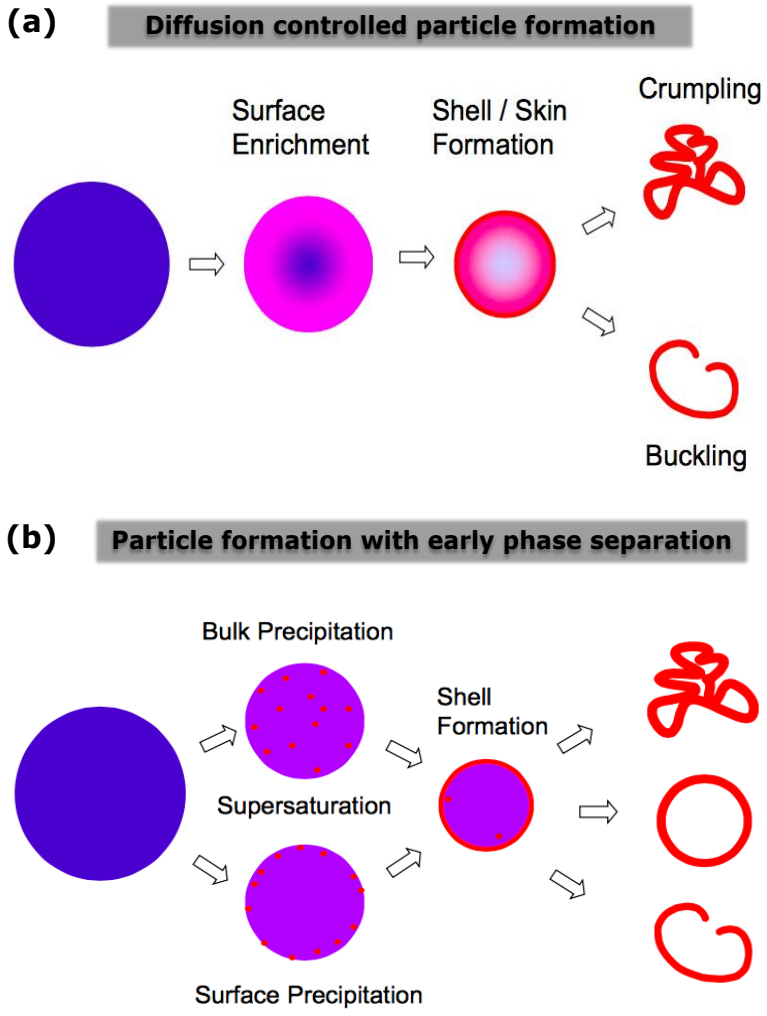

Figure 1.11 Proposed particle formation for (a) high and (b) changing Peclet number (Vehring 2008).

Low Peclet number particle formation: For Peclet numbers equal to or smaller than one ($Pe \leq 1$), the diffusion of the solute is faster or of the same order, compared to the radial velocity of the receding droplet surface. This means that the solute remains evenly distributed in the droplet during evaporation. Particularly for small Peclet numbers and high solute solubility (to avoid supersaturation during drying) the obtained dry particles are expected to be spherical with little or no void space and thus their density is close to the true density of the dried bulk material.

High Peclet number particle formation: High Peclet numbers cause enrichment of the solute at the surface leading to shell or skin formation. The obtained particles are expected to exhibit significantly lower density than the true density of the dried bulk material. This is explained by the large void space in the particles (Fig. 1.11a). It should be noted that when spray drying nanoparticles from suspensions, the nanoparticles are considered to exhibit very high Peclet numbers. This may be explained by the fact that nanoparticles are considered immobile compared to the receding droplet surface (Tsapis et al., 2002).

Changing Peclet number: The third and most challenging case in terms of particle engineering is when the Peclet number changes during the evaporation process. While for the two previous cases both the evaporation rate and the diffusion coefficient of the solute were considered to be constant during the whole process, in reality the diffusion coefficient of a solute is changing during droplet evaporation, especially in co-solvent systems, as one solvent evaporates faster than the other. For molecules with low solubility in the solvent system used and high diffusion coefficient, the initial Peclet number will be small and the concentration of the solute will increase without any surface enrichment. However, if the initial saturation is efficient, a supersaturation will be reached early during the drying process causing the precipitation of a separate phase at the surface or throughout the bulk of the droplet. The separated phase exhibits much lower mobility than the dissolved phase and as a result the diffusion coefficient of the separated phase is much lower than the one of the dissolved phase. In other words, the Peclet number increases and the separated phase tend to accumulate at the particle surface (Fig.1.11b). The approach of changing Peclet number can explain the properties of excipients such as L-leucine and trileucine as surface modifiers accumulating in the surface of particles. In many studies, L-leucine and trileucine have been used as force control agents in spray-dried formulations

for inhalation as they have been found to alter the interparticle forces in the aerosol powder and thus improving powder dispersibility (Seville et al., 2007; Vehring, 2008; Xu et al., 2014).

1.6. Nanoparticles in drug delivery

The use of nanoparticles has gained momentum in drug delivery, and research on nanoparticulate formulations is expanding in recent years. This is mainly because many of the new chemical entities (NCEs) arising from combinatorial screening (>40%) suffer from poor solubility in aqueous media and some of them simultaneously in organic solvents (Lipinski, 2002). Benet (2007) puts the figure of NCEs suffering from poor solubility at 90%, while only 40% of marketed drugs are poorly soluble. The limitation of poor solubility, that constitutes one of the main reasons for the discontinuation of development of NCEs, makes their formulation very challenging. In the past, the industry considered these compounds as highly risky development candidates. However, nowadays mainly due to their prevalence, '*industry consensus has shifted from an attitude of avoidance to one of acceptance and increasing research dedication is given to solving solubility challenges*' (Brough and Williams, 2013). Nanotechnologies are considered one of the most prevalent improvement methods and have been used to overcome the problem of poor solubility and thus bioavailability, as well as to achieve targeted drug delivery.

Despite the importance of nanoparticles, there is no single definition of nanoparticles. This may be due to the highly multidisciplinary nature of nanotechnology. The term nanotechnology was first used by the scientist Norio Taniguchi in 1974, at the University of Tokyo in Japan, for any material in the nanometre size range (Taniguchi, 1974).

According to the U.S. Food and Drug Administration, materials are classified as being in the nanoscale range if they have at least one dimension at the size range of approximately 1-100 nm. However, the 100 nm limit is often considered constraining and according to a more expanded and inclusive definition: particles below 1000 nm in each dimension (sub-micron particles) are designated as nanoparticles (Keck and Müller, 2006). The latter definition is applicable in the pharmaceutical field as physical behaviour and material properties such as aggregation, solubility and dissolution, start to alter once

the size of particles is reduced to the sub-micron level, due to the increased surface area to volume ratio (Florence and Attwood, 2015).

Different types of nanotherapeutics have been applied in drug delivery, such as nanocomplexes, nanoemulsions, polymeric micelles, liposomes, virosomes, polymeric nanoparticles, and nanocrystals (Fig. 1.12).

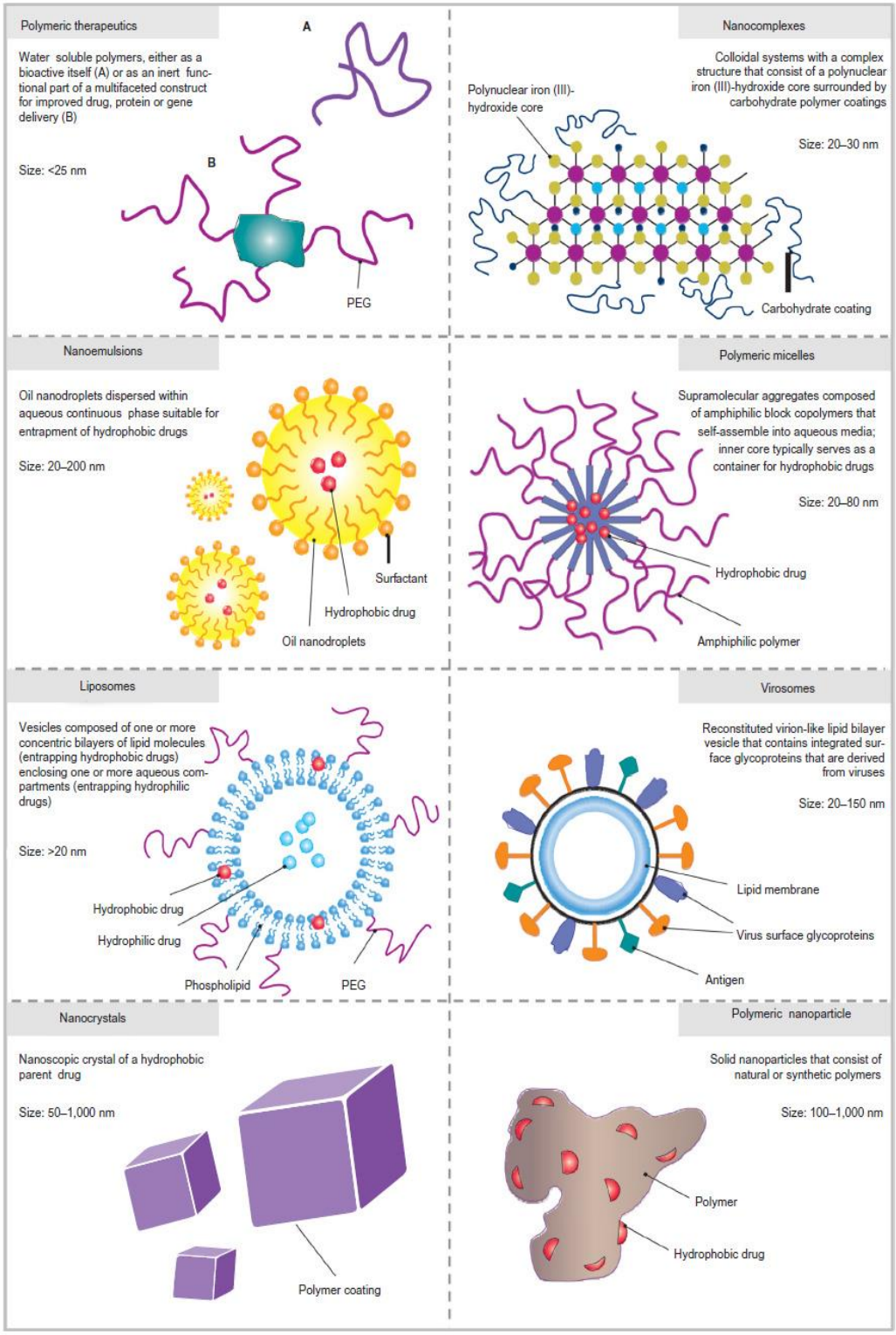

Figure 1.12 Types of nanotherapeutics marketed in the EU (Hafner et al., 2013).

1.6.1. Nanocrystals

Nanocrystals are nanosized drug particles. Nanocrystals are typically produced in the form of nanosuspensions, which are submicron, colloidal dispersions of nanosized drug particles, stabilised by surfactants, polymers, or a mixture of both (Chingunpituk, 2007). According to a stricter definition, a formulation should have a volume median diameter (D_{50}) below 1 μm and a volume diameter 90% undersize (D_{90}) below 2.5 μm to be classified as a nanosuspension (Wong et al., 2008; Yue et al., 2013). The term nanocrystals, although implying the particles are in a crystalline state, which is true for the majority of reported cases, has been extended to describe nanosized suspensions of partially crystalline or even amorphous drugs (Lindfors et al., 2007).

From the different types of nanotherapeutics, specific focus will be given on nanocrystals in the context of this thesis. Nanocrystals possess a high drug loading (close to 100%) in contrast to matrix nanoparticles consisting of polymeric or lipid matrices. Thus, the main advantage of nanocrystals is the low amount of excipients used allowing high drug concentration at the site of action and reduction of the potential toxicity of the excipients in the lungs.

1.6.1.1. Advantages of nanocrystals in drug delivery

In general, the main advantages of nanocrystals are:

- increased dissolution rate and enhanced saturation solubility with consequent bioavailability improvement
- low toxicity
- improved chemical stability

The reduced particle size and high surface area per unit mass of the nanoparticles lead to a more rapid dissolution as described by the Nernst and Brunner equation (Eq.1.7, Nernst, 1904; Brunner, 1904):

$$\frac{dm}{dt} = \frac{D*S}{h}(C_s - C) \quad . \quad . \quad . \quad \text{Equation 1.7}$$

where $\frac{dm}{dt}$ is the dissolution rate of non-formulated drug particles, D is the diffusion coefficient, S is the surface area of drug particles, h is the thickness of the diffusion layer, C_s is the saturation solubility of the drug particles and

m is the concentration of the drug in solution. Therefore, by reducing the particle size, the total surface area, *S*, will increase resulting in a more rapid dissolution, particularly under sink conditions (*C* << *Cs*).

Regarding the saturation solubility, which for drug particles in the micrometre size range and above is a constant depending on temperature and dissolution medium, in the case of submicron particles, it depends on their size and is reported as 'apparent' saturation solubility (Buckton and Beezer, 1992). The enhanced 'apparent' saturation solubility of nanosuspensions has been attributed to the increased curvature of nanoparticles resulting in increased dissolution pressure and hence drug solubility as described by a modified Kelvin and Ostwald-Freundlich equation (Eq.1.8)

$$ln\frac{S}{S_0} = \frac{2\gamma * V_m}{r * R * T} = \frac{2\gamma * M}{r * \rho * R * T} \quad . \quad . \quad . \quad \text{Equation 1.8}$$

where *S* is the drug solubility at temperature *T*, S_0 is the solubility of infinite big particle material, *R* is the gas constant, V_m is the molar volume, *T* is the temperature, *r* is the particle diameter, *γ* is the surface free energy, M and ρ are the molecular weight and density of the compound, respectively.

Due to the increased dissolution rate and enhanced saturation solubility, nanosuspensions result in improved bioavailability (Kesisoglou et al., 2007; Shegokar and Muller, 2010). More specifically, regarding the oral drug delivery, nanosuspensions have been used as a way to address the issue of low bioavailability with reduced food effect compared to micronized drug (Rabinow, 2004). Nanosuspensions also increase adhesiveness to the gastrointestinal mucosa, leading to prolonged gastrointestinal residence and

thus enhanced uptake via the gastrointestinal tract (Jacobs et al., 2001). Mucoadhesive nanosuspensions of the antiprotozoal drug buparvaquone containing chitosan were proposed as a drug delivery system against intestinal *Cryptosporidium* infections due to their increased gastrointestinal residence time and thus prolonged action (Kayser, 2001). The high drug loading of nanosuspensions compared to other formulation approaches (e.g. cyclodextrin formulations) is beneficial as it is associated with reduced toxicity due to the very small amounts of stabilisers/excipients used (Verma and Burgess, 2010). Recently, there is increasing concern regarding nanotoxicology mainly due to the ability of nanoparticles to enter the cells. The toxicity of nanoparticles is related to their cellular uptake and intracellular fate. According to the nanotoxicological classification system proposed by Müller et al (2011), nanocrystals are in the low/non-risk group. Their typical size (100 nm < d < 1000 nm) does not allow cell endocytosis and their biodegradable nature is associated with low danger of biopersistency. However, studies should be conducted on the interaction of nanocrystals with cells and their cellular uptake has to be considered when developing nanocrystalline-based products.

Formulating a drug as a nanosuspension has also been proposed as a method of improving chemical stability with respect to solution formulations. For example, quercetin nanosuspensions exhibited no significant change in drug content or colour over one month. In contrast, for the solution, a 28.3% reduction in drug content and discoloration was observed over the same period (Gao et al., 2011). Formulating drugs as nanosuspensions may change their pharmacokinetic profile and extend their therapeutic use, as in the case of melarsoprol, an organoarsenic compound. Melarsoprol as a nanosuspension was unable to cross the blood-brain barrier, but rather accumulated preferentially in the Mononuclear Phagocyte System, which is a family of cells comprising bone marrow progenitors. The high concentration of the drug in the bone marrow resulted in reduced arsenic-related encephalopathies, due to the inability of the formulation to cross the blood-brain barrier, and opens the way for the use of melarsoprol against refractory leukemias and other cancer diseases (Ben Zirar et al., 2008).

Apart from their superior clinical performance, nanosuspensions have attracted the interest of drug formulators as they can extend the life cycle of an active pharmaceutical ingredient (API) after patent expiration, as

occurred for a fenofibrate nanosuspension launched by Abbott Laboratories (Shegokar and Muller, 2010). Nanosuspensions are also suitable formulations for preclinical animal studies mainly due to their quantitative and easy oral administration (Niwa et al., 2011). Moreover, the techniques for the production of nanosuspensions (e.g. wet milling) are easy to scale-up and can provide the amount of formulation required (10 mL up to a few liters) for toxicological and pharmacokinetic studies in animals and for clinical trials under current good manufacturing practices (Möschwitzer, 2013). All these characteristics have resulted in the rapid commercialisation of nanosuspensions.

1.6.1.2. Stabilisation of nanocrystals

The formation of nanocrystals almost always takes place in a liquid (usually water) as a nanosuspension (colloidal system). The nanosuspensions by definition are thermodynamically unstable systems due to their large interfacial area, and thus they possess high interfacial free energy. The surface free energy (ΔG) termed 'Gibb's energy' associated with this area is given by Eq.1.9:

$$\Delta G = \gamma_{SL} * \Delta A - T * \Delta S \quad . \quad . \quad . \quad \text{Equation 1.9}$$

where ΔA is the change in surface area, γ_{SL} is interfacial tension between the solid and liquid interface, T is the absolute temperature and ΔS is the change in entropy of the system. Therefore, a nanosuspension can spontaneously increase its stability by reducing the interfacial area and consequently the surface free energy. This can be achieved in several different ways: i) aggregation (flocculation), ii) sedimentation or floating and iii) Ostwald ripening.

For a nanosuspension to be stable it must contain a third component known as stabiliser additional to the solid particles and liquid, such as a surfactant and/or polymer. Several theories have been proposed to explain how stabilisers function and contribute to the stability of nanosuspensions: i) the lowering of the interfacial tension, ii) the DLVO theory (Derjaguin and Landau, 1941; Verwey and Overbeek, 1948) and iii) the steric stabilisation theory.

Lowering of the interfacial tension: Surfactants are amphiphilic molecules having a hydrophilic and a hydrophobic part. The combination of the two opposite affinities in the same molecule causes them to orient and adsorb to the interface. Thus, in the case of suspensions, they reduce the interfacial tension between the continuous (liquid) and disperse (solid) phases. By reducing the interfacial tension, the surface free energy of the system is reduced resulting in a stable nanosuspension.

Steric stabilisation theory: Steric stabilisation is a general term that includes all the aspects of the stabilisation of uncharged particles in a colloidal dispersion system by using non-ionic macromolecules (surfactants or polymers), Fig.1.13.

The non-ionic macromolecules orientate themselves at the solid-liquid interface in such a way that the hydrophilic portions are directed towards the liquid (water) and the hydrophobic portions towards the solid particle where they are adsorbed and adhered on the particle surface. A stabiliser layer is formed around the particles and water penetrates into the layer possibly allowing the stabiliser macromolecular chains to gyrate. When two particles of radius a having adsorbed stabiliser layer with an average thickness δ approach one another closely as a result of Brownian motion, two effects will lead to repulsion termed 'steric repulsion' between the particles.

The first called the 'osmotic effect' occurs if $\delta \leq H \leq 2\ \delta$, where H is the distance between particle surfaces. The adsorbed surfactant layers on the opposing surfaces of the two particles start to overlap and the macromolecular chains will interpenetrate each other. This will cause water molecules to be forced out of the overlapped layers and will be a free energy change (energy of steric repulsion). The repulsion increases with the chain length of the stabiliser, the ability of the liquid to solubilise the chain and with the number of chains per unit area of the particle surface (Fischer, 1958).

The second effect, called the 'volume restriction effect' occurs if $H < \delta$; then both interpenetration and compression of the macromolecular chains may occur. The interpenetration of the chains give rise to the 'osmotic effect' described above, while their compression may produce two effects: a) intermolecular self-interpenetration accompanied by a corresponding 'osmotic effect' and b) deformation of the adsorbed layer which contributes to the 'steric repulsive' energy of the system (Napper, 1977).

Similar to steric stabilisation is the 'depletion stabilization of colloids', which involves unanchored (free) polymeric macromolecules creating repulsive forces between the approaching particles, Fig 1.13.

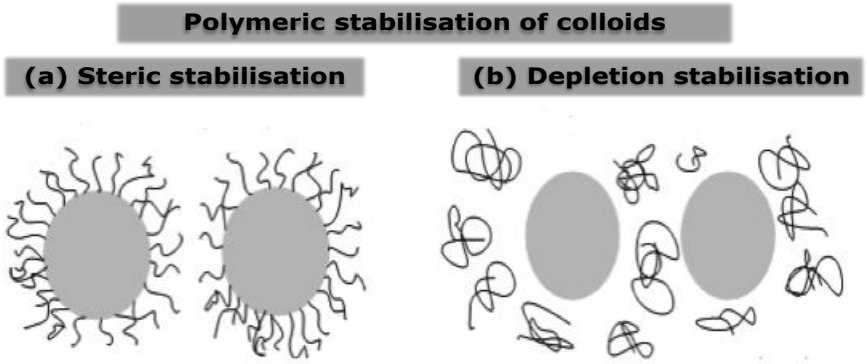

Figure 1.13 (a) Steric and (b) depletion stabilisation of colloids.

Common pharmaceutical excipients that are suitable as polymeric stabilisers are hydroxypropylcellulose (HPC), hydroxypropylmethylcellulose (HPMC), polyvinyl pyrrolidone (PVP K30) and poloxamers (Pluronic F68 and F127). Tween 80 and sodium lauryl sulfate (SLS) are widely used as non-ionic and anionic surfactants, respectively. For nanosuspensions, apart from reducing the interfacial tension, it is necessary that a stabiliser acts as wetting agent and provides a barrier between the particles (van Eerdenbrugh et al., 2008a).

It should be noted that currently selection of a suitable stabiliser for a drug nanosuspension is based on trial and error. Few studies attempt to develop a rational approach for the selection of the appropriate stabiliser based on the physicochemical characteristics of the API in question. In this direction, George and Ghosh (2013) studied the wet milling of six APIs with four different stabilisers in order to identify the material property variables (API and stabiliser) that control the critical quality parameters, which play a role in nanosuspension stability. They identified, the log *P*, the melting point and the enthalpy of fusion as the key drug properties that have a direct effect on nanosuspension stability, proposing a generic formulation strategy for the production of nanosuspensions based on the drug properties (Fig. 1.14). The most likely candidate for wet milling is a drug with a high enthalpy of fusion and hydrophobicity which can be stabilised either electrostatically or sterically.

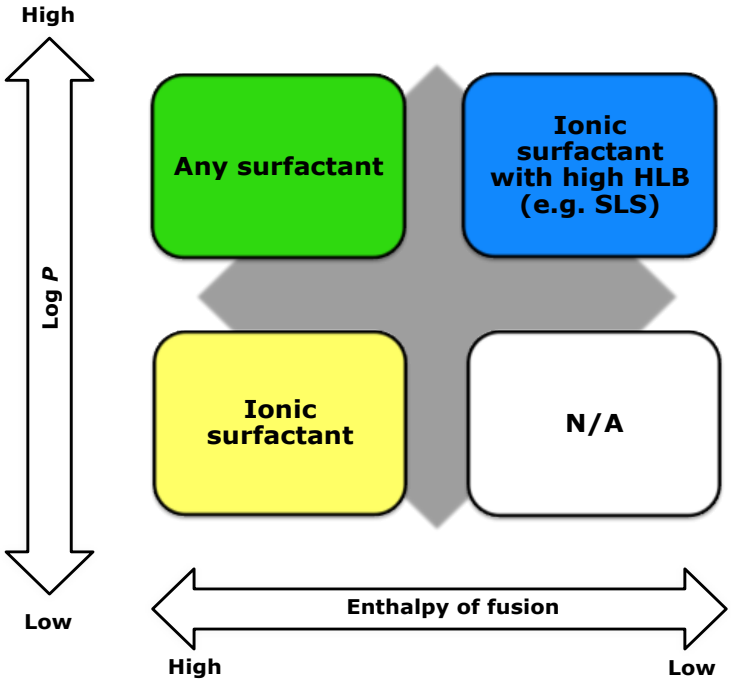

Figure 1.14 Proposed generic formulation of nanosuspension based on drug properties (HLB: hydrophilic lipophilic balance, George and Ghosh, 2013).

1.6.1.3. Formation of nanocrystals

Methods for the production of nanosuspensions can be categorised as top-down and bottom-up methods, depending on the starting material. In top-down methods, such as wet milling, high-pressure homogenisation (HPH) and microfluidisation, the starting material comprises larger solid particles than the resulting nanoparticles and mechanical processes are the fundamental mechanism causing particle size reduction. In bottom-up methods, particles are formed from the molecular level. Such methods are further subdivided into solvent evaporation (e.g. spray drying, electrospraying, cryogenic solvent evaporation, etc.) and antisolvent methods (e.g. liquid antisolvent, supercritical antisolvent, etc.) (Zhang et al., 2011).

The main advantage of top-down over bottom-up methods is the production of nanosuspensions with high drug loading. Moreover, they do not involve harsh organic solvents since the solvent in which drug is dispersed, but not dissolved, is water for the majority of poorly water-soluble drugs, making the top-down methods eco-friendly. This permits the formulation of many poorly soluble APIs, characterized as 'brick dust', suffering from poor solubility in a

wide range of solvents. In general, because of the more streamlined process-flow and the solvent-free feature of top-down methods, the majority of marketed and developmental nanosuspension-based pharmaceutical formulations have been produced by top-down methods. From the various methods for the production of nanocrystals, the method of wet milling will be presented in depth, as it is the method used in this thesis for the formation of nanosuspensions.

1.6.1.3.1. Wet milling

This process involves feeding the milling chamber with the milling medium (water, buffer or organic solvent), the milling beads, the particulate material and the stabiliser (Fig. 1.15). The milling chamber is rotated at the desired speed generating very high shear forces between the particles and the beads. These forces lead to size reduction by breakage and abrasion of the particles along the weak points (cracks, crystal imperfections and slip planes) and finally yields particles with smaller size.

Wet milling is an efficient way to produce drug material in the nanosized range (nanocrystalline material) with a typical size ranging from 200-500 nm. The majority of nanocrystals that have been offered as commercial products are produced by this method (Table 1.2).

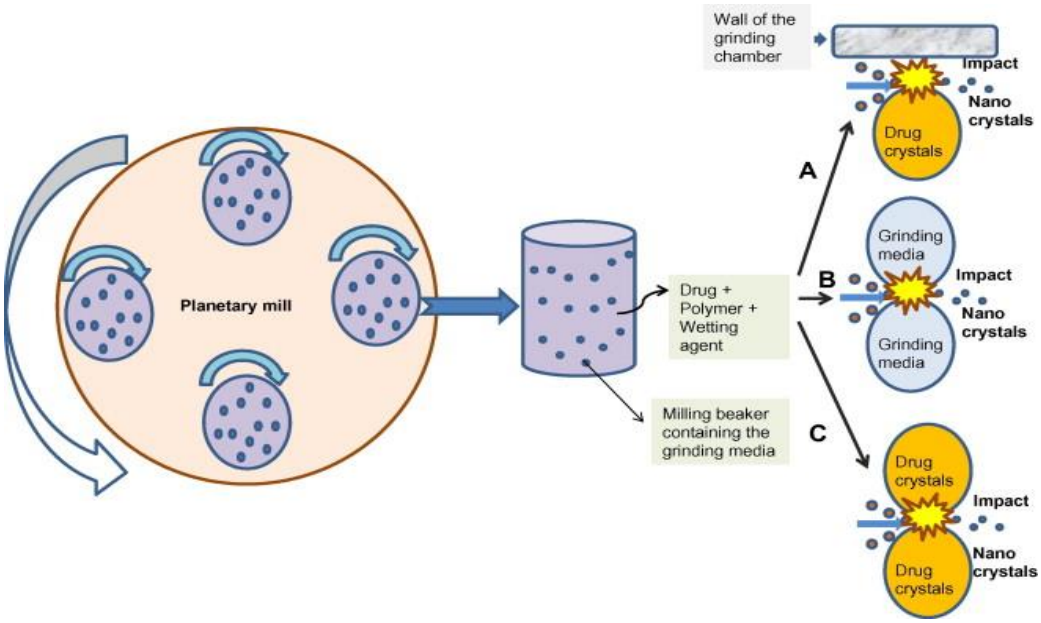

Figure 1.15 Formation of nanocrystals using a planetary mill showing different grinding mechanisms (A- drug-wall, B- drug-bead and C- drug-drug) (Ghosh et al., 2012).

Table 1.2 Commercial products based on nanomilling (Möschwitzer, 2013; Van Eerdenbrugh et al.,2008b).

Trade Name, Company	Active substance	FDA approval	Reasons for the development/ reformulation as a nanocrystalline dosage form
Rapamune® [a], Wyeth	Sirolimus	2000	Reformulation of the oral solution, which required refrigeration storage and was difficult to administer due to special dispensing protocol and unpleasant taste (Merisko-Liversidge and Liversidge, 2011).
Emend®, Merck	Aprepitant	2003	Original dosage form exhibited significant food effect (3-fold increase under fed conditions). As aprepitant is an antiemetic drug, reformulation as a nanosuspension and elimination of the food effect is significant as patient's compliance may have been limited if the drug should be administered with food (Merisko-Liversidge and Liversidge, 2011; Brough and Williams, 2013).
Tricor®, Abbott	Fenofibrate	2004	More flexible dosing regime. Life-cycle extension after patent expiration due to superior performing product (Shegokar and Müller, 2010).
Megace ES®, PAR Pharmaceuticals	Megestrol acetate	2005	Enhanced solubility, increase in the dissolution rate of the oral suspension and reduction of its volume and viscosity. Reduced bioavailability variation between fed/fasted state.
Invega Sustenna®, Janssen	Paliperidone palmitate	2009	Once monthly intramuscular extended release in injectable dosage form with physical stability for a two-year shelf life. As paliperidone palmitate is an atypical antipsychotic, the once monthly intramuscular injection facilitates patient compliance, a special concern for this population (Brough and Williams, 2013).

[a] Rapamune® was the first product reaching the market using wet milling technology and was a patented technology of Elan® drug technologies (known as Nanocrystals®)

Nanomilling is always conducted under controlled temperature, a crucial parameter especially for thermolabile drugs or drugs with low melting point. The increase of temperature during milling is considered as an additional mechanism behind the reduction of particle size. More specifically, the temperature-related stress relaxation due to intraparticle crack formation is followed by crack propagation and finally particle fracturing (Peltonen and Hirvonen, 2010).

The quality of the final nanosuspension is influenced by several critical parameters (Table 1.3), which should be selected carefully during the optimisation of the process.

Table 1.3 Critical process variables in nanomilling. Modified from (Peltonen and Hirvonen, 2010).

Process Variables	Range
Drug Amount	2-30% w/w
Amount of milling beads	10-50% w/v of the slurry
Size of milling beads	0.1-20.0 mm
Milling speed and duration	Low milling speed (80-90 rpm) & long milling time (1-5 days)
	High milling speed (1800-4800 rpm) & short milling time (30-60 min)

The milling beads are made of a hard and dense material such as yttrium-stabilised zirconium oxide, stainless steel, glass alumina, titanium or certain polymers as highly cross-linked polystyrene and methacrylate (Verhoff et al., 2003). The beads size may vary from less than 0.1 mm to 20 mm. As a general rule, the smaller the size of the milling beads the finer the nanoparticles produced, due to increased collision frequency between drug particles and beads. However, it has been reported that too small beads (e.g. 0.03 mm) may not be suitable for milling as they cannot generate sufficient energy for particle breakage when they impact with drug particles due to their light weight. Rotation speed is a parameter of critical importance. Low rotation speeds will lead to the rolling of the beads inside the milling vessel, impacting the material with insufficient force to achieve comminution. On the

other hand, too high speeds may result in the sticking of the beads on the walls of the milling vessel and therefore no milling will occur.

Nanomilling is especially beneficial for poorly soluble drugs with less than 200 μg ml^{-1} solubility, as well as for materials with high melting point and high molecular weight. It is characterised as a reproducible, cost-effective, scalable and quick process with little or no batch-to-batch variation (control over particle size) once the formulation and the process have been optimised. The most significant concern of nanomilling includes the risk of contamination of the final product with residues of the milling media. This risk, together with the risk of degradation, stability issues and microbial growth becomes even more increased when nanocrystals are obtained by low milling speeds and extended milling times.

Another concern associated mainly with dry milling is the mechanical activation of the particle surfaces above a critical pressure value or crystal defection concentration leading to the formation of local amorphous regions. The risk of material amorphisation may be linked with the main mechanism of particle size reduction during milling. In particular, friction and fracture are dominant phenomena during milling contributing to the transformation of about 90% of the mechanical energy into dislocation and distortion energy of the crystalline lattice. However, for wet milling unlike dry milling, the concern of amorphisation is reduced as the particles are formed in liquid media and amorphous regions may undergo recrystallisation (Kayaert and Van den Mooter, 2012).

1.7. Nanoparticles and pulmonary drug delivery

1.7.1. Applications and advantages of nanosuspensions in pulmonary drug delivery

The application of nanosuspensions in pulmonary drug delivery has been limited until recently. However, many of the advantages outlined in Section 1.6.1.1 can be extended to this route of administration. Additionally, nanosuspensions have been proposed as a formulation approach to increase the dissolution rate and thus absorption of poorly water-soluble inhaled corticosteroids such as fluticasone propionate and budesonide (Yang et al., 2008). Regarding pulmonary drug delivery, drug absorption and local bioavailability depends upon the fraction of deposited drug that dissolves in the lungs. Mucociliary clearance and absorption are two competing mechanisms and this can lead to bioavailability reduction for drug particles with low dissolution velocity (Forbes et al., 2015). Nanoparticle-based formulations have been found to promote more rapid absorption following inhalation of poorly water-soluble drug that have dissolution-limited drug absorption (e.g. beclometasone dipropionate, budesonide, itraconazole, fentanyl) (Tolman and Williams III, 2010). Britland et al. (2012) compared the bioavailability, emission characteristics and efficacy of a budesonide nanoparticulate formulation with those of a proprietary micronised suspension of the drug after delivery as a nebulised aerosol to a human airway epithelial culture cell line. For an equivalent dose, the budesonide nanosuspension achieved improved uptake, retention and efficacy in the culture cells.

Furthermore, there are two key advantages in using nanosuspensions instead of solution formulations for pulmonary delivery of drugs with poor aqueous solubility. Preparation of solutions requires the use of organic co-solvents while the need for co-solvents is limited or even non-existent for the production of nanosuspensions. As a result, the danger of potential co-solvent related toxicity is reduced (Chiang et al., 2009). In nanosuspensions, the drug concentration is not limited by the solubility in the vehicle, as is the case for solutions, allowing the delivery of higher doses in the lungs. Exploiting this advantage, Rundfeldt et al. (2013) prepared itraconazole nanosuspensions which achieved high and long-lasting lung tissue concentrations well above the minimum inhibitory concentration against *Aspergillus* species, when administered using standard mesh nebuliser

technology. The high concentration achieved indicates the potential of itraconazole nanosuspensions as a treatment for allergic bronchopulmonary aspergillosis in patients with cystic fibrosis, administered only once daily.

Finally, nanosuspensions can be used as formulations facilitating pulmonary drug discovery, as they are easy to dose with a syringe-type delivery device in preclinical animal studies (e.g. intratracheal instillation, Yang et al., 2008).

1.7.2. Delivery of nanocrystals as dry powders for inhalation: challenges and opportunities

Liquid nanosuspensions are associated with physical instability issues including sedimentation, creaming, crystal growth (also known as Ostwald ripening), aggregation and solid state transformation. A detailed review of the physical and chemical instability issues of drug nanoparticles has been provided by Wu et al. (2011). These instability phenomena make it difficult to ensure that the particle size of the nanosuspensions will remain the same upon storage. Moreover, nanosuspensions, due to their liquid media, are prone to microbial growth. On the other hand, solid dosage forms exhibit enhanced physical and chemical stability.

For pulmonary delivery the particles should have an aerodynamic diameter between 1-5 μm so as to deposit in the lungs. Therefore, delivery of individual nanoparticles to the lungs (with the exception of particles below 100 nm) appears to be problematic, as due to their submicron size, the probability of exhalation before deposition is increased (Byron, 1986; Rogueda and Traini, 2007). Moreover, nanoparticles tend to strongly aggregate upon aerosolisation under the normal airflow rates in passive DPIs and their cohesive nature makes their handling extremely difficult (Watts and Williams III, 2011). In order to overcome these limitations, the controlled agglomeration of nanoparticles to micron-sized clusters has been recently proposed as *"an approach to harmonise the advantages of nanoparticles with the aerodynamics of small microparticles so as to achieve an improved bioavailability and aerosolisation behaviour of the drug"* (El-Gendy et al., 2009). It is clear then, that solidifying nanosuspensions to respirable nanoparticle agglomerates of 1-5 μm, is a highly desirable strategy for administering nanoparticles effectively to the lungs using DPIs.

1.7.3. Formation of nanoparticle agglomerates as dry powders for inhalation

Spray drying, spray-freeze drying, freeze drying and aerosol flow reactor have been applied as solidification approaches for the preparation of inhalable micron-sized nanoparticle agglomerates with suitable aerodynamic properties for delivery to the lungs using DPIs (Fig. 1.16.).

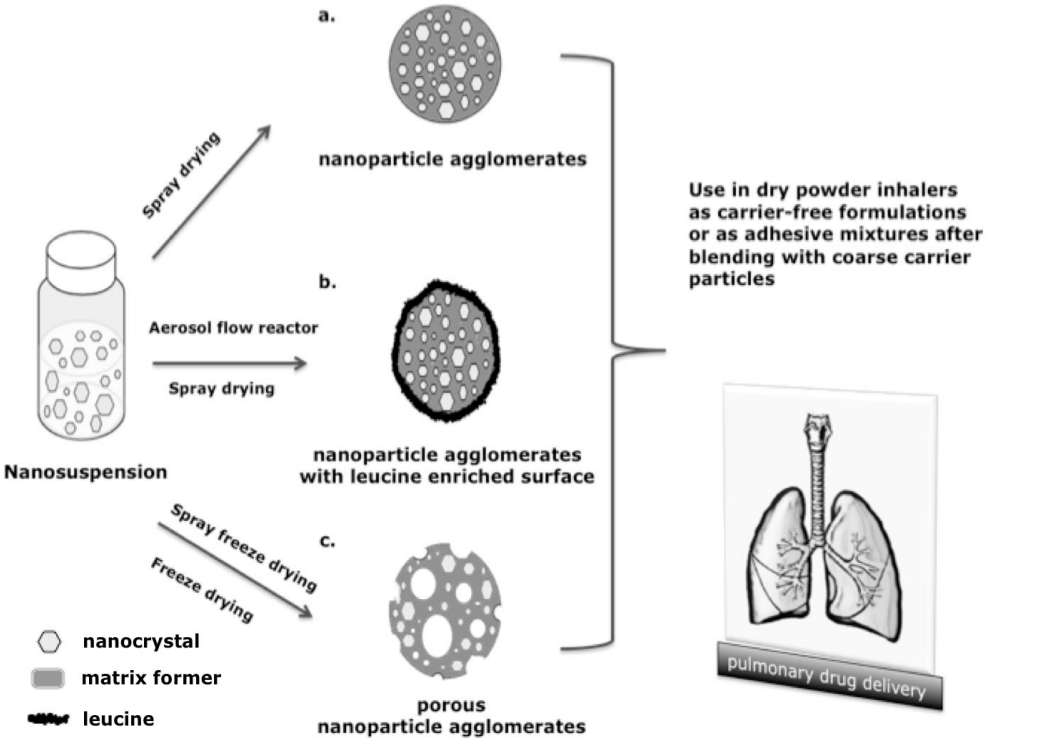

Figure 1.16 Schematic representation of the various solidification approaches for the preparation of inhalable micron-sized nanoparticle agglomerates.

1.7.3.1. Spray drying

Spray drying has a long tradition as a fundamental particle engineering technique for pulmonary drug delivery and until now the majority of reported studies on the development of inhalable particles by this methodology have focused on spray drying of drug solutions. But, as spray drying is a rapid solidification procedure, the obtained particles (at least from solution feed) are usually amorphous with the characteristic example being that of salbutamol sulfate after spray drying from aqueous solution (Fig.1.17a, Chawla et al., 1994). Amorphicity is regarded as a disadvantage for respirable particles as it is associated with the danger of recrystallisation

upon storage, which may influence adversely the stability, dissolution, absorption and aerosolisation efficiency of the product (Chow et al., 2007). Recently, a few studies on solidified nanosuspensions for the development of pulmonary formulations by applying spray drying have been reported.

Pilcer et al. (2009) prepared carrier-free respirable agglomerated nanoparticle formulations of tobramycin with enhanced dispersion properties by combining high-pressure homogenisation with spray drying. This can be considered as an attractive formulation approach for treating lung infections as a high dose can be delivered to the site of infection reducing the side effects related to systemic antibiotic administration.

Yamasaki et al. (2011) prepared nanosuspensions of ciclosporin A by anti-solvent precipitation (bottom-up technique) using a multi-inlet vortex mixer. The nanosuspensions were spray dried after the addition of different amounts of mannitol (Fig.1.17b), resulting in respirable nanoparticle agglomerates with enhanced fine particle fraction (FPF> 50%). The drug in the nanoparticle agglomerates was found to be in the amorphous state and this was attributed to the method of nanosuspension production rather than to the spray-drying step. The authors also investigated the effect of ciclosporin A to mannitol mass ratio on the dissolution rate and on the aerosolisation performance of the solidified nanosuspensions and concluded that mannitol, as a hydrophilic excipient, improved the dissolution rate of the drug, while it did not influence its aerosolisation behaviour.

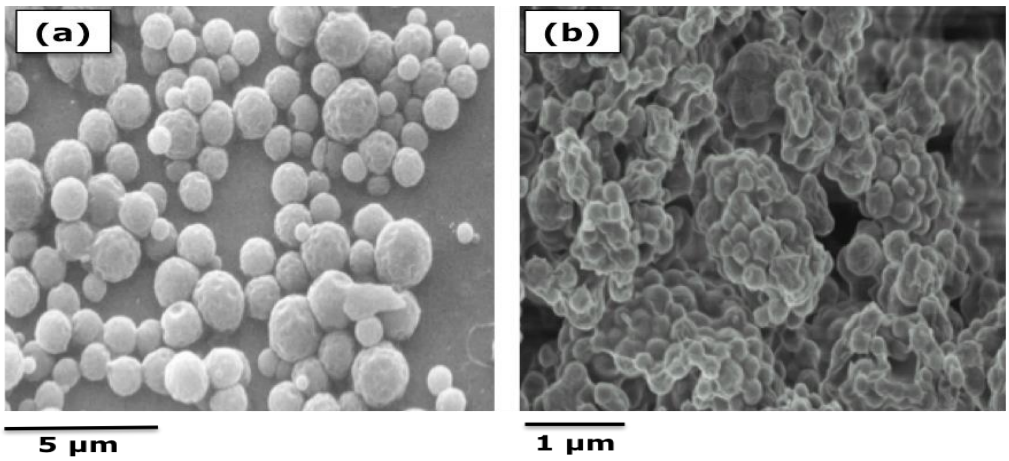

Figure 1.17 SEM images of (a) spray-dried salbutamol sulfate from 10% w/v aqueous solution (Chalwla et al., 1994) and (b) spray dried nanosuspension of ciclosporin A containing mannitol (1:0.5 mass ratio, Yamasaki et al., 2011).

Pomázi et al. (2013) developed respirable nanoparticle agglomerates of meloxicam embedded in mannitol and other adjuvants (polymers and L-leucine), by applying high-pressure homogenisation followed by spray drying. The presence of the amino acid L-leucine was found to enhance the aerosolisation of the nanoparticle agglomerates due to decreased particle-to-particle adhesion (Sou et al., 2011). The nanoparticle agglomerates of meloxicam were crystalline and exhibited enhanced in vitro aerosolisation (FPF > 53%; mass median aerodynamic diameter, MMAD < 3.52 μm) and dissolution performance. Similar results have been reported for nanoparticle agglomerates of itraconazole as a formulation approach for the treatment of pulmonary aspergillosis (Duret et al., 2012).

From the above, it can be summarised that spray drying of nanosuspensions has great potential for the production of solid formulations with predefined solid state and enhanced dissolution and aerosolisation properties that can be administered via a DPI.

1.7.3.2. Spray-freeze drying

Spray-freeze drying is an alternative technique to spray drying, which has been used for the preparation of thermolabile inhalable particles, especially proteins (Maa et al., 1999). In the spray-freeze drying process, the liquid feed is atomised by a nozzle and the atomised droplets are snap frozen in liquid N_2. The iced droplets are then lyophilized in order to remove the frozen solvent (water) via sublimation and obtain a powdery product. In comparison to spray drying, the spray-freeze drying is a low-temperature solidification process that produces porous particles (Mumenthaler et al., 1991).

Few studies have been published regarding the spray-freeze drying of drug nanosuspensions to produce particles suitable for inhalation. Cheow et al. (2011) prepared inhalable composite particles by spray-freeze drying suspensions of levofloxacin-loaded polycaprolactone (PCL) nanoparticles, in order to avoid problems associated with the low melting point of PCL and the limitation of elevated temperature use, which is inevitable in spray drying. Prior to the spray-freeze drying, adjuvants such as mannitol or polyvinyl alcohol (PVA) were added to the nanosuspensions to act as cryoprotectants and also to ensure redispersibility of the particles produced. Porous inhalable particles with suitable flowability and redispersibility were produced when

high adjuvant concentrations were used (Fig.1.18). Regarding pulmonary drug delivery, spray-freeze drying allows the preparation of particles with large geometric diameters but still having suitable aerodynamic properties due to their high porosity/low particle density (Cheow et al., 2011). In this way the poor flowability problems usually associated with inhalable particles can be overcome.

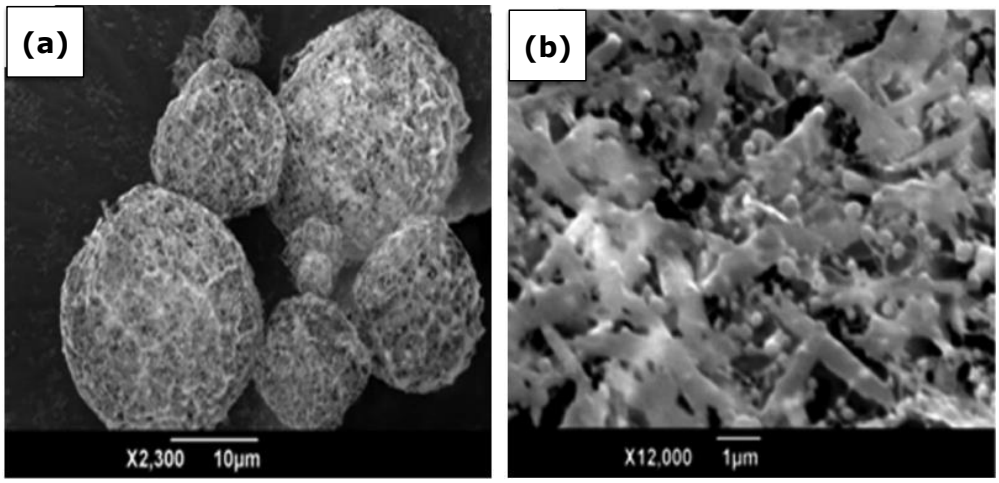

Figure 1.18 SEM images of (a) large, spherical and porous morphologies of levofloxacin-loaded PCL nanoparticles containing mannitol as an adjuvant, prepared by spray-freeze drying and (b) PCL nanoparticles dispersed in the porous mannitol matrix (Cheow et al., 2011).

1.7.3.3. Freeze drying

Freeze drying or lyophilisation is a classical process of removing water from high value products (e.g. antibiotics, enzymes, vaccines, etc.) without excessive damage, enhancing stability on storage and reconstitution by adding water, or other suitable aqueous vehicle, prior to use (Tang and Pikal, 2004). In freeze drying, the liquid solution or suspension is firstly frozen under atmospheric pressure and subsequently heated under vacuum to remove the ice crystals by sublimation. At the end of the process, a highly porous cake with low moisture content is obtained.

For the formation of respirable nanoparticle agglomerates, El-Gendy et al. (2009) employed freeze drying for the transformation of the nanosuspensions obtained by a controlled flocculation process (protocol under the name NanoClusters™, owned by Savara Pharmaceuticals).

Budesonide nanoparticle agglomerates prepared by this protocol, exhibited enhanced dissolution rate compared to the raw drug and had MMAD 2.1 ± 1.8 μm (mean ± SD) on aerosolisation, appropriate for deep lung deposition of the particles (Fig.1.19). The NanoClusters™ protocol has been applied for the preparation of nanoparticle agglomerates of various drugs, such as ciprofloxacin, paclitaxel, diatrizoic acid, nifedipine and fluticasone propionate (El-Gendy et al., 2009; Plumley et al., 2009; El-Gendy et al., 2011).

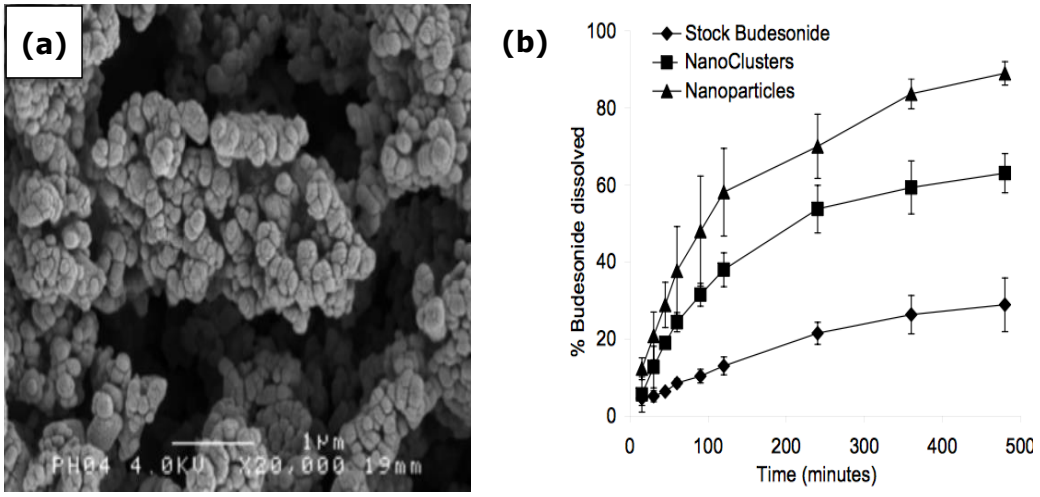

Figure 1.19 (a) SEM image of budesonide nanoparticle agglomerates prepared by the NanoClusters™ technology and (b) dissolution profiles budesonide from budesonide stock, nanoparticles and nanoparticle agglomerates (El-Gendy et al., 2009).

1.7.3.4. Aerosol flow reactor

The aerosol flow reactor, patented by Teicos Pharma (Finland), has been used for the solidification of nanosuspensions. It is a one-step continuous process involving the atomisation of a liquid feed into a carrier gas (usually N_2) for drying. More specifically, the liquid feed is atomised by an ultrasonic air-jet nebuliser and the droplets produced, suspended in the carrier gas, are directed into a heated tubular laminar flow reactor with constant temperature where evaporation takes place (Eerikainen et al., 2003).

Using the aerosol flow reactor technology, inhalable microparticles for the concomitant pulmonary administration (combination therapy) of budesonide and salbutamol sulfate have been prepared (Fig.1.20, Raula et al., 2013). Combination therapy has been found to be advantageous for the treatment of respiratory diseases by reducing the need for multiple therapies and as a

result it holds potential to improve patient adherence to medication and therapeutic outcomes. Especially for COPD, combination therapy enables simultaneous delivery of more than one drug to the same area of the lungs where they can exhibit synergistic action (Arun et al., 2012).

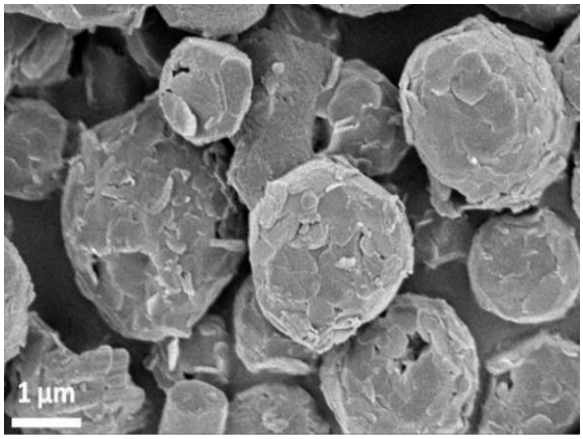

Figure 1.20 SEM image of L-leucine coated and encapsulated aerosol particles composed of budesonide nanocrystals embedded in mannitol matrix with salbutamol sulfate, prepared using the aerosol flow reactor (Raula et al., 2013).

The budesonide nanosuspension was prepared by wet milling. It was further diluted with an aqueous solution of salbutamol sulfate, mannitol and L-leucine and then solidified using the aerosol flow reactor. The obtained microparticles exhibited improved dissolution properties, with budesonide nanocrystals dissolving in 20 min and at the same rate as salbutamol sulfate, ensuring that the drugs will have a synergistic effect at the site of deposition/action. The microparticles also had enhanced aerosolisation efficiency with FPF: ≈ 50%, due to the leucine coating, which reduced the adhesion between particles.

1.8. RESEARCH HYPOTHESIS

Controlled agglomeration of nanoparticles to micrometre-sized clusters, which can "fall apart" once they reach the lung environment so as to reform nanoparticles, has been suggested as a way to combine the advantages of nanoparticles with the aerodynamics of microparticles for pulmonary drug delivery. Spray drying is a suitable technique for producing respirable particles. While spray drying of solutions may lead to the production of (partially) amorphous materials due to the rapid transition of droplets to the solid state, spray drying of material from a suspension often yields crystalline particles. Excipients such as mannitol and the endogenous amino acid L-leucine have been used in many studies for the engineering of dry powders for inhalation. Additionally, mannitol has been reported to exhibit excellent spray-drying properties as the size and shape of particles can be adjusted by changing the process parameters, while L-leucine is a commonly used aerosolisation enhancer. Therefore, it is hypothesised that it is possible to engineer respirable particles with a tailored crystalline form for a range of drugs with different physicochemical properties, by preparing nanoparticles and spray drying them in the presence of suitable excipients in order to produce inhalable microcomposite particles with predictable performance.

1.9. THESIS AIMS AND OBJECTIVES

The aim of this thesis is to develop a drug delivery platform based on wet milling and spray drying for the engineering of crystalline nanoparticle agglomerates suitable for inhalation, which can be applicable to a range of drugs with different physicochemical properties. To achieve this aim, the objectives of the thesis are:

- To engineer nanoparticle agglomerates using wet milling and spray drying for three model drugs, namely indometacin, ibuprofen and theophylline, which possess different physicochemical properties.
- To characterise the particles produced regarding their micromeritic properties, solid state, dissolution profile and aerosolisation behaviour.
- To investigate in a systematic way the effect of formulation parameters on the in-vitro performance of the nanoparticle agglomerates.

- To develop an initial "road map" to guide the selection of formulation and process parameters that should be adjusted in order to engineer inhalable nanoparticle agglomerates, by taking into account the physicochemical properties of the drug in question.

CHAPTER 2

NANOPARTICLE AGGLOMERATES OF INDOMETACIN

2. NANOPARTICLE AGGLOMERATES OF INDOMETACIN

2.1. INTRODUCTION

Several of the drugs used for the treatment of respiratory diseases exhibit poor aqueous solubility (antifungals, corticosteroids, oligopeptides and opioids) affecting their availability and retention in the lung tissue and subsequently their therapeutic efficacy, safety and dosing (Tolman and Williams, 2010). Reduction of drug particle size to the nano-range is considered an appropriate method to overcome the obstacle of poor water solubility (Brough and Williams, 2013).

The controlled agglomeration of nanoparticles to micro-sized clusters has been recently proposed as *"an approach to harmonize the features of nanoparticles with the aerodynamics of small microparticles so as to achieve an improved bioavailability and aerosolisation behaviour of the drug"* (El-Gendy et al., 2009).

The formation of nanoparticle agglomerates involves two processing steps: a) the preparation of a nanosuspension and b) the removal of liquid from the nanosuspension with simultaneous controlled assembling of the nanoparticles to micrometer-sized particles (agglomeration).

Considering the various nanosizing techniques, wet bead milling has been characterized as a reproducible, cost-effective and scalable way of producing nanosuspension (Möschwitzer, 2013). Especially for poorly water-soluble drugs, wet milling can take place in water avoiding the use of organic solvents, producing crystalline nanosuspensions due to the plasticizing effect of water on the potentially generated amorphous material, triggering recrystallisation (Kayaert and Van den Mooter, 2012).

For the water removal from nanosuspensions and controlled nanoparticle agglomeration, processes such as freeze drying and spray drying have been evaluated. The high energy consumption, long processing times and reduced flowability of freeze-dried products limit the use of freeze drying for the preparation of nanoparticle agglomerates in the respirable size range (Zhang et al., 2014). On the other hand, spray drying is a manufacturing technique of particular interest for respiratory drug delivery as particle characteristics (e.g. size, flowability, redispersibility and moisture content) can be controlled by formulation and process parameters (Van Oort and Sacchetti, 1996).

Prior to spray drying, the addition of matrix formers and surface-active agents may enhance the dissolution rate and the aerosolisation behaviour of the particles, respectively. More specifically, incorporation of mannitol as matrix former in nanoparticle agglomerates was found to improve their dissolution rate by preventing the irreversible aggregation of nanoparticles during drying (Chaubal and Popescu, 2008; Van Eerdenbrugh et al., 2008a; Yamasaki et al., 2011; Cerdeira et al., 2013). The amino acid, L- leucine, was found to act as an aerosolisation enhancer forming a coat (shell) on the dry particle surface, preventing particle fusion and therefore by preserving the individual particles as collected from the spray dryer (Seville et al., 2007; Sou et al., 2011).

In this chapter, the use of wet bead milling followed by spray drying was investigated for the preparation of inhalable nanoparticle agglomerates. Three poloxamers selected as amphiphilic, non-ionic copolymers differing in their molecular domains, were used for the production of nanosuspensions. In this way the effect of stabiliser characteristics (total molecular weight and molecular weight of the hydrophilic polyoxyethylene, EO, moiety) on the nanosuspension formation will be elucidated. Besides poloxamers, D-α-tocopherol polyethylene glycol succinate (TPGS) was selected as a stabiliser for comparative purposes, since it has been reported as an efficient stabiliser for drugs with different functional groups and for different pharmaceutical applications (Van Eerdenbrugh et al., 2008b; Duret et al., 2012;). Moreover, the effect of mannitol and L-leucine addition during the spray drying of nanosuspensions on the solid state, dissolution rate, redispersibility (reformation of nanoparticles after rehydration) and aerosolisation efficiency of the nanoparticle agglomerates will be investigated. Indometacin was selected as a model, poorly water-soluble drug, prone to polymorphic transformations and amorphisation during milling and spray drying (Karmwar et al., 2012; Legendre and Feutelais, 2004; Martena et al., 2012).

2.2. MATERIALS

Indometacin (IND, LKT Laboratories, USA) with a volume mean diameter $D_{4,3}$: 54.10 ± 8.12 µm was used. Poloxamers: 407, 188 and 184 (Pluronics®: F127, F68, and L64 respectively) from BASF Co. (Ludwigshafen, Germany) and D-α- tocopherol polyethylene glycol 1000 succinate (TPGS, Sigma Aldrich Co., St. Louis, USA) were used as stabilisers. Mannitol (Pearlitol 160C, Roquette Freres, Lestrem, France) and L- leucine (Sigma®) were used as matrix formers of the nanoparticle agglomerates. The chemical structures of indometacin, stabilisers and matrix formers are given in Fig. 2.1. and their physicochemical properties are summarised in Table 2.1. Hyclone™ water for injection quality water (Thermo Scientific, UK) was used for the preparation of nanosuspensions. Potassium dihydrogen phosphate and sodium hydroxide (from Fisher Scientific UK, Loughborough, UK) and deionised water were used for the preparation of the dissolution medium. Ethanol (96% v/v, analytical reagent grade) and acetonitrile (HPLC grade) both from Fisher Scientific UK, Loughborough, UK and trifluoroacetic acid (TFA, Sigma Aldrich Co., St Louis, USA) were used for the HPLC analysis.

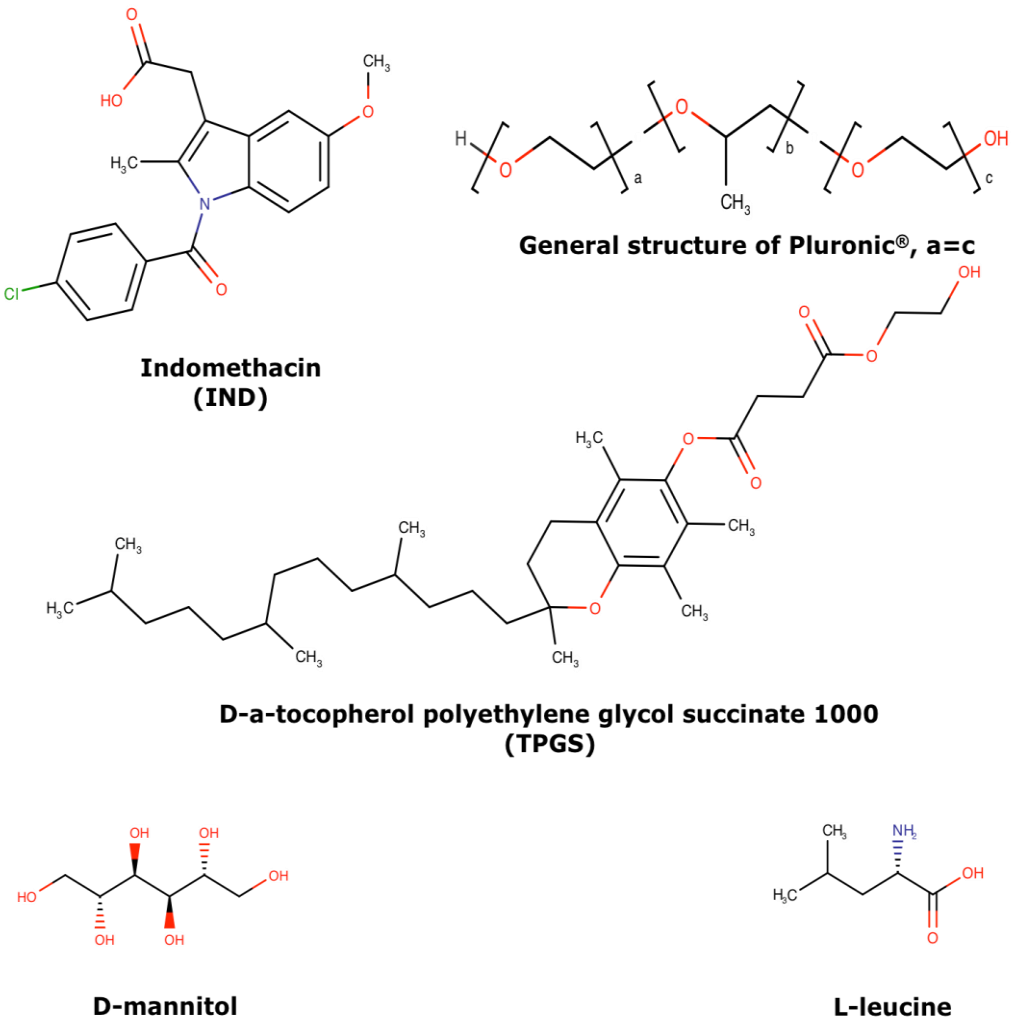

Figure 2.1 Chemical structures of indometacin, stabilisers and matrix formers.

Table 2.1 Physicochemical properties of indometacin, stabilisers and matrix formers.

Compound	Molecular weight ($g\ mol^{-1}$)	Melting point (^oC)	Aqueous solubility
Indometacin	357.79	159 (γ-form)[a]	16 ± 1 $\mu g\ mL^{-1}$ [b]
Mannitol	182.17	166-168[c]	Soluble[c]
L-leucine	131.17	145-148 (sublimation) 293-295 (decomposition)[c]	Soluble[c]

Stabiliser	Properties (provided by the manufacturers)						
	Molecular weight ($g\ mol^{-1}$)	Melting point (^oC)	PO units	EO units	PO/EO	PO ($g\ mol^{-1}$)	HLB
Pluronics® F127	12600	56	65	2 × 100	0.33	3780	18-23
Pluronics® F68	8400	52	29	2 × 76	0.19	1680	>24
Pluronics® L64	2900	16	30	2 × 13	1.15	1740	12-18
TPGS 1000	1513	38	-	-	-		13

[a] Legendre and Feutelais, 2004, [b] Van Eerdenbrugh et al., 2008b, [c] Rowe et al., 2012
PO = propylene oxide, EO = ethylene oxide, HLB = hydrophilic- lipophilic balance

2.3. METHODS

2.3.1. Solubility measurements

The solubility of indometacin in 0.5% w/v stabiliser solutions (corresponding to that of nanomilling) and distilled water was measured. The solvents were placed in stoppered vials and excess indometacin was added and stored at 25°C, in a shaking water bath for 24 h. The saturated solutions were filtered through a 0.1 μm disposable syringe filter (Millex® Durapore®) to separate the undissolved drug and the amount of drug dissolved was assayed by HPLC as described below in drug content determination. All determinations were made in triplicate.

2.3.2. Preparation of nanosuspensions

Nanosuspensions were prepared by wet bead milling using a planetary micro mill (Pulverisette 7 Premium, Fritsch Co., Germany) with two grinding bowls of 80 mL (Fig. 2.2). 2 g of IND and the stabiliser (10% w/w of IND) were added in each milling bowl containing 100 g of milling beads (YTZ grinding beads, 0.4 mm, GSK Comet) and 40 mL of sterile purified water. Rotation speed of bowls (600 rpm), milling duration (12 cycles of altered bowl rotation direction) and stabiliser concentration (10% w/w of IND) were selected based on preliminary experiments. Each milling cycle comprised of 15 min rotation followed by 3 min pause. In order to cool down the milling vessels and avoid overheating of the instrument's rotors, an additional 30 min pause followed the completion of 3 milling cycles. At each pause, the nanocrystal size was determined and at the end of the milling procedure, the nanosuspensions were left to cool to room temperature. The nanosuspensions were removed from the milling pots using transfer pipettes with openings smaller than the size of the milling beads. In the case of the nanosuspensions which were further diluted with an aqueous solution prior to spray drying (Section 2.3.4), part of this solution was used to repeatedly rinse the beads in order to increase the recovery of the nanosuspensions.

Figure 2.2 Planetary micro mill Pulverisette 7 premium line. Adapted from Fritsch, 2007.

2.3.3. Characterisation of nanosuspensions

Dynamic light scattering (DLS) and transmission electron microscopy (TEM) measurements were carried out during the milling process, at each pause, for monitoring the particle size reduction and the final size of the nanocrystals. Physical short-term stability of the nanosuspensions after 7 days was also determined by DLS.

2.3.3.1. Dynamic light scattering (DLS)

Malvern Nano ZS (Malvern Instrument, UK) was used for size measurements yielding the intensity-weighted mean diameter of the bulk population (z-average) and the polydispersity index (PI) as a measure of the width of size distribution. 20 µL of nanosuspension was diluted with 10 mL of saturated IND solution, prepared by filtration of a suspension through a 0.22 µm disposable syringe filter (Millex® sterile) to avoid extensive dissolution and then was shaken vigorously for 30 s by hand before being transferred into disposable sizing cuvettes. The measuring parameters were: dispersant reflective index of 1.338 and viscosity value of the dispersion medium 0.89 cP. The measurement was performed in triplicate, at 25°C, and mean value and standard deviation were calculated.

2.3.3.2 Transmission electron microscopy (TEM)

One drop of nanosuspension was placed on a 300 mesh copper grid and stained with 1% uranyl acetate. The liquid was then allowed to dry and examined by TEM (Philips Electron Optics BV, Netherlands).

2.3.4. Preparation of nanoparticle agglomerates

The obtained nanosuspensions were solidified by spray drying either immediately after preparation as collected without any further pre-treatments or after diluting 25 mL of nanosuspension with 75 mL aqueous solution of matrix formers (mannitol and L- leucine at contents of 120% and 16% w/w of IND, respectively). Spray drying was performed using a laboratory scale spray dryer (Mini B-290, Buchi Labortechnik Ab, Flawil, Switzerland) fitted with a high performance cyclone (Fig. 2.3). On the basis of preliminary 'one-factor-at-a-time' experiments, inlet temperature of 130 ^{o}C, outlet temperature of 42 ± 2 ^{o}C, feed rate of 5 mL min^{-1} and atomizing gas flow rate of 0.5 L s^{-1} were selected. The collected nanoparticle agglomerates were stored in a desiccator over silica gel until testing.

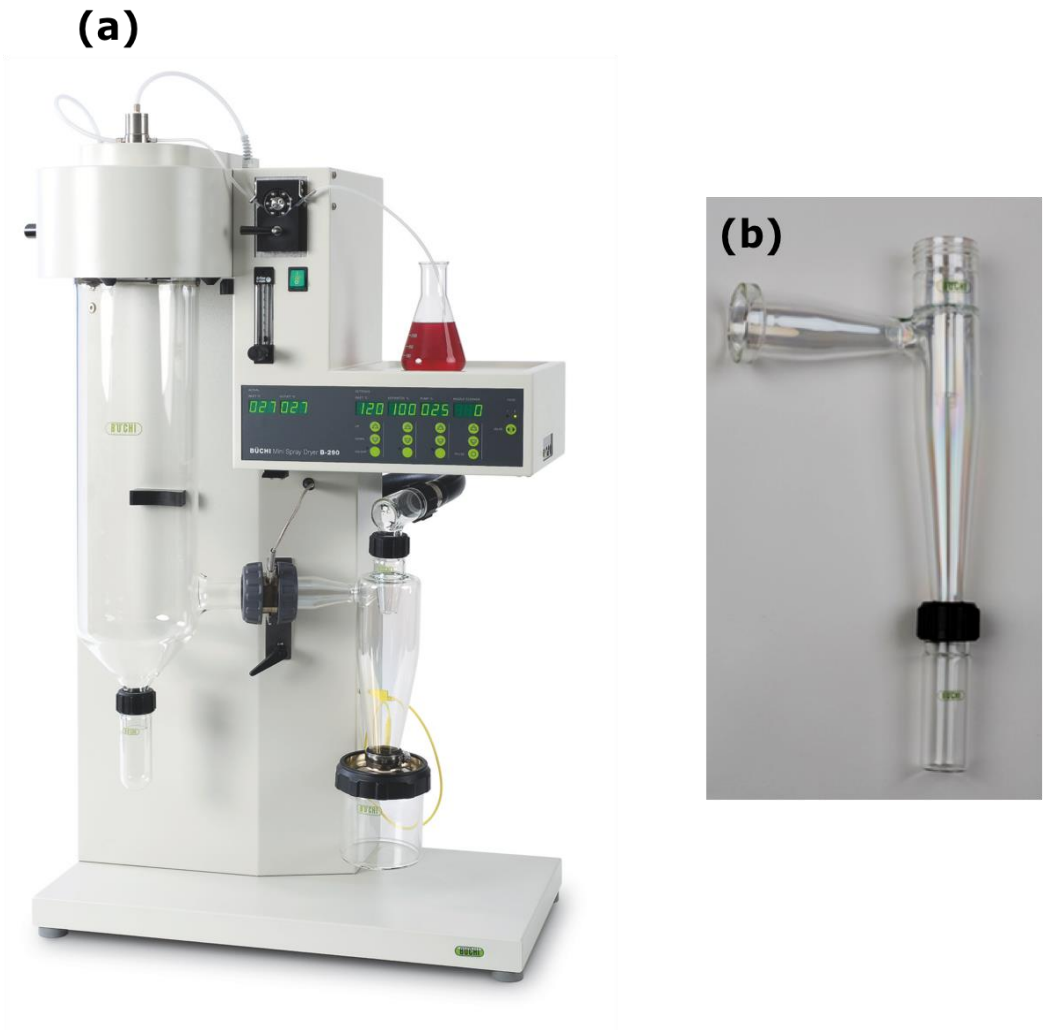

Figure 2.3 (a) Büchi Mini Spray Dryer B-290 and (b) high performance cyclone. Adapted from Büchi, 2010.

2.3.5. Characterisation of nanoparticle agglomerates

The nanoparticle agglomerates were characterized with respect to: surface morphology by SEM; particle size distribution (PSD) by laser diffractometry; solid state form by X-ray powder diffractometry (XRPD) and differential scanning calorimetry (DSC); drug loading and dissolution testing by HPLC analysis of indometacin content; redispersibility by DLS after dispersion in water; and in- vitro aerosol performance using the next generation impactor (NGI).

2.3.5.1. Scanning electron microscopy (SEM)

Samples were placed on double-side electroconductive adhesive tape, which was fixed onto an aluminium stub and then sputter-coated with gold under

argon atmosphere to a thickness of 10 nm (Quorum model 150). SEM micrographs were taken using a FEI Quanta 200 FEG ESEM (Netherlands), at 5.00 kV.

2.3.5.2. Laser diffraction

The particle size distribution of the samples (n=3) was determined using a HELOS/ BR laser diffractometer (Sympatec GmbH, Germany) which was fitted with the micro-dosing unit ASPIROS and the dry disperser RODOS. Samples were placed in the feeder and pressurised air at 4 bar was used to disperse them in the measurement chamber while the feeding velocity kept constant at 50 mm s^{-1}. A pressure of 4 bar was selected based on preliminary studies where increase of the primary pressure from 2 to 4 bar did not change the particle size distributions of the samples indicating that there is no particle de-agglomeration at elevated pressure. An R2 lens detector (0.25- 87.5 μm) and the particle size distribution (PSD) analysis software Windox 5 were used. The d_{10}, d_{50} and d_{90} particle sizes (i.e. the size in microns at which 10%, 50% and 90% of the particles are smaller) were recorded.

The particle size distribution of the starting materials was measured with Malvern Mastersizer 3000 equipped with a dry sampling system (Aero S, Malvern Instruments, UK), as the particle size range covered by this laser diffractometer is 0.1-3500 μm. The standard operating conditions used were: refractive index: 1.52, vibration feed rate: 25%, measurement time: 5 s, dispersive air pressure: 4 bar.

2.3.5.3. X-ray powder diffractometry (XRPD)

XRPD patterns were obtained with a bench-top diffractometer (Rigaku Miniflex 600, Japan) to assess crystallinity. Cu Kα radiation at 15 mA and 40 kV with a step of 0.02 deg and a speed of 5 deg min^{-1} was used, covering a 2 θ of 3-40 °. Miniflex Guidance was the analysis software.

2.3.5.4. Differential scanning calorimetry (DSC)

DSC was performed using a TA DSC Q200 calorimeter at constant pressure previously calibrated with indium. Weighted powder samples (1-3 mg) were sealed into crimped standard aluminium pans (TA) and heated under

nitrogen flow (50 mL min^{-1}) from 25 °C to 180 °C at a heating rate of 10 °C min^{-1}.

2.3.5.5. Drug loading

5 mg of nanoparticle agglomerates was dissolved in 100 mL ethanol 96% v/v and indometacin concentration was assayed using a HPLC system (Agilent 1100 Series, Agilent technologies, Germany). The stationary phase was a Synergi 4u Polar- RP 80 A (250 x 4.60 mm, 4 micron) column (Phenomenex Co., California, USA) kept at 40 °C. The mobile phase was composed of acetonitrile and aqueous trifluoroacetic acid solution (0.1% v/v) at 60/40 volumetric ratio. The mobile phase flow rate was 1 $mLmin^{-1}$, the injection volume was 20 µL and the detection wavelength 318 nm. The retention time for indometacin was 6.1 min. The correlation coefficient of the calibration curve was R^2: 0.9995 for a concentration range of 5-350 µg mL^{-1}, indicating acceptable linearity. Drug loading measurements were conducted in triplicate for each formulation (n=3).

2.3.5.6. Redispersibility

For the measurement of redispersibility, around 100 mg of each spray-dried powder was added in 10 mL of water in a glass vial and vortexed for 30 s. Redispersibility index (*RDI %*) was determined according to Yue et al., 2013:

$$RDI\% = \frac{z-average}{z-average_0} * 100 \quad \ldots . \quad \text{Equation 2.1}$$

where, *z-average*$_0$ is the intensity-weighted mean particle diameter of the nanosuspensions prior to spray drying measured by PCS and *z-average* is the corresponding value of nanosuspension reconstituted from nanoparticle agglomerates upon rehydration. A RDI% value close to 100% would mean that the spray-dried nanosuspensions can be completely reconstituted to the original particle size of liquid nanosuspensions upon rehydration.

2.3.5.7. *In-vitro* dissolution testing

A paddle method was employed using the USP apparatus type II (Pharma Test, Heinburg, Germany), at 37°C and 100 rpm stirring speed. The dissolution medium was 900 mL phosphate buffer BP, pH: 6.8. Weighted amounts of formulations corresponding to about 75 mg of IND were filled in gelatin capsules (size 2). Sink conditions were maintained during the

dissolution tests (solubility of IND in phosphate buffer pH: 6.8 is 0.835 mg ml^{-1}, Bahl and Bogner, 2008). At specific time intervals up to 60 min, 5 mL of dissolution medium was withdrawn, filtered through 0.1 µm disposable syringe filter and placed in HPLC vials for assay, while immediately being replaced with 5 mL of fresh medium. The HPLC conditions for the assay were as described in section 2.3.5.5. Dissolution tests were made in triplicate for each formulation (n=3). The percentage of dissolution efficiency (DE%), as a parameter of the extent of dissolution, was calculated from the ratio of the area under the curve up to time (t), to that of the rectangle described by 100% dissolution at the same time as follows:

$$\%DE = \left(\frac{\int_0^t y.dt}{y_{100}.t}\right).100 \qquad \ldots . \qquad \text{Equation 2.2}$$

where, *y* is the percentage of drug dissolved (Khan, 1975). Also, the mean dissolution time (*MDT*), as a parameter of the rate of dissolution, was calculated:

$$MDT = \frac{\sum_{n-1}^{n} t_{mid}\Delta \mathrm{M}}{\sum_{i-1}^{n}\Delta \mathrm{M}} \qquad \ldots . \qquad \text{Equation 2.3}$$

Where, *i* is the dissolution sample number, *n* is the number of dissolution times, t_{mid} is the time at the midpoint between times t_i and t_{i-1}, and ΔM is the amount of drug dissolved (mg) between times t_i and $t_{i-1.}$ (Brockmeier et al., 1983).

2.3.5.8. *In-vitro* aerosol performance

Deposition profiles were determined with Ph. Eur. Apparatus E (Next Generation Impactor, NGI, Copley Instruments Ltd, UK) connected to a high-capacity vacuum pump (Model HCP5, Copley Instruments Ltd, UK) (Fig. 2.4). Prior to use, the impaction cups in each of the seven stages were coated with 1% v/v silicone oil in hexane, and allowed to dry for 1 h, in order to minimize particle bounce and entrapment of particles between the stages. The final stage of the impactor was fitted with a fibreglass filter (nylon 0.45 µm, Millipore, UK). The actual flow rate was measured using a calibrated flow meter (Flow Meter Model DFM 2000, Copley Instrument Ltd, UK) prior to each run, to ensure that a flow at 60 L min^{-1} was achieved.

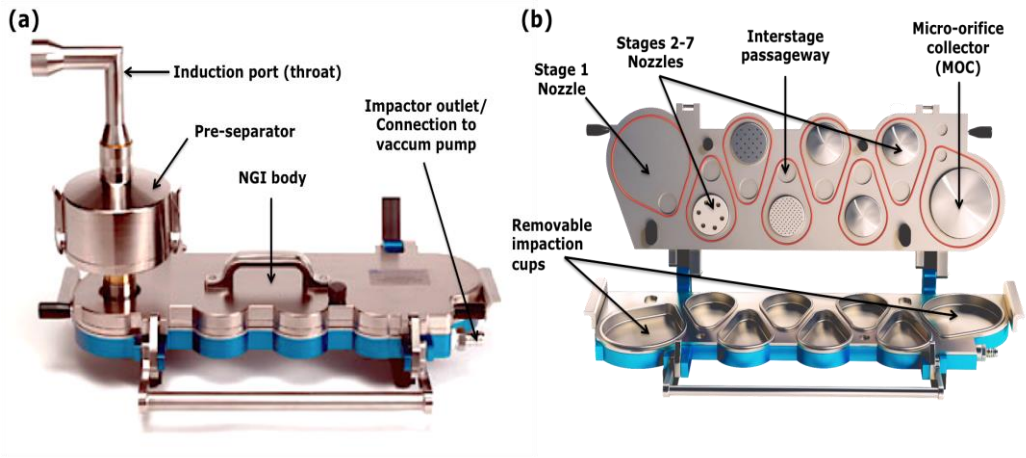

Figure 2.4 The Next Generation Impactor apparatus (a) closed with induction port and pre-separator attached and (b) open showing component parts. Adapted from Copley, 2007.

Gelatin capsules (size 3) were filled with accurately weighted amounts of product corresponding to about 15 mg of IND and tested at 60 L min^{-1} for 4 s. The inhaler device (Cyclohaler®) was connected to the impactor via an airtight rubber adaptor. The capsules were discharged into the NGI and after dispersion the powder deposited on each inhaler and NGI part was collected by exhaustively washing with ethanol 96% v/v, transferred into volumetric flasks and made up to volume and assayed. *In-vitro* aerosol performance tests were conducted in triplicate for each formulation (n=3). The HPLC conditions for the assay were identical to those for drug content determination. To characterise the aerosol performance the following parameters were determined: the emitted fraction (EF%) was calculated as the ratio of the sum of drug mass depositing in the mouthpiece, induction port, pre-separator and impactor stages (1 to MOC) to the loaded dose. The fine particle fraction (FPF %) was the ratio of the drug mass depositing on stages 2 to MOC to the loaded dose (initial mass of drug loaded in the capsules). The fine particle dose (FPD) was calculated as the ratio of mass deposited on stage 2 to MOC, to the number of doses (n=3). The mass median aerodynamic diameter (MMAD) defined as the median particle diameter of the formulation deposited within the NGI; and the geometric standard deviation (GSD) determined as the square root of the ratio of the particle size at 84.13^{th} percentile to that of 15.87^{th} percentile were calculated. Both MMAD and GSD were determined from the linear region in the plot of the cumulative mass distribution versus the logarithm of aerodynamic diameters.

2.3.6. Statistical data analysis

The analysis of variance (one-way ANOVA) with Tukey's multiple comparison test was carried out to evaluate differences between the mean values using Prism 6 (GraphPad Software, Inc., USA). Probability values less than 0.05 were considered as indicative of statistically significant differences.

2.4. RESULTS AND DISCUSSION

2.4.1. Preparation and characterization of nanosuspensions

All the stabilisers used in this study (except Pluronic® L64) generated nanosuspensions with a mean particle size around 260 nm after 12 cycles of milling (Fig. 2.5). Longer milling times resulted in finer nanosuspensions with narrow particle size distribution indicated by smaller polydispersity index (PI) values. Furthermore, the achieved rate of size reduction (breakage rate) was reduced with the milling duration but in a manner dependent on the nature of the stabiliser used (Fig. 2.6.). TPGS generated nanoparticles of 263 nm even from the first 45 min of milling, followed by Pluronic® F68 and F127. More specifically, Pluronic® F127 with the higher molecular weight, Table 2.1, exhibited a slower rate of size reduction (mean particle size of 505 nm after 45 min of milling) compared to small molecular weight stabilisers such as TPGS or Pluronic® F68 (mean particle sizes of 263 and 363 nm after 45 min of milling, respectively). This suggests a trend between the molecular weight of the polymer and the rate of size reduction which may be explained by the less kinetically restricted adsorption process of the low molecular weight stabilisers compared to those of higher molecular weight (Lee et al., 2008; Rachmawati et al., 2013).

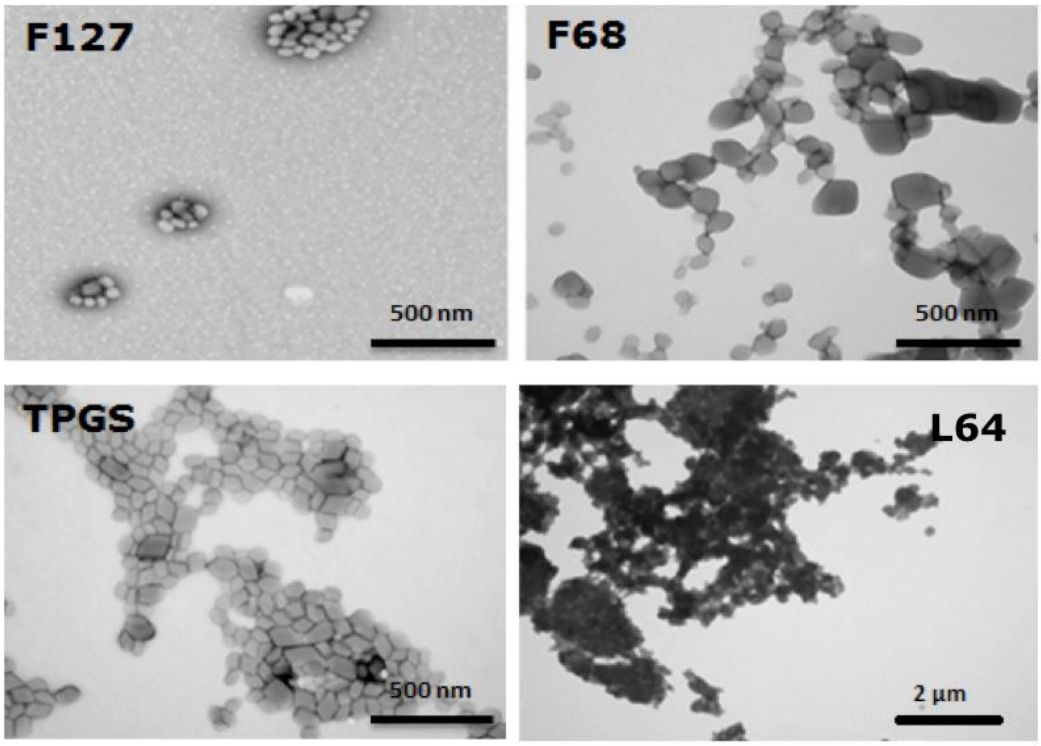

Figure 2.5 TEM images of liquid nanosuspensions prepared with different stabilisers (10% w/w IND) after 180 min milling.

The initial faster breakage of IND crystals, from 54.10 ± 8.12 μm (volume mean diameter of raw indometacin crystals) to below 500 nm during the first 45 min of milling, for all the nanosuspensions prepared (apart from that with liquid Pluronic® L64) can be attributed to the existence of more cracks and crystal defects in the larger crystals which propagate breakage relatively easily. After this initial fast breakage stage, size reduction continues but at a remarkably slower rate until a plateau is reached (Fig. 2.6). The slower size reduction rate and achievement of the plateau (steady state) suggests that in the later stages of milling, abrasion becomes the main mechanism behind size reduction as shear stress of nanosuspensions increases with decreasing particle size (Peukert et al., 2003; Plakkot et al., 2011).

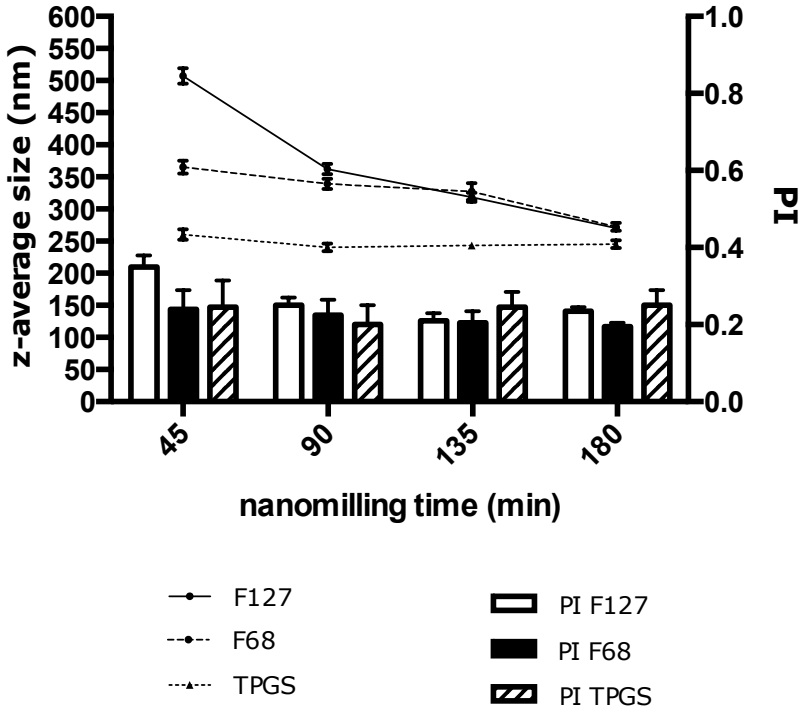

Figure 2.6 Mean nanoparticle size (hydrodynamic diameter) and polydispersity index (PI) of nanosuspensions of indometacin with increasing wet milling time (mean ± SD, three samples from one batch of each nanosuspension were analysed).

The size reduction dependence on the stabiliser's nature and the existence of similar nanoparticle size plateau for different stabilisers (steady state), may be explained by the fact that the fracture of drug crystals depends on two groups of factors based on: the transfer of mechanical energy and the intrinsic physico-mechanical properties of the crystalline material (Lee, 2003). For the transfer of mechanical energy, factors such as stabiliser type, slurry viscosity, size of milling beads and milling speed are involved, influencing particle size distribution as a function of time (size reduction rate) but not the steady state particle size of the nanoparticles obtained. The latter mainly depends on the intrinsic physico-mechanical properties of the drug crystals such as brittleness, yield stress, plasticity and elasticity (Lee, 2003; Plakkot et al., 2011).

The inability of Pluronic® L64 to stabilise the indometacin nanosuspensions seems to be interesting, especially when compared with the high success rate of Pluronic® F68 in stabilising nanosuspensions of indometacin (Fig. 2.5) and of other poorly water-soluble drugs. Pluronics® L64 and F68 have approximately the same molecular weight of the hydrophobic poly-

oxypropylene (PO) segment (1680 and 1740 g mol^{-1}, respectively). However, L64 has a small hydrophilic poly-oxyethylene (EO) segment of 1160 g mol^{-1}, while F68 has a EO segment of 6720 g mol^{-1}, Table 2.1. Therefore the poor stabilisation ability of L64 can be attributed to its small EO segment indicating the importance of both segments for the stabilisation of drug nanocrystals. While the hydrophobic PO segment adsorbs and adheres on the hydrophobic drug crystal surface the hydrophilic EO segment has to be of sufficient size to protrude from the particle size in order to give suitable stabilisation. The difference in stabilisation efficiency of Pluronics® L64 and F68, can be explained by considering previous studies on the adsorption and coating thickness of different types of Pluronics® on polystyrene latex particles (Carstensen et al., 1991; Illum et al., 1987). According to Carstensen et al. (1991) the coating thickness of Pluronic® L64 and F68 on polystyrene particles (60 nm hydrophobic particles) was 2.4 and 7.6 nm, respectively. The lower coating thickness of Pluronic®L64 was explained by the fact that its EO segment protrudes to a smaller extent from the particle surface than the EO segment of Pluronic® F68. In the case of indometacin nanosuspensions, L64 due to its lower coating thickness cannot make the hydrophobic drug surface sufficiently hydrophilic so as to secure steric stabilisation and as a result aggregation occurs. Liu et al. (2015) reported similar results after studying the affinity of polymers onto drug surfaces using surface plasmon resonance and contact angle measurements.

No significant change ($p > 0.05$) was found in mean hydrodynamic diameter of the nanocrystals after one-week storage at room temperature. The one week can be considered as a reasonable time period between the procedures of wet bead milling and spray drying and the short term physical stability of the nanosuspensions is thus considered adequate.

2.4.2. Characterisation of nanoparticle agglomerates

For the evaluation of the nanoparticle agglomerates prepared with different stabilisers, the particle size distribution results are given in Table 2.2 and SEM images in Figure 2.7. Figures 2.8 and 2.9 show the XRPD patterns and DSC curves, respectively, of the raw materials used and nanoparticle agglomerates prepared, while Table 2.3 summarises the contents of nominal components and assayed IND together with the calculated drug loading efficiency (%) and the parameters of reconstitution ability. The *in-vitro*

dissolution parameters of nanoparticle agglomerates are listed in Table 2.4, while Figure 2.10 summarizes the corresponding drug dissolution profiles. Finally, the parameters of *in-vitro* aerosol performance of nanoparticle agglomerates are given in Table 2.5 and their drug deposition profiles are presented in Figure 2.11.

2.4.2.1. Particle size and morphology

The SEM images (Fig. 2.7) reveal the spherical and composite structure of the nanoparticle agglomerates that consist of micron-sized clusters of nanoparticles. Also, they show that the nanoparticles were generally 200-400 nm in diameter, confirming the results of PCS and TEM for the original nanosuspensions.

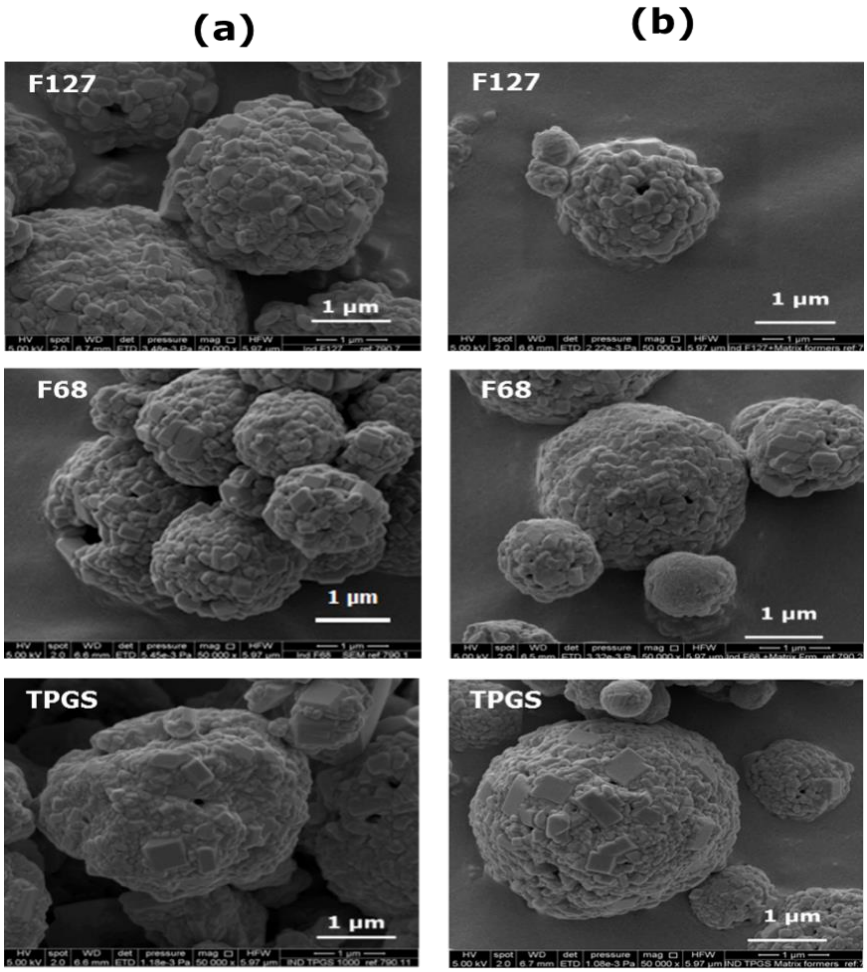

Figure 2.7 SEM images of nanoparticle agglomerates of indometacin: (a) without and (b) with matrix formers prepared with different stabilisers (10 % w/w of IND).

From the particle size distribution results (Table 2.2) it is seen that nanoparticle agglomerates without matrix formers (mannitol and L-leucine) have significantly higher median diameter d_{50} compared to the nanoparticle agglomerates containing matrix formers ($p < 0.05$). Moreover, the nanoparticle agglomerates without matrix formers exhibit d_{90} values higher than the size range that is suitable for pulmonary drug delivery (0.5-5 μm). This can be attributed to the presence of some secondary agglomerates (nanoparticle agglomerates attached together).

Table 2.2. Particle size distribution (d_{10}, d_{50} and d_{90}, μm) of nanoparticle agglomerates of indometacin prepared with different stabilizers (10% w/w of IND) at 4 bar dispersion pressure and 50 mm s^{-1} feeding velocity (mean ±SD, n=3).

Stabiliser	Matrix Formers	Particle size distribution d_{10}, d_{50}, d_{90} (4 bar, 50 mm s^{-1})		
		d_{10} (μm)	d_{50} (μm)	d_{90} (μm)
Pluronic® F127	without	1.63 ± 0.02	4.03 ± 0.03	47.96 ± 1.65
	with	0.89 ± 0.04	2.08 ± 0.02	3.88 ± 0.04
Pluronic® F68	without	1.35 ±0.05	3.37 ± 0.11	6.96 ± 1.50
	with	1.06 ± 0.02	2.49 ± 0.02	4.68 ± 0.11
TPGS	without	1.26 ± 0.02	4.03 ± 0.03	18.03 ± 9.3
	with	0.87 ± 0.02	2.17 ± 0.08	3.98 ± 0.10

2.4.2.2. Solid state characterisation

The solid state properties of the nanoparticle agglomerates were examined as these are important for drug stability, solubility, dissolution and therapeutic efficacy and may change for the drug during milling and for both the drug and the matrix formers during spray drying. The XRPD patterns (Fig. 2.8) showed that for indometacin raw material the diffraction angles observed are characteristic of the γ- form (2 theta: 11.6^o, 16.8 ^{o}, 19.6 ^{o}, 21.8^o, 26.6^o) (Legendre and Feutelais, 2004), while for spray-dried mannitol, XRDP patterns are characteristic for the β- form (2 theta: 10.6^o, 14.7^o, 16.9^o, 21.2^o, 23.9^o, 29.5^o) (Hulse et al., 2009). Figure 2.8a did not show any apparent difference between pure indometacin and the nanoparticle agglomerates prepared with different stabiliser and without matrix formers, while for the nanoparticle agglomerates containing matrix formers, the diffraction patterns (Fig. 2.8b) were essentially a summation of the patterns of indometacin and spray-dried mannitol and L-leucine with the expected relative reduction in intensities. Reduction in the intensities, as well as broadening of the peaks observed, for the patterns of both nanoparticle agglomerates with and without matrix formers compared to the patterns of the starting materials, can be attributed to the smaller size of nanoparticles, the dilution of the particles with stabilisers and strain caused by the milling process (Hecq et al., 2005; Van Eerdenburgh et al., 2008b).

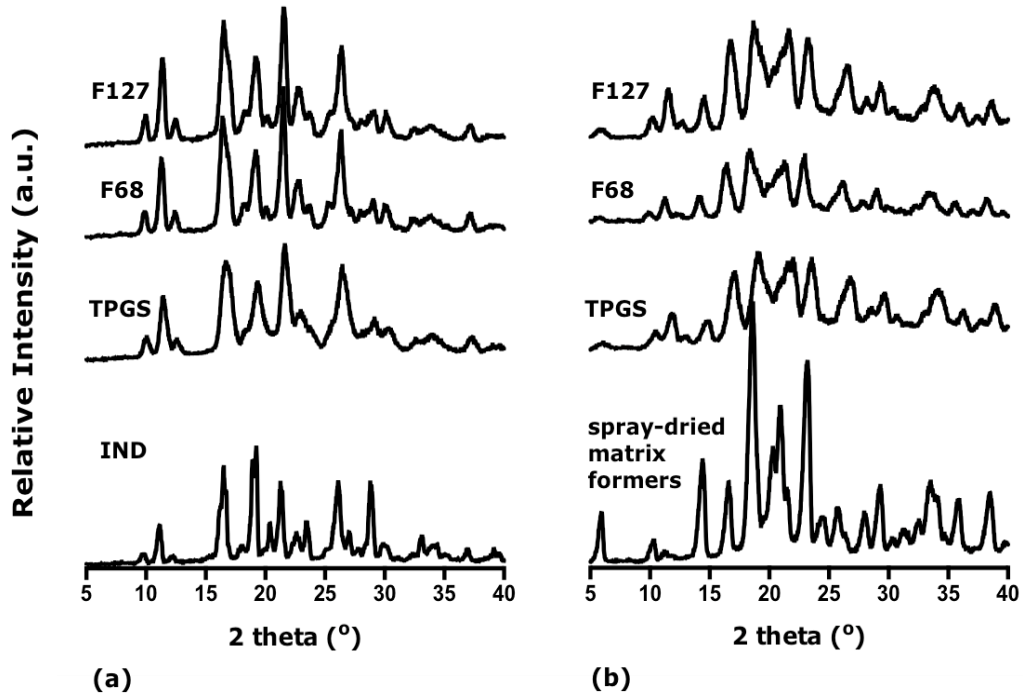

Figure 2.8 XRPD patterns of nanoparticle agglomerates of indometacin prepared with different stabilisers: (a) without matrix formers and (b) with matrix formers, comparatively to raw indometacin and spray-dried aqueous solution of matrix formers (mannitol and L- leucine).

The DSC curve of raw indometacin (Fig. 2.9) showed an endothermic melting peak at 159 °C (γ- form), while the curves of nanoparticle agglomerates without matrix formers containing different stabilisers presented two endothermic peaks corresponding to their components; a small peak in the range 30 to 50 °C due to the melting of the stabiliser used in each formulation and a melting peak at 157 °C due to the melting of indometacin. Regarding DSC curves of spray-dried aqueous solution of mannitol and L-leucine in the same proportion as in the agglomerates, a large endothermic melting peak at 165 °C appeared due to the melting of mannitol while for the nanoparticle agglomerates containing matrix formers an additional smaller melting peak at around 155 °C was observed, due to the melting of indometacin. Absence of an endothermic peak for the incorporated stabilisers indicated their existence as molecular dispersions in the spray-dried nanoparticles. Also, in the DSC curves of all nanoparticle agglomerates, as expected, the peaks shifted slightly to lower temperatures compared to the starting materials due to the fact that the agglomerates consist of more than one substance (Sharma et al., 2009).

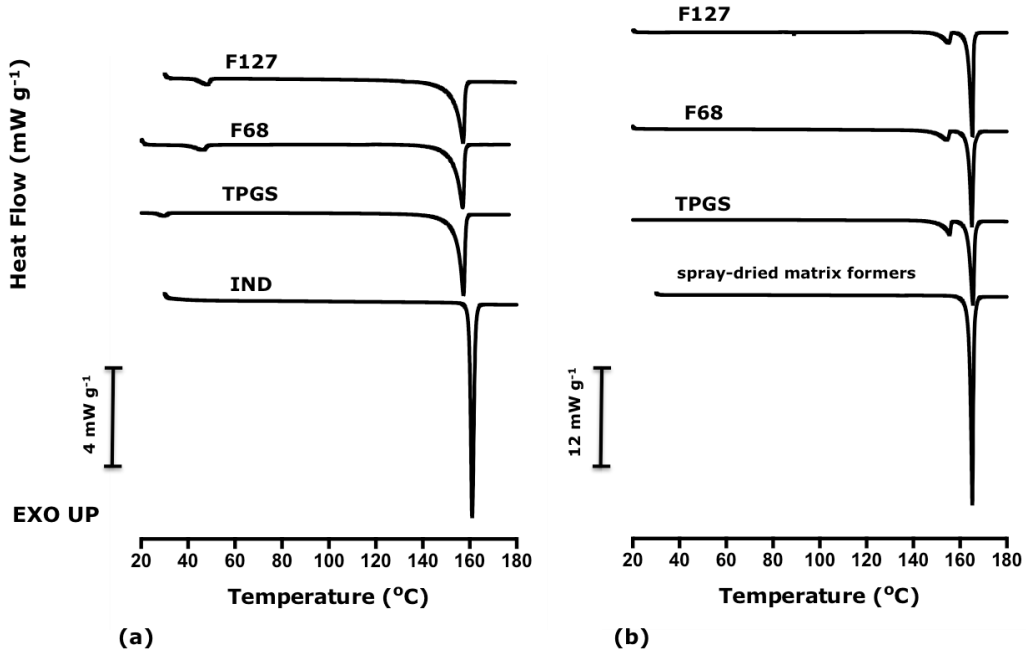

Figure 2.9 DSC curves of nanoparticle agglomerates of indometacin prepared with different stabilizers: (a) without matrix formers and (b) with matrix formers, comparatively to raw indometacin and spray-dried aqueous solution of matrix formers (mannitol and L- leucine).

According to both XRPD and DSC data, nanoparticle agglomerates with and without matrix formers retain their crystallinity. The preservation of the crystalline state when wet bead milling and spray drying are coupled is advantageous ensuring long-term physical stability during storage, compared with other size reduction methods that may result in amorphisation (total or partial) of indometacin. More specifically, production of indometacin nanocrystals by using a nano-spray dryer and ethanol:water solution resulted in a mixture of amorphous indometacin and two polymophs, the stable γ- form and the metastable α- form (Martena et al., 2012). The production of an entirely 'X-ray amorphous' indometacin was also observed when cryo-milling in an oscillatory ball mill was employed as size reduction method (Karmwar et al., 2012). According to Kayaert and Van den Mooter (2012) the absence of drug amorphisation when wet bead milling is employed, can be attributed to the function of water as plasticiser on the potentially generated amorphous material, lowering the glass transition temperature sufficiently to trigger recrystallisation.

2.4.2.3. Drug loading and redispersibility

The results of assayed indometacin content in the nanoparticle agglomerates (Table 2.3) show that the drug content is very close to the nominal content, meaning that there was very little indometacin loss or powder segregation during the production process. Regarding the redispersibilty, for the nanoparticle agglomerates it is desirable that they rapidly redisperse and give primary nanoparticles upon contact with biological fluids (Chaubal and Popescu, 2008). Comparison of redispersibility index data (Table 2.3) shows that nanoparticle agglomerates without matrix formers could not reform nanoparticles upon their rehydration. Specifically, rehydration of nanoparticle agglomerates without matrix formers resulted in particles with z-average size above 1 μm and 2 μm in the case of stabilisation with TPGS and Pluronics®, respectively. At this point, it should be noted that while the upper limit of dynamic light scattering (DLS) is at 5 μm, the technique is not accurate for particles above 1 μm. This means that the z-average values above 1 μm should only be used as an indication of the poor redispersibility of the nanoparticle agglomerates. This may be because spray drying can cause thermal stress, which leads to irreversible aggregation, probably due to the inactivation of steric stabilisation provided by the stabiliser in the liquid state. More specifically, removal of water between the nanoparticles

during spray drying may induce entanglement of the stabiliser chains or stabiliser fusion which can lead to irreversible particle aggregation (Yue et al., 2013). Another possible explanation for the inability for particles to redisperse, is that stabilisers, such as Pluronics®, which are coating nanoparticles during spray drying, may recrystallize, compromising their ability to prevent aggregation (Chaubal and Popescu, 2008). On the contrary, for nanoparticle agglomerates containing matrix formers the reformed nanoparticles exhibited a mean z-average size of around 450 nm upon their dispersion in water (Table 2.3). The higher z-average size of the redispersed nanoparticles compared to the nanoparticles after wet milling (Fig. 2.6) indicates that addition of matrix of formers reduced the irreversible aggregation induced by spray drying but could not completely prevented. However, as the reformed particles are in the nano-range, it can be assumed that spray drying in the presence of matrix formers did not comprise the advantages of nanosuspensions.

Previous studies have highlighted the role of mannitol as matrix former which enhances the redispersibility of nanoparticle agglomerates by decreasing the inter-nanoparticle contacts and as a result preserves the rapid dissolution characteristics of the nanoparticles (Van Eerdenbrugh et al., 2008a). Therefore, the protective action of matrix formers for the nanoparticle agglomerates can be attributed to mannitol and particularly to its function as a continuous solid matrix where nanoparticles are interdispersed. Upon contact with water mannitol is dissolved and nanoparticles are reformed.

Table 2.3 Nominal component and assayed Indometacin content (%w/w) of nanoparticle agglomerates, together with calculated drug loading efficiency (%) and parameters of nanosuspension reconstitution: z-average size, polydispersity index, PI, and redispersibilidy index, RDI % (mean ± SD, n=3).

Formulation	Matrix Formers	Content (% w/w)					Drug loading Efficiency (%)	Reconstituted Nanosuspension		
		Nominal				Assayed IND		z-average size (nm)	PI	RDI%
		IND	Stab	Man	Leu					
Pluronic® F127	Without	90.9	9.1	-	-	88.4 ± 0.7	97.2 ± 0.8	2749 ± 773[a]	0.63	1042
	With	40.6	4.0	49	6.5	38.3 ± 0.4	94.3 ± 1.0	422 ± 0.8	0.19	160
Pluronic® F68	Without	90.9	9.1	-	-	90.7 ± 0.7	99.8 ± 0.8	2460 ± 414[a]	0.48	918
	With	40.6	4.0	49	6.5	36.3 ± 0.3	89.4 ± 0.8	417 ± 4	0.20	156
TPGS	Without	90.9	9.1	-	-	91.1 ± 0.9	100.2 ± 1.0	1293 ± 83[a]	0.33	475
	With	40.6	4.0	49	6.5	41.0 ± 0.5	101.0 ± 1.3	468 ± 31	0.35	172

[a] Large sedimenting particles, Stab= stabilizer, Man= mannitol, and Leu= leucine

2.4.2.4. *In-vitro* dissolution tests

The dissolution profiles of nanoparticle agglomerates (Fig. 2.10), and the corresponding dissolution parameters (DE% and MDT; Table 2.4) show that % $DE_{60\ min}$ is lowest for raw indometacin (47.4%) and increases remarkably for its physical mixtures with stabilisers (58.7 – 70.6 %) and furthermore for the nanoparticle agglomerates without matrix formers (88.2 – 98.1%) and even more for those containing matrix formers (97.1– 99.2%). More specifically due to the different stabiliser, the $\%DE_{60min}$ increases in the order F68 < TPGS < F127, which is the same with that of indometacin solubility in aqueous (0.5% w/v) solutions of F68 and F127 (Table 2.5) apart from the case of TPGS. The exception of TPGS might be attributed to the slow diffusion of surfactant-loaded micelles despite the surfactant enhanced solubility (Balakrishnan et al., 2004). The results of %DE at 10 and 30 min and MDT are in accordance with $\%DE_{60min}$, with some variation, probably due to differences in the dissolution area caused by the differences in the size of nanoparticle agglomerates and their primary nanoparticles.

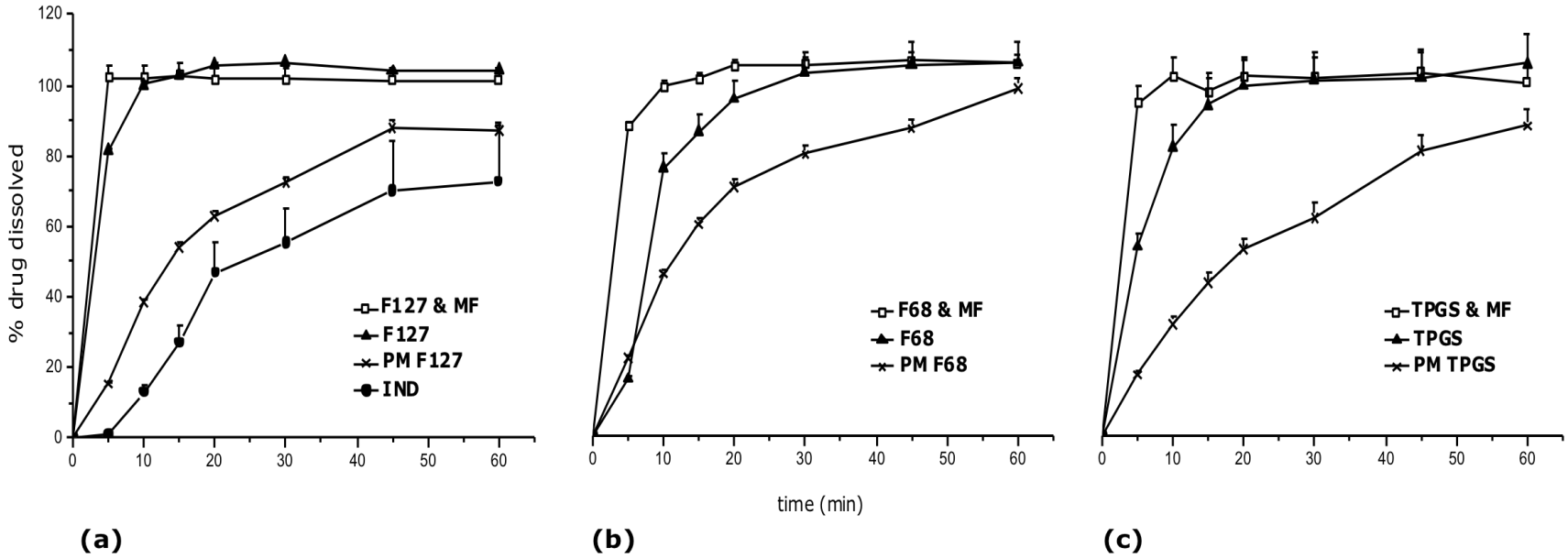

Figure 2.10 Dissolution profiles of nanoparticle agglomerates of indometacin prepared with and without matrix formers (MF) and different stabilizers: (a) Pluronic® F127, (b) Pluronic® F68 and (c) TPGS, comparatively to raw indometacin (IND) and its physical mixtures with each stabilizer (PM) (mean + SD, n=3).

The increase in dissolution rate for the nanoparticle agglomerates can be attributed to the following reasons:

i) The action of both Pluronics® and TPGS as solubilisers enhancing the saturation solubility of indometacin besides its wetting and dissolution rate (Chiappetta and Sosnik, 2007; Guo et al., 2013).

ii) The increase in surface area as a result of size reduction (nanoparticle formation) compared to raw indometacin and physical mixtures of indometacin with stabilisers.

iii) The additional enhancement of dissolution rate by the use of mannitol as a hydrophilic matrix former, resulting in quicker nanoparticle reconstitution and highest dissolution efficiencies, even at 10 min, and lowest mean dissolution times (MDT)

Table 2.4 *In-vitro* dissolution parameters (dissolution efficiency, %DE at 10, 30 and 60 min and mean dissolution time, MDT) of NP-agglomerates prepared with different stabilisers (10% w/w of IND), raw indometacin powder and its physical mixtures with stabilisers (n=3).

Formulation	Stabiliser	Matrix Former	DE_{10} (%)	DE_{30} (%)	DE_{60} (%)	MDT (min)
IND powder	-	Without	3.61	27.5	47.4	15.2
Agglomerates	F127	Without	65.8	91.6	98.1	4.9
Agglomerates		With	76.5	93.5	97.5	2.9
Physical mix		Without	17.3	45.8	64.9	14.0
Agglomerates	F68	Without	27.2	71.1	88.2	10.7
Agglomerates		With	68.8	92.1	99.2	4.1
Physical mix		Without	22.8	52.5	70.6	17.1
Agglomerates	TPGS	Without	47.4	80.1	91.4	8.7
Agglomerates		With	72.8	91.8	97.1	4.3
Physical mix		Without	16.8	39.2	58.7	17.8

Table 2.5 Solubility of indometacin in aqueous stabiliser solutions (0.5% w/v) before nanocommunition (at 25 °C for 24 hs), (mean ± SD, n=3).

Stabiliser	Indometacin solubility ($\mu g\ mL^{-1}$)
Distilled water	12.34 ± 0.70
Pluronic F127	29.02 ± 1.62
Pluronic F68	25.76 ± 0.15
TPGS 1000	185.23 ± 3.47

Dissolution testing indicated that nanoparticle agglomerates achieve a higher available amount of drug for absorption, as their dissolution is faster compared to the raw indometacin and its physical mixtures with stabilisers. This is especially advantageous for indometacin, which according to the BCS is a class II drug (poor water solubility, high permeability), meaning that its *in vivo* dissolution is the rate-limiting step in its absorption. Thus, the improved *in-vitro* dissolution of nanoparticle agglomerates may result in enhanced *in vivo* bioavailability of indometacin. This is important in both the cases of oral and pulmonary delivery of nanoparticle agglomerates of poorly water-soluble drugs as indometacin.

2.4.2.5. *In-vitro* aerosol performance

The drug deposition profiles (Fig. 2.11) and the parameters FPF% and MMAD, Table 2.6, show significant differences due to incorporation of the matrix formers. FPF% becomes higher (48.9 - 61.9 instead of 34.9 - 43.2%) and MMAD lower (3.4 - 3.5 instead of 3.8 - 4.5 μm) indicating improved aerosolisation. Applying ANOVA has shown significant effects of the matrix formers' incorporation on FPF% and MMAD (p=0.001-0.03, p= 0.001-0.1). For the nanoparticle agglomerates with matrix formers, those with F68 and TPGS exhibited higher FPF% (p=0.36) compared to those with F127 (p= 0.001-0.04) while no significant differences were found for the MMAD (p= 0.97-1.0). The type of stabiliser employed was found to have non- significant influence for both FPF% and MMAD (p=0.13-0.49) of nanoparticle agglomerates without matrix formers.

Table 2.6 Parameters of *in-vitro* aerosol performance (recovered fraction, RF%, emitted fraction, EF%, fine particle fraction, FPF%, fine particle dose, FPD, mass median aerodynamic diameter, MMAD, and geometric standard deviation, GSD) of NP-agglomerates prepared with different stabilizers, 10% w/w of IND (mean ± SD, n=3).

Stabiliser	Matrix Formers	RF (%)	EF (%)	FPF (%)	FPD (mg)	MMAD (μm)	GSD
Pluronic F127	Without	82.3 ± 4.3	70.2 ± 5.3	36.6 ± 3.8	5.5 ± 0.6	4.5 ± 0.2	1.7 ± 0.1
	With	79.7 ± 4.6	61.2 ± 2.6	48.9 ± 4.2	7.3 ± 0.7	3.4 ± 0.1	1.6 ± 0.1
Pluronic F68	Without	82.4 ± 1.7	62.1 ± 4.9	43.2 ± 2.4	6.5 ± 0.3	4.1 ± 0.3	1.7 ± 0.1
	With	81.5 ± 7.5	77.9 ± 2.2	61.9 ± 1.6	9.3 ± 0.1	3.4 ± 0.1	1.8 ± 0.3
TPGS	Without	81.4 ± 5.6	60.7 ± 4.3	34.9 ± 2.5	5.2 ± 0.4	3.8 ± 0.2	1.7 ± 0.2
	With	83.2 ± 5.4	76.3 ± 3.1	57.0 ± 2.2	8.6 ± 0.4	3.4 ± 0.1	1.6 ± 0.1

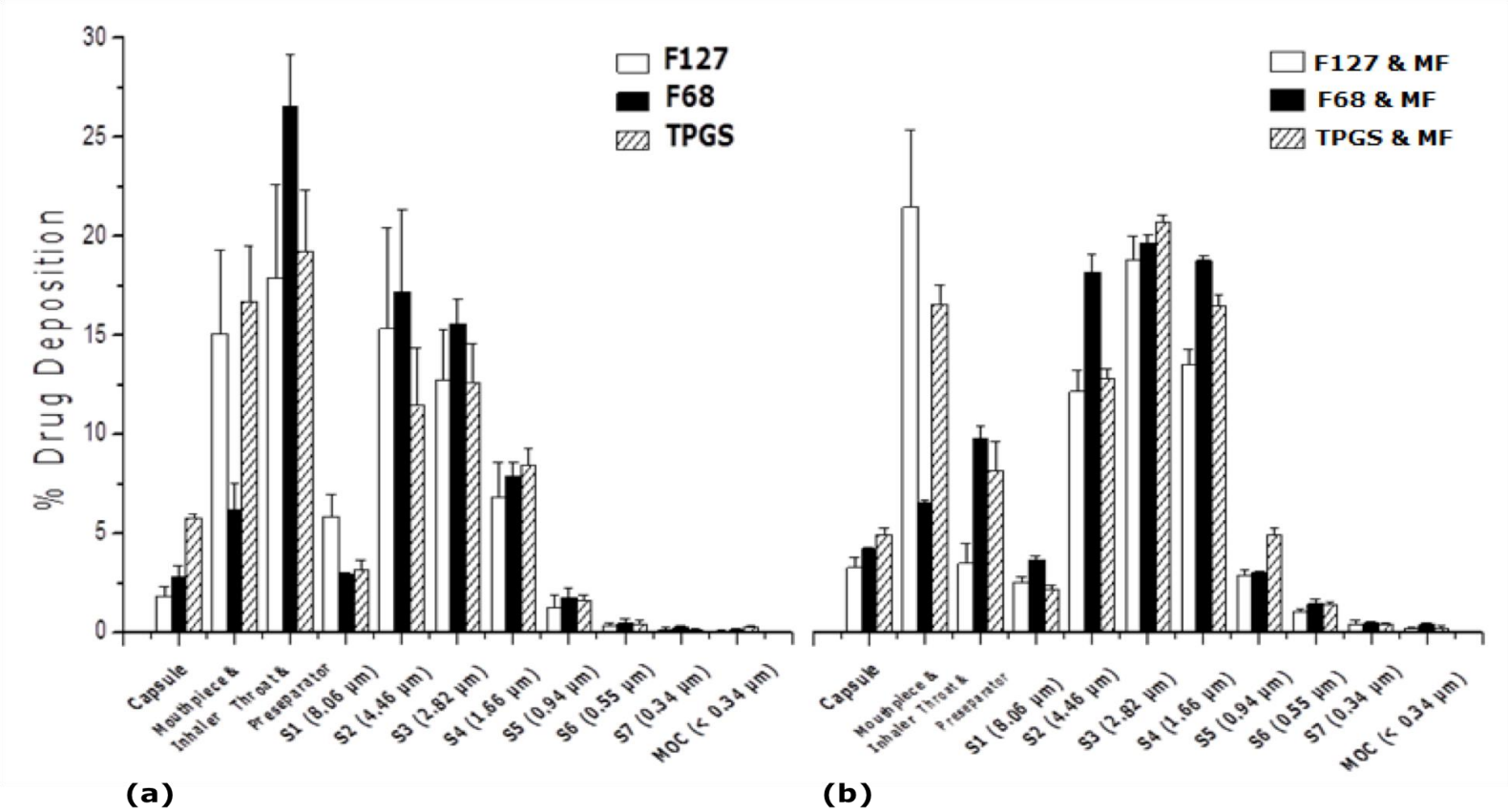

Figure 2.11 Drug deposition profiles of nanoparticle agglomerates prepared with different stabilizers (10% w/w of IND): (a) without matrix formers and (b) with matrix formers (mean + SD, n=3).

The improved aerosolisation indicated by higher FPF% and lower MMAD for the nanoparticle agglomerates containing matrix formers, Table 2.6, can be attributed to the significantly smaller particle size according to the laser diffraction measurements, Table 2.2. On the contrary, the high throat and pre-separator deposition of the nanoparticle agglomerates without matrix formers (Fig. 2.11a) may be due to the presence of secondary nanoparticle agglomerates (agglomerates attached together) observed also by the SEM images (Fig. 2.7a). Moreover, the presence of leucine is of benefit to the aerosolisation performance of the particles. Leucine as a surface active molecule was found to improve the dispersibility of particles by forming a coat (shell) on the surface. Also, inclusion of leucine as an additive in a precursor solution for spray drying was found to enhance the aerosol behaviour of the resulting powders (Lechuga-Ballesteros et al., 2008; Rabbani and Seville, 2005; Seville et al., 2007). More specifically, the addition of leucine to a mannitol-based spray-dried powder for inhalation, was found to enhance the performance of DPI formulations, by forming a coating on the dry particle surface preserving the individual particles as collected from the dryer, preventing any particle fusion (Sou et al., 2011). Therefore, the property of leucine on improving dispersibility of particles and thus reducing their cohesiveness may explain the remarkably reduced throat and pre-separator deposition (Fig. 2.11b) in the case of nanoparticle agglomerates containing matrix formers and particularly those with Pluronic® F127 resulting in an approximately 2- fold decrease, compared to corresponding formulation without matrix formers.

2.5. CONCLUSIONS

Based on the aforementioned results presented in this chapter, it can be concluded that:

1. Nanosuspensions of the poorly water-soluble drug indometacin stabilised with different Pluronics® (F127 and F68) and TPGS were successfully produced and further spray dried with or without the addition of matrix formers (mannitol and L-leucine).
2. Under the milling conditions applied, the molecular weight of stabilisers used influences the rate but not the limit of particle size reduction of the nanosuspensions, which is probably determined by the physico-mechanical properties of the drug tested (IND).
3. The nanoparticle agglomerates obtained after spray drying were crystalline and IND was of the same polymorphic form as the raw drug (γ- IND), which is beneficial for their long-term physical stability.
4. Incorporation of matrix formers during the spray-drying step improved the aerosol performance, the dissolution rate as well as the redispersibility of the formulations.

CHAPTER 3

NANOPARTICLE AGGLOMERATES OF IBUPROFEN

3. NANOPARTICLE AGGLOMERATES OF IBUPROFEN

3.1. INTRODUCTION

Nanosuspensions have been suggested as a beneficial formulation approach for class IIa drugs of the Biopharmaceutical Classification System (BCS), for which the dissolution rate is the rate-limiting step of absorption (Butler and Dressman, 2010). Solidification of the nanosuspensions has been explored to combine the advantages of liquid nanosuspensions (i.e. enhanced dissolution and solubility) with the benefits of solid formulations (i.e. stability, easier handling, enhanced patient compliance) producing nanoparticle agglomerates suitable for oral and pulmonary delivery. Preparation of nanosuspensions by wet milling followed by solidification, using spray drying, has been suggested as a formulation approach for nanoparticle agglomerates with enhanced dissolution and aerosolisation efficiency (Yamasaki et al., 2011).

Compounds with high melting points and poor water-solubility have been highlighted as successful candidates for nanomilling. According to the study by George and Ghosh (2013) the melting point is one of the key drug properties that showed a direct influence on the stability of the nanosuspension with respect to the particle size distribution. This may be explained by the fact that the higher the melting point, the more stable is the drug compound, with no solid state transformations expected. Thus, it is evident that low melting point drugs can be challenging candidates to be processed by wet milling and spray drying as considerable amount of heat is generated in these operations.

The aim of the present work is to study the preparation of nanoparticle agglomerates for low melting point APIs. In this way, the use of wet milling followed by spray drying as a universal and industrially feasible formulation-based approach for the nanoparticle agglomerates with tailored properties for pulmonary and oral delivery will be evaluated.

Ibuprofen was selected as a poorly water-soluble model drug with low melting point. Moreover, it is a drug with challenging mechanical properties as it is a ductile material with a high brittle-ductile transition point of 854 μm (Leuenberger, 1982). Below this point, it is difficult to reduce the size of particles by dry milling, as the particles tend to deform rather than fragment.

Despite the high ductility of ibuprofen, it was reported that wet milling using a Micros Ring Mill resulted in particles with diameter about 8-11 μm (much smaller than the critical diameter of 854 μm). The superior size reduction performance of wet milling was attributed to the contribution of shear forces, which cause ductile fracture of crystals (Larsson and Kristensen, 2000). Besides the ductility of ibuprofen, its low-melting point poses additional challenges on the conventional nano-comminution techniques.

According to the ICH Q8 (R2) guideline, quality by design (QbD) is the systematic approach to pharmaceutical development with predefined objectives emphasizing product and process understanding (ICH, 2009). The main tools of QbD are the design of experiments (DoE), risk assessment and process analytical technology (PAT). DoE helps in the identification of critical versus non-critical parameters affecting product quality attributes and also identifies any interactions between critical parameters impacting the quality attributes

In this chapter, wet milling of ibuprofen using two different stabilisers, namely hypromellose (HPMC) and D-α- Tocopherol polyethylene glycol 1000 succinate (TPGS), followed by spray drying, after the addition of matrix formers, was assessed. The effect of the type of stabiliser on the size reduction of nanosuspensions was investigated. The solid state, particle morphology and the dissolution profiles were also assessed. A full factorial design was employed to understand the critical process parameters as well as any interactions between them involved in the wet milling and spray drying process. The critical formulation parameters investigated were: type of stabiliser, mannitol to drug ratio and leucine to drug ratio. The yield of the process, the particle size distribution, the redispersibility (as redispersibility index) and the fine particle fraction were investigated as responses.

3.2. MATERIALS

Ibuprofen (IBU, Shasun Pharmaceuticals Ltd, India) with a volume mean diameter $D_{4,3}$: 64.5 ± 8.3 μm was used. Pharmacoat 603 (low viscosity hypromellose 2910 Shin-Etsu, Chemical Co. Ltd, Japan) and D-α- Tocopherol polyethylene glycol 1000 succinate (TPGS, Sigma Aldrich Co., St Louis, USA) were used as stabilisers. Mannitol (Pearlitol® 160C, Roquette Frères, Lestrem, France) and L-leucine (Sigma) were used as matrix formers of the nanoparticle agglomerates (Fig. 3.1 and Table 3.1). Hyclone™ water for Injections (Thermo Scientific, UK) was used for the preparation of nanosuspensions. Methanol and acetonitrile were HPLC grade and all other reagents of analytical grade.

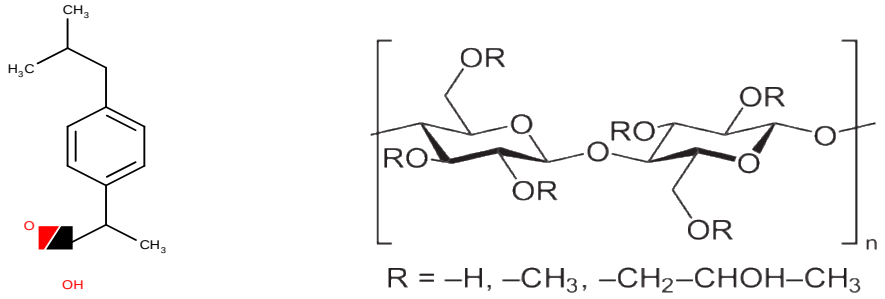

Ibuprofen (IBU)

Hypromellose (HPMC)

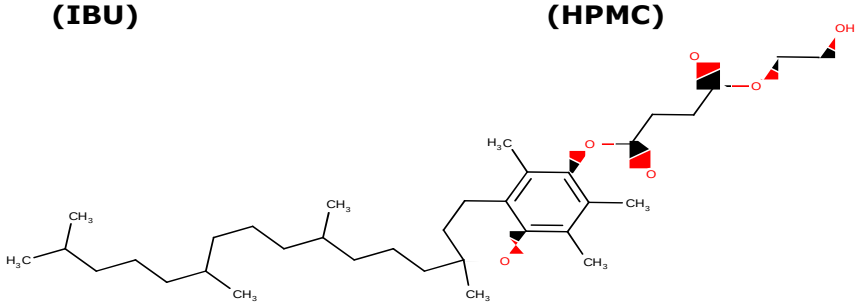

D-α-tocopherol polyethylene glycol succinate 1000 (TPGS)

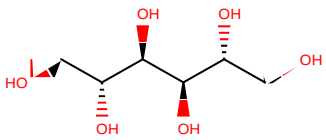

D-mannitol

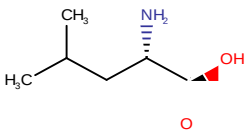

L-leucine

Figure 3.1 Chemical structures of ibuprofen, stabilisers and matrix formers.

Table 3.1 Physicochemical properties of ibuprofen and stabilisers.

Compound	Molecular weight (g mol^{-1})	Melting point (° C)	Aqueous solubility
Ibuprofen	206.3	76 ° C	318.98 µg mL^{-1} [a]
Pharmacoat 603 (HPMC)	13000	170-180 °C (glass transition temperature) 225–230 °C (charring) [b]	soluble
TPGS 1000	1513	38 ° C	soluble

[a] Attari et al., 2015
[b] Rowe et al., 2012

3.3 METHODS

3.3.1. Preparation of nanosuspensions

Nanosuspensions were prepared by wet bead milling using a laboratory planetary mill (Pulverisette 5, Fritsch Co., Germany). 0.5 g of IBU, the stabiliser (10% w/w of IBU) and 10 g of milling beads (0.5 mm diameter aluminum borosilicate glass grinding beads, Gerhardt Ltd, UK) were weighed into each glass vial of 14 mL capacity and suspended in 10 mL water for Injections. The vials were placed into a stainless steel milling pot with a maximum loading capacity of 8 vials (Fig. 3.2.).

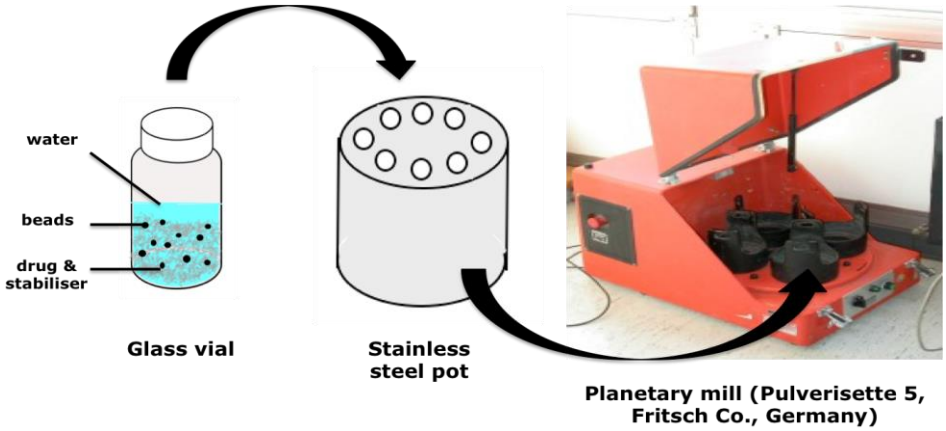

Figure 3.2 Schematic diagram of the wet bead milling process for the production of drug nanosuspension using the planetary mill Pulverisette 5.

Rotation speed (200 rpm), milling duration (6 cycles) and stabiliser concentration (10% w/w of IBU) were selected based on preliminary studies. Each milling cycle comprised 30 min rotation followed by 20 min pause to cool down the milling vessels and avoid overheating of the instrument's rotors. At each pause the nanocrystal size was determined and at the end of the milling procedure, the nanosuspensions were allowed to cool to room temperature and collected by withdrawal using a pipette for separation from the milling beads.

3.3.2. Characterisation of nanosuspensions

3.3.2.1. Nanoparticle size

Measurements were carried out during the milling process, at each pause, for monitoring the particle size reduction and the final size of the nanocrystals in the nanosuspensions. Dynamic light scattering (DLS) was used as previously described in Section 2.3.3.1.

3.3.3. Preparation of nanoparticle agglomerates

The obtained nanosuspensions were solidified by spray drying immediately after preparation. 10 mL of nanosuspension were diluted to 100 mL with an aqueous solution of matrix formers (mannitol and/or L- leucine) to obtain the proportions reported in Table 3.2. Spray drying was performed using a laboratory scale spray dryer (Mini B-290, Buchi Labortechnik Ab, Flawil, Switzerland) fitted with a high performance cyclone Section 2.3.4). On the basis of preliminary 'one-factor-at-a-time' experiments the following parameters were employed: inlet temperature of 70 °C, outlet temperature of 50 ± 2 °C, feed rate of 5 mL min^{-1} and atomizing gas flow rate of 0.5 L s^{-1}. The collected nanoparticle agglomerates were weighed and stored in a desiccator over silica gel for subsequent testing.

Table 3.2 Matrix of full factorial design

Formulation number	Pattern	Independent experimental variables		
		Stabiliser	Mannitol to drug ratio	Leucine to drug ratio
1	100	HPMC	0.5	0.25
2	200	TPGS	0.5	0.25
3	1++	HPMC	1	0.5
4	100	HPMC	0.5	0.25
5	2+−	TPGS	1	0
6	1−+	HPMC	0	0.5
7	2−−	TPGS	0	0
8	2−+	TPGS	0	0.5
9	1+−	HPMC	1	0
10	2++	TPGS	1	0.5
11	200	TPGS	0.5	0.25
12	1−−	HPMC	0	0

3.3.4. Determination of yield

Yield was calculated as the ratio of the mass of the particles collected after spray drying to the mass of solids (drug, stabiliser, matrix formers) introduced in the feed solution. The drug quantity used in the calculations was the amount weighed in the milling pots before the wet milling step.

3.3.5. Characterisation of nanoparticle agglomerates

The nanoparticle agglomerates were characterized with respect to: surface morphology by SEM, particle size distribution (PSD) by laser diffractometry; solid state form by X-ray powder diffractometry (XRPD) and differential scanning calorimetry (DSC), redispersibility by DLS after reconstitution in water. Details of the methods applied have been described in Sections 2.3.5.1-4 and 2.3.5.6.

The drug loading and the dissolution testing were assessed by HPLC analysis of ibuprofen content and the in-vitro aerosol performance using the fast screening impactor (FSI).

3.3.5.1. Drug loading

5 mg of nanoparticle agglomerates were dissolved in 50 mL methanol and ibuprofen concentration was assayed using an HPLC system (Agilent 1100 Series, Agilent technologies, Germany). The stationary phase was a Luna® (150 x 4.60 mm, 5 micron) column (Phenomenex Co., California, USA) kept at 30 ° C. The mobile phase was composed of acetonitrile and aqueous trifluoroacetic acid solution (0.1% v/v) at 50/50 volumetric ratio. The mobile phase flow rate was 1 mL min^{-1}, the injection volume was 10 µL and the detection wavelength 214 nm. The retention time for ibuprofen was 7.4 min. The correlation coefficient of the calibration curve was R^2=0.9999 for a concentration range of 5-600 µg mL^{-1}, indicating acceptable linearity.

3.3.5.2. *In-vitro* dissolution testing

The paddle method was applied by using USP apparatus type II (Pharma Test, Heinburg, Germany), at 37 °C and 50 rpm stirring speed. The dissolution medium was 500 mL of deionised water (freshly boiled and cooled, pH: 6-7). Weighted amounts of formulations corresponding to about 30 mg of IBU were filled in gelatin capsules (size 2), thus sink conditions were maintained during the dissolution tests. At specific time intervals up to 120 min, 5 mL of dissolution medium was withdrawn, filtered through a 0.1 µm disposable syringe filter and placed in HPLC vials for assay, whilst being immediately replaced with 5 mL of fresh medium. The HPLC conditions for the assay were similar to those for drug content determination (section 3.3.5.1). Dissolution tests were conducted in triplicate for each formulation (n=3).

3.3.5.3. *In-vitro* aerosol performance

The aerodynamic assessment of the nanoparticle agglomerates was carried out using the fast screening impactor, FSI (MSP 185 FSI, Copley Scientific, UK, Fig. 3.3). The FSI was developed based on the abbreviated impactor measurement (AIM) concept. The use of multistage cascade impactors for determining the aerodynamic particle size distribution (APSD) is a laborious and time-consuming process that may not be necessarily needed for initial screening and development studies of inhalation formulations (Despres-Gnis

and Williams, 2010). The AIM concept reduces the 7 or 8 data points required for the typical full resolution APSD to two mass fractions; fine (FPF) and coarse (CPF). According to the AIM concept, eliminating all stages from a multistage cascade impactor apart from those required to establish fine and coarse particle fractions can be used as a simpler, faster and more precise way with less operator error in order to assess the quality of inhaled drug products (Mitchell et al., 2013).

The fast screening impactor, FSI, is a device based around the NGI pre-separator. Equipped with a fine particle collector and an induction port, it focuses on the fine particle fraction (i.e. the particles with an aerodynamic diameter smaller than 5 μm that is considered to deposit in the lung). The coarse fraction collector (CFC) is equipped with an insert that enables a cut-off of 5μm at a specific flow rate. A range of inserts is available, generating a 5 μm cut-off diameter within the flow rate range of 30-100 L min^{-1}. The particles not captured in the CFC follow the airstream and deposit in the fine fraction collector (FFC) where they are captured by a filter. The external filter holder, with quick release catches allows rapid removal of the filter holder for gravimetric or chemical analysis (Copley et al., 2013). The FSI is a valuable tool as it reduces the time (up to 40% compared to NGI) and the analytical burden required to assess information regarding the aerodynamic particle size of inhaled drug products. It is especially useful for process optimization, QbD and DoE development, batch release and quality control (Rogueda et al., 2010).

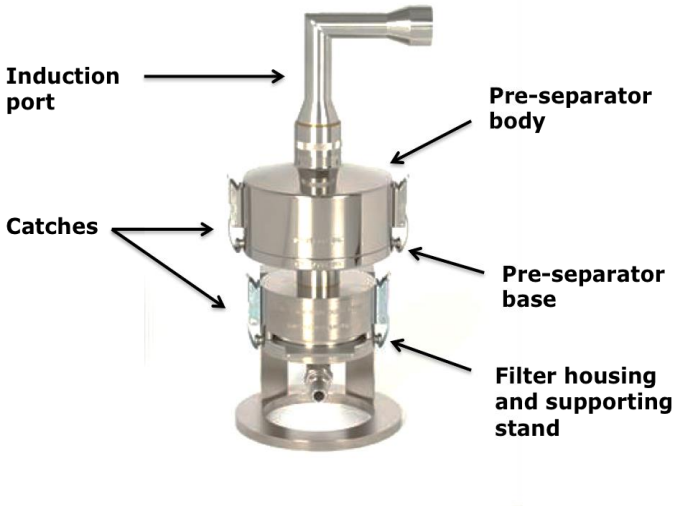

Figure 3.3 Model 185 Fast Screening Impactor (FSI).

In our study, deposition profiles of all the formulations were determined with a FSI connected to a high-capacity vacuum pump (Model HCP5, Copley Instruments, Ltd, UK). Based on results from preliminary studies the bottom plate of the pre-separator was coated with 1% v/v silicone oil in hexane in order to reduce particle bounce that is created from the additional 5 μm cut-off plate. The actual flow rate was measured using a calibrated flow meter (Flow Meter Model DFM 2000, Copley Instrument Ltd, UK) prior to each run, to ensure that a flow at 30 L min^{-1} was achieved. Gelatin capsules (size 3) were filled with accurately weighted amounts of product corresponding to about 10 mg of IBU, placed in the inhaler device (Cyclohaler®) fitted to the impactor via an airtight rubber adaptor and tested at 30 L min^{-1} for 8 seconds (total volume of 4L).

The capsules were discharged into the FSI and after dispersion the particles were collected on a glass fiber filter (76 mm, Pall Corporation, USA) and extracted in methanol. Analysis of the extracts from the coarse and fine particle fractions of the FSI was performed with HPLC. The HPLC conditions for the assay were identical to those for drug content determination. Each formulation was tested in triplicate (n=3).

3.3.6. Design of Experiment

A full factorial design 2^3 (3 factors at 2 levels) was used allowing the estimation of the main effects and the two-way interactions (Table 3.2). The three independent variables used at two levels in the design were: type of stabiliser (X_1), mannitol to drug ratio (X_2) and leucine to drug ratio (X_3). Dependent variables: yield, volume median diameter (D_{50}), redispersibility index (RDI%) and fine particle fraction (FPF%), were selected as critical quality attributes (CQAs). The design matrix included 8 runs plus four centre points. Centre points were added to the design space to identify any non-linearity in the responses. The design space was constructed and analysed using the JMP 12.1.0 software (SAS Institute Inc., USA). To reduce systematic errors, all the experiments were completely randomised. The standard least squares model (including multiple linear regression analysis and ANOVA) was fitted in to model the data and develop a mathematical expression. More specifically the data were fitted according to the following polynomial equation (Eq. 3.1):

$$Y = a_o + a_i X_i + a_j X_j + a_k X_k + a_{ij} X_i X_j + a_{ik} X_i X_k + a_{jk} X_j X_k + \varepsilon \quad \ldots \text{ Equation 3.1}$$

where Y is the dependent variable or response, a_o is the intercept, a_i, a_k, a_j are the main effects coefficients, a_{ij} , a_{ik} , a_{jk} are the two-way interactions coefficients, X_i, X_i, X_i are the independent factors and ε is the noise of the measurement. The significance and validity of the model was estimated by ANOVA. For the sorted parameter estimates of the effects and two-way interactions of each response, the t-ratio and prob>|t| values are given. The t-ratio value is the ratio of the estimate to its standard error and prob>|t| list the probability value of the test. Probability values less than 0.05 were deemed to be statistically significant.

3.4. RESULTS AND DISCUSSION

3.4.1. Preparation and characterisation of nanosuspensions

In this study, both stabilisers were able to produce nanosuspensions of ibuprofen after 180 min of wet milling. The results of hydrodynamic diameter and polydispersity index (PI) of nanosuspensions obtained with both stabilisers as a function of milling time are presented in (Fig. 3.4). More specifically, after 180 min nanosuspensions stabilised with HPMC and TPGS exhibited a z-average size of 533 ± 28 nm and 663 ± 12 nm, respectively.

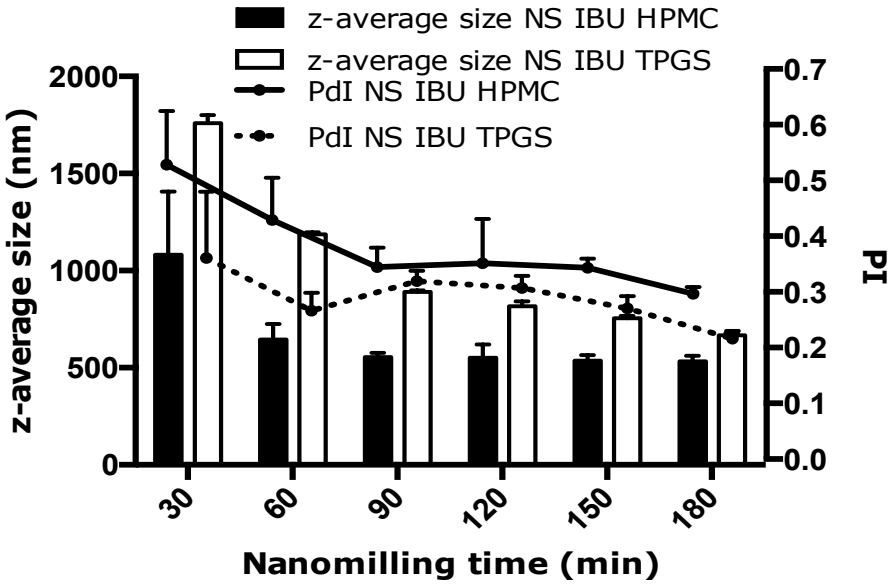

Figure 3.4 Nanoparticle size (hydrodynamic diameter) and polydispersity index (PI) of ibuprofen nanosuspensions with increasing wet milling time (mean + SD, n=3, i.e. three batches of each nanosuspension were produced and analysed).

The starting material, with a volume mean diameter $D_{4,3}$: 64.5 ± 8.3 μm (Fig. 3.5) initially showed rapid size reduction during milling, especially with HPMC as stabiliser. In the case of HPMC, submicron particles of ibuprofen were produced in 60 min while for TPGS this occurred in 90 min. The breakage rate of crystals was high initially and with further milling time the size continued to decrease but at a remarkably slower rate for both stabilisers. This is a common profile as breakage rate kinetics have been found to follow a first-order exponential decay (Afolabi et al., 2014). The ability of HPMC to stabilise the ibuprofen nanosuspensions can be attributed to the conformation of stabiliser molecules on the ibuprofen surface. The polymeric chains were found to be completely uncoiled and adsorbed in an open extended conformation on the ibuprofen surface (Verma et al., 2009a).

Various techniques have been employed for the nanocomminution of ibuprofen crystals. More specifically, Mauludin et al. (2012) produced ibuprofen nanosuspensions with a z-average size of 929 nm after 40 homogenisation cycles using different stabilisers (sodium dodecyl sulfate, Tween 80, Poloxamer 188 and polyvinyl alcohol 90000). Plakkot et al. (2011) managed to produce nanosuspensions of ibuprofen around 450 nm using a new comminution technology (Dena DM 100 processing system) equipped with a heat exchanger. The heat exchanger attached to the size reduction

system enables the temperature of the sample suspensions to be controlled during processing and thus avoid the melting of thermolabile compounds.

In this study, the results of ibuprofen size reduction are similar to those reported by Plakkot et al. (2011) and can be favorably compared with those obtained by Mauludin et al. (2012) using high pressure homogenisation and by Cristini et al. (2003) using rapid expansion of supercritical solutions.

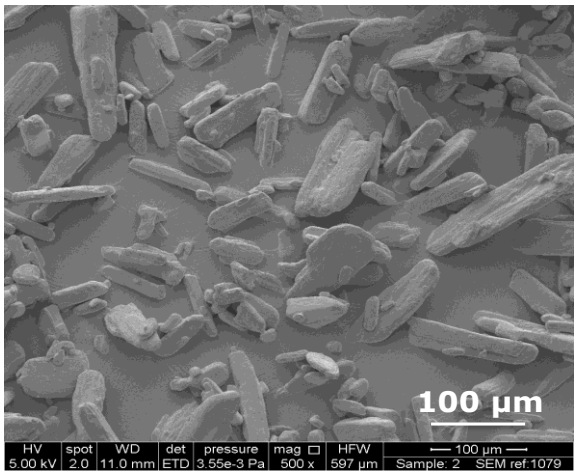

Figure 3.5 SEM image of ibuprofen starting material.

3.4.2. Preparation of nanoparticle agglomerates

During spray drying, the particles are never heated above the outlet temperature of the dryer, despite the fact that the inlet temperature may be considerably higher (Anandharamakrishnan and Ishwarya, 2015). However, in this study based on preliminary trials an inlet temperature of 70 ^{o}C, lower than the melting point of ibuprofen, was selected in order to avoid melting and irreversible aggregation of nanoparticle agglomerates that would hinder their reconstitution upon hydration. Similar results were reported regarding the spray drying of fenofibrate nanosuspensions (Zhu et al., 2014).

3.4.3. Yield

The yield was selected as a response characterising quantitatively the overall productivity of the process. For the experimental conditions applied the yield ranged from 27.3% to 72.5% (Table 3.3). The generated model was significant and the response was modeled with high accuracy (adjusted R^2: 0.96) and low root mean square error (RMSE= 2.4516, Fig.3.6).

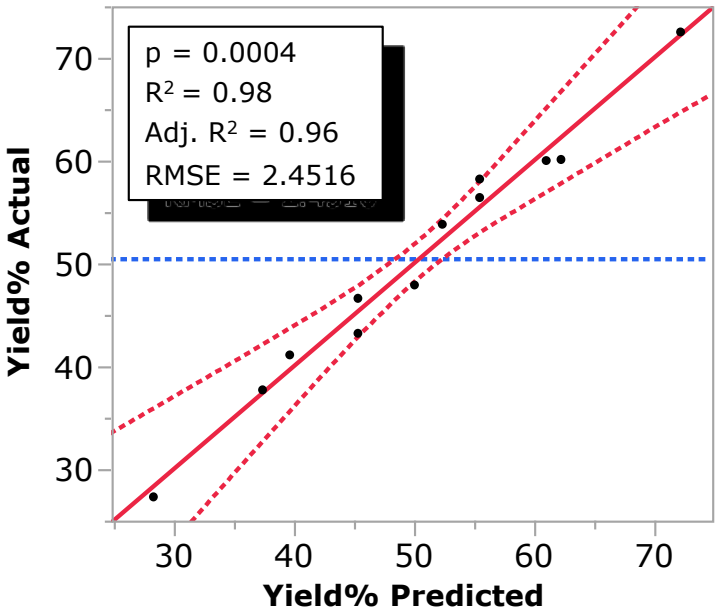

Figure 3.6 Actual vs predicted plot for the process yield of nanoparticle agglomerates of ibuprofen.

Table 3.3 Yield of process and characteristics of spray dried nanoparticle agglomerates of ibuprofen: volume diameter, redispersibility (RDI%) and fine particle fraction (FPF%) (mean ± SD, three samples of one batch of each formulation were analysed).

Sample number	Pattern	Yield (%)	Volume diameter (μm)			RDI (%)	FPF (%)
			D_{10}	D_{50}	D_{90}		
1	100	58.2	0.92 ± 0.02	3.02 ± 0.04	7.02 ± 0.23	420	58.20 ± 4.2
2	200	46.6	0.85 ± 0.01	6.20 ± 0.05	9.02 ± 0.13	250	46.62± 5.6
3	1++	72.5	0.85 ± 0.00	3.57 ± 0.03	6.82 ± 0.07	283	68.55 ± 3.8
4	100	56.4	0.83 ± 0.01	2.27 ± 0.01	6.23 ± 0.16	400	45.11 ± 6.1
5	2+−	41.1	1.13 ± 0.05	9.88 ± 0.39	24.39 ± 2.70	181	9.32 ± 2.5
6	1−+	60.1	0.99 ± 0.02	2.30 ± 0.08	3.83 ± 0.11	751	22.93 ± 1.2
7	2−−	27.3	1.56 ± 0.04	16.04 ± 0.33	53.22 ± 1.51	765	6.68 ± 2.7
8	2−+	53.8	0.88 ± 0.02	2.15 ± 0.02	3.81 ± 0.01	600	40.00 ± 2.3
9	1+−	47.9	1.02 ± 0.06	3.22 ± 0.04	5.92 ± 0.34	307	29.56 ± 3.4
10	2++	60.0	0.77 ± 0.01	2.23 ± 0.04	6.21 ± 0.01	148	43.63 ± 4.1
11	200	43.2	0.87 ± 0.01	5.20 ± 0.04	7.31 ± 0.30	280	40.23 ± 2.7
12	1−−	37.7	0.96 ± 0.03	4.29 ± 0.09	6.87 ± 1.01	938	5.84 ± 2.8

All the three independent variables (independent formulation factors) were identified as significant with a positive effect on the yield of the process ($p < 0.05$, Table 3.4). More specifically, the positive effect of increasing the leucine and mannitol to drug ratios may be attributed to the increased concentration of the solids dissolved in the feed suspension, prior to the spray-drying step. Spray drying of nanosuspensions stabilised with TPGS led to the lowest yield of 27.3% yield. This low yield may be attributed to the low melting point of TPGS resulting in melting and adhesion of the nanoparticle agglomerates to the drying chamber and cyclone. Similar results have been reported for spray drying nanosuspensions of indometacin containing low glass transition temperature sugars (Kumar et al., 2014). Replacing TPGS with HPMC, which is a non-thermolabile stabiliser (Table 3.1), increased the yield. Furthermore, the yield of the process was found to maximize by increasing leucine to drug ratio. This may be explained by the fact that leucine accumulates on the surface of the particles forming a coating around them and thus protecting them from being exposed to high temperatures during the spray-drying step. Similar results were reported by Rabbani and Seville (2005) regarding the spray drying of hydroalcoholic solutions of β-estradiol. They reported that the powder yield was increased with increasing leucine content in the formulation. The explanation proposed by the authors was that when increasing leucine content was used, the drug was encapsulated in micelle-like structures of leucine and thus it was protected from the relative harsh spray-drying conditions.

As shown in the response surface plot (Fig. 3.7) higher yields were obtained when HPMC was used as the stabiliser of ibuprofen nanosuspensions and when high leucine and mannitol to drug ratios were used in the formulations prior to the spray-drying step.

Table 3.4 Sorted parameter estimates of the effects and two-way interactions of factors on the process yield of nanoparticle agglomerates of ibuprofen.

Term	t-ratio	prob > |t|
Leucine to drug ratio (0,0.5)	13.33	< 0.0001 *
Type of stabiliser [HPMC]	7.16	0.0008 *
Mannitol to drug ratio (0,1)	6.14	0.0017 *
Mannitol to drug ratio * Leucine to drug ratio	-0.78	0.4714
Type of stabiliser [HPMC] * Mannitol to drug ratio	0.37	0.7231
Type of stabiliser [HPMC] * Leucine to drug ratio	0.23	0.8267

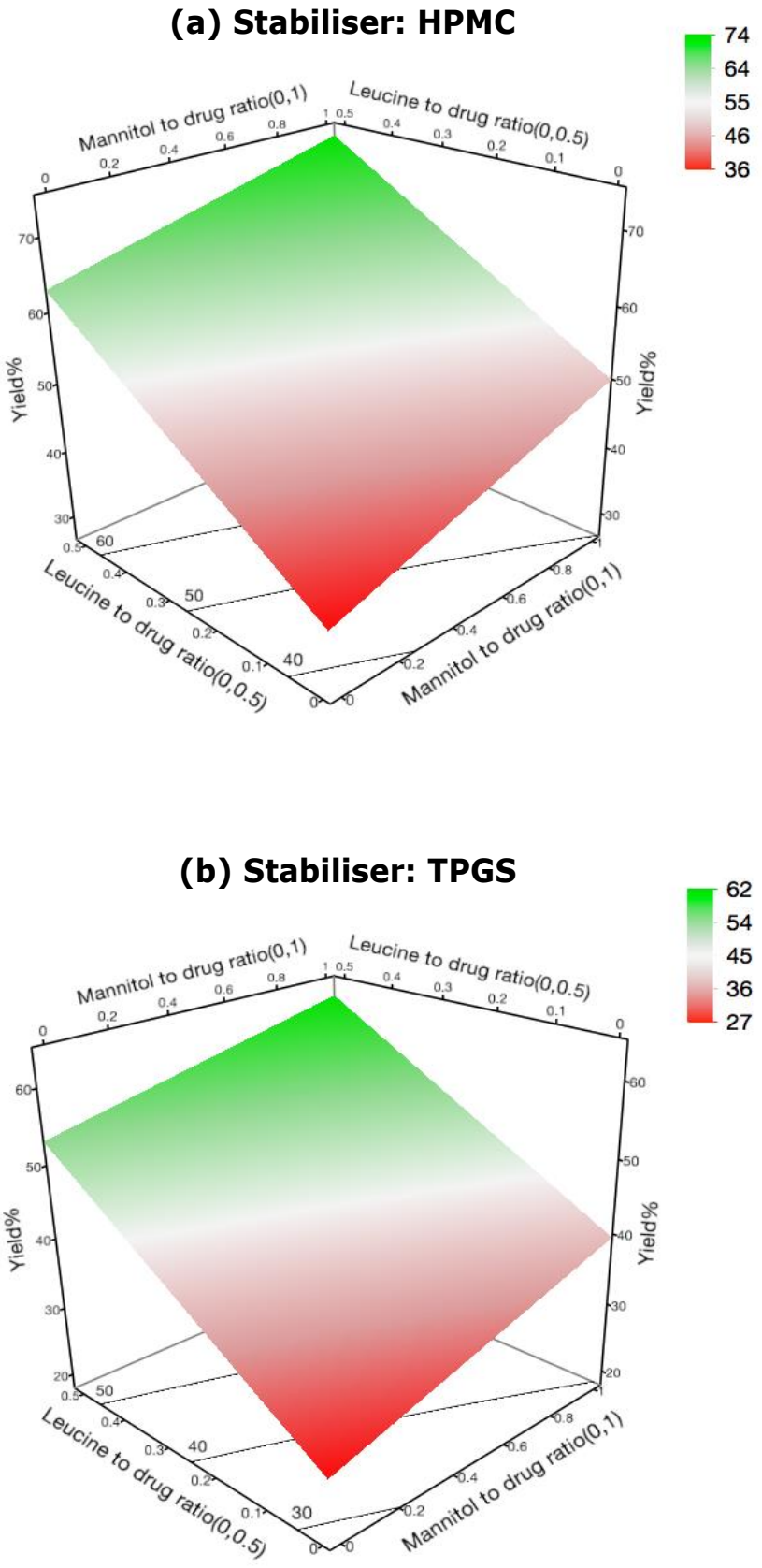

Figure 3.7 Response surface plots showing the influence of the independent formulation variables mannitol to drug ratio and leucine to drug ratio on the yield of the nanoparticle agglomerates of ibuprofen. The stabiliser is (a) HPMC and (b) TPGS.

3.4.4. Characterisation of nanoparticle agglomerates

3.4.4.1. Particle size and morphology

The SEM images of the formulations prepared based on the full factorial design are shown in Figs. 3.8 and 3.9. Spray drying of ibuprofen nanosuspensions stabilised either by HPMC or TPGS in the absence of matrix formers resulted in aggregated particles of irregular morphology with size outside the acceptable range for deposition to the respiratory tract. In the case of HPMC, the particles exhibit irregular morphology where elongated fine crystals of ibuprofen coexist with larger particles (pattern 1--, Fig. 3.8). In the case of TPGS, the SEM images at low magnification shows particles with size larger than 50 μm. SEM images of the same formulation using higher magnification indicate that the lumps may have been created due to melting and sintering of smaller particles (pattern 2--, Fig.3.9).

Addition of mannitol and/or leucine resulted in the promotion of spherical particles with mean size around 2-3 μm that is suitable for pulmonary drug delivery. The surface of the spray-dried particles appears not to be smooth and a closer look reveals the presence of nanoparticles indicating the composite structure of the particles where ibuprofen nanocrystals are embedded in a matrix of mannitol and/or leucine (i.e. nanoparticle agglomerates).

The nanoparticle agglomerates containing leucine consist of individual particles (e.g. patterns 1-+, 2-+). This may be attributed to the accumulation of leucine to the surface of the particles preventing any particle fusion. Addition of high leucine to drug ratio resulted in wrinkled particles (patterns 1++, 2++). A wrinkled morphology was interpreted as an indication of hollow particles as the particle density was found to decrease as the "wrinkleness" of the particles was increased (Raula et al., 2010).

Furthermore, the nanoparticle agglomerates appear to be porous with holes and dimples in the particle surface. The presence of the holes in the particle shell can be attributed to the evaporation of liquid that escapes from the inner of the droplet through the solid crust built in the course of the drying process on the surface of the droplet (Vehring, 2008; Maas et al., 2011). Engineering of porous particles is considered beneficial for pulmonary drug delivery as particles with high porosity have smaller aerodynamic diameter

compared to nonporous particles of the same size, increasing the probability for deposition in the lower respiratory tract (Edwards et al., 1997).

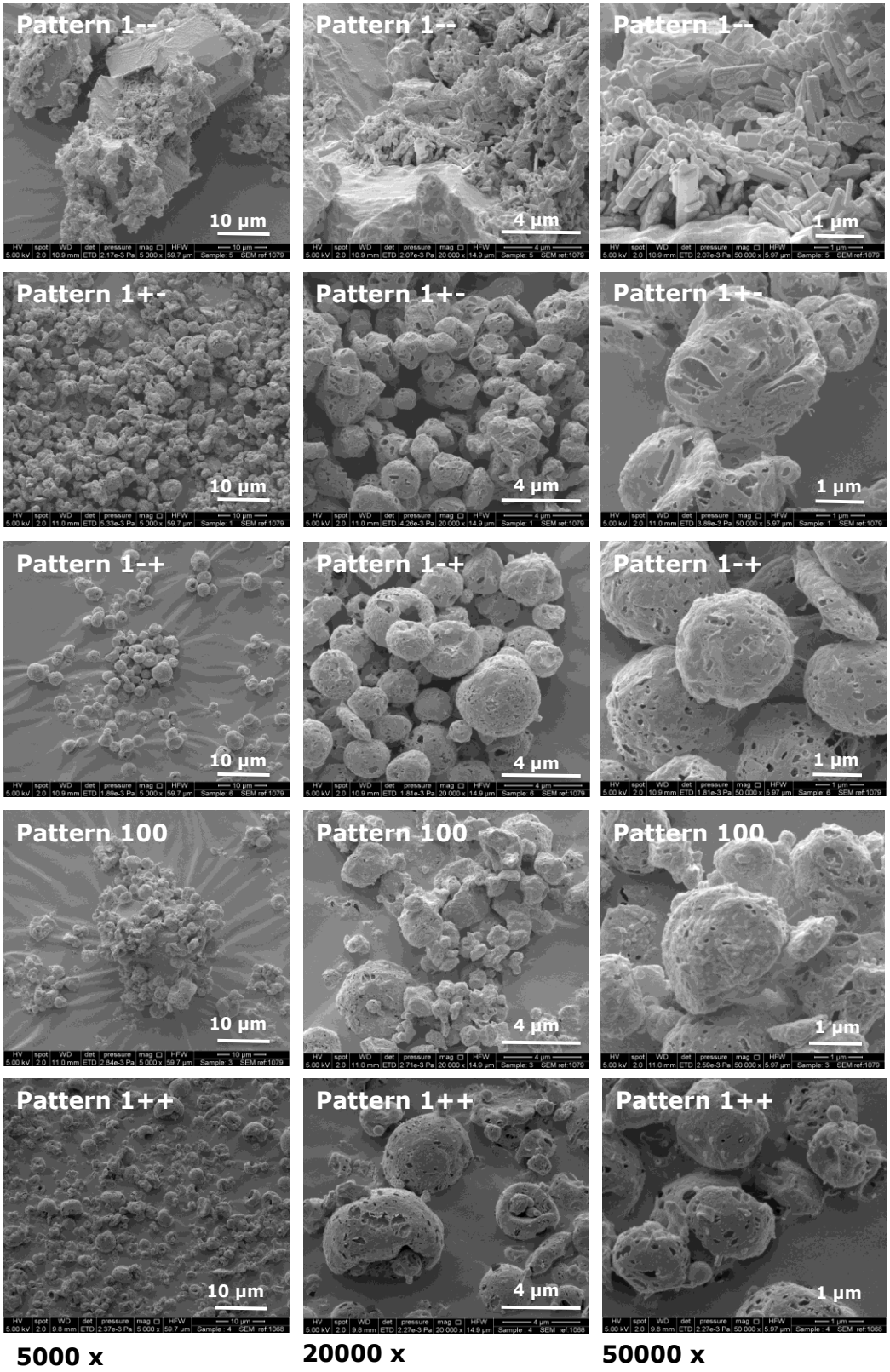

Figure 3.8 SEM images of nanoparticle agglomerates of ibuprofen stabilised with HPMC included in the full factorial design.

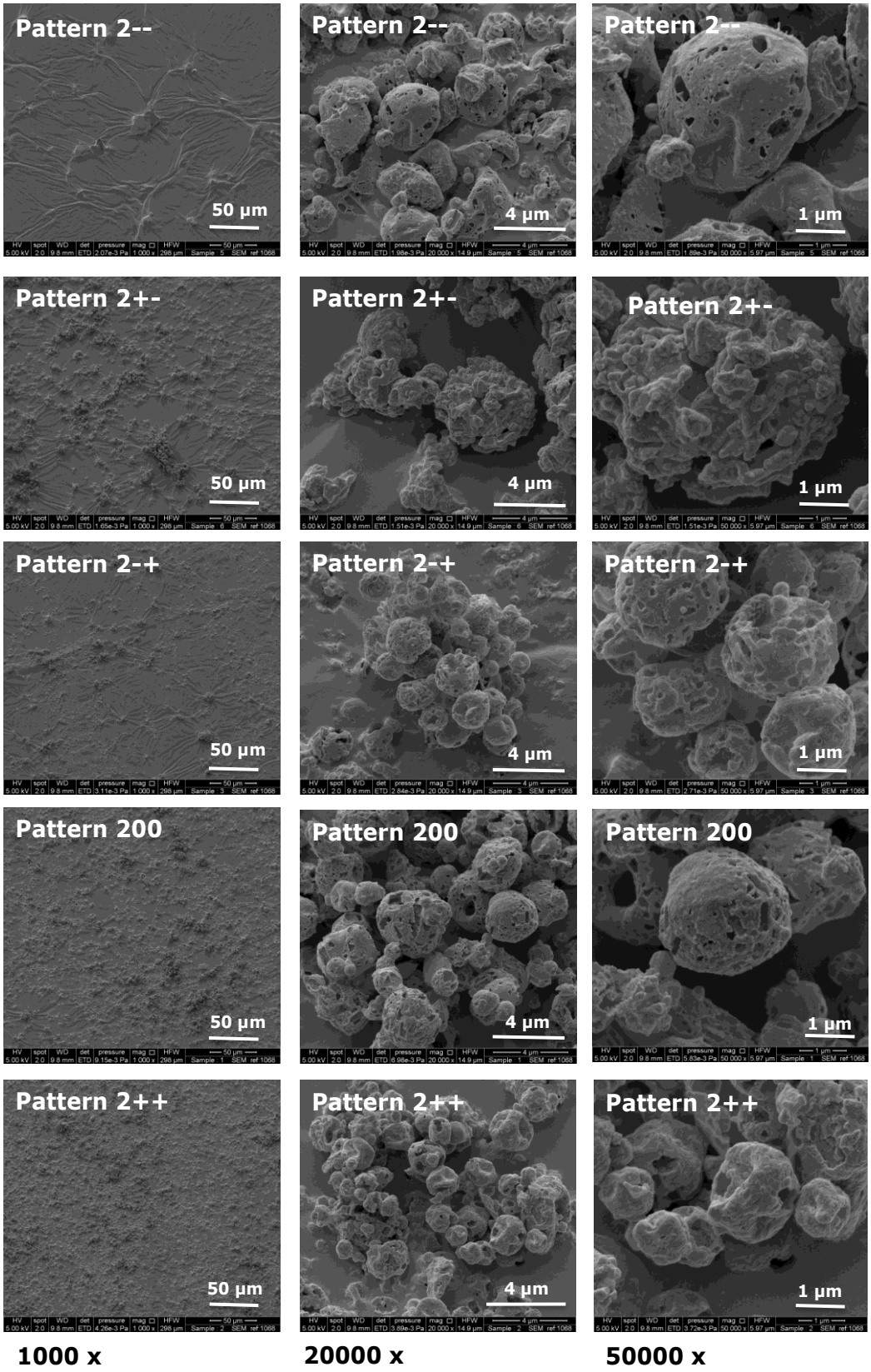

Figure 3.9 SEM images of nanoparticle agglomerates of ibuprofen stabilised with TPGS included in the full factorial design.

The particle size of the nanoparticle agglomerates obtained was measured by laser diffraction as volume diameter (Table 3.3) The dried powders obtained exhibited a median diameter D_{50} between 2.15 and 16.04μm and the data are in good agreement with the particle size observed by SEM. The results were analysed in the experimental design performing ANOVA for particle size focusing on the D_{50} value and the model was found significant ($p < 0.05$, Fig.3.10).

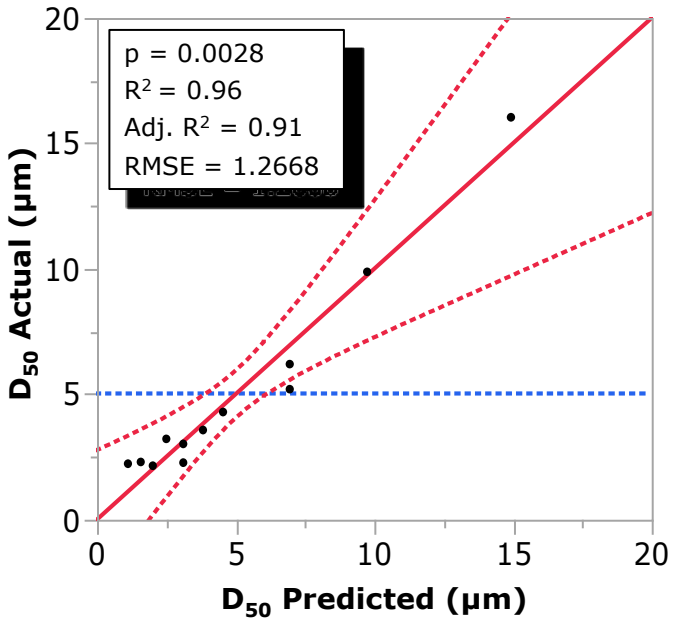

Figure 3.10 Actual vs predicted plot for the D_{50} particle size of the nanoparticle agglomerates of ibuprofen.

Leucine to drug ratio and the type of stabiliser were identified as formulation variables with the most significant effects on the D_{50} (Table 3.5). Their "negative" effect is interpreted as size reduction that is desirable for pulmonary drug delivery. It is likely that increased leucine to drug ratio formed a surface coating around the particles which prevented the particles from melting and sintering, as observed for the process yield. Moreover, a significant interaction was identified between leucine to drug ratio and the type of stabiliser with a positive t-ratio, despite the fact that the factors had individually negative effects on the D_{50} (Table 3.5).

Table 3.5 Sorted parameter estimates of the effects and two-way interactions on the D_{50} particle size of nanoparticle agglomerates of ibuprofen.

Term	t-ratio	prob > |t|
Leucine to drug ratio (0,0.5)	-6.47	0.0013 *
Type of stabiliser [HPMC]* Leucine to drug ratio	5.55	0.0026 *
Type of stabiliser [HPMC]	-5.25	0.0033 *
Mannitol to drug ratio * Leucine to drug ratio	2.39	0.0620
Type of stabiliser [HPMC] * Mannitol to drug ratio	1.75	0.1400
Mannitol to drug ratio (0,1)	-1.64	0.1627

This means that the interaction between HPMC and leucine to drug ratio is synergistic rather than additive. Use of the non-melting HPMC as a nanosuspension stabiliser and the addition of a high leucine to drug ratio leads to further particle size reduction than the individual factors alone.

As shown in the response surface plot, spray drying of ibuprofen nanosuspensions stabilised with HPMC and containing a high leucine to drug ratio was able to produce nanoparticle agglomerates with particle size around 2-3 μm that is suitable for pulmonary drug delivery (Fig. 3.11a). On the other hand, spray drying of ibuprofen nanosuspensions stabilised with TPGS produced larger particles while addition of both high leucine and mannitol to drug ratios is required in order to produce particles smaller than 4 μm (Fig. 3.11b). This indicates that the selection of stabiliser is vital not only for the step of nanosuspension production but it may also influence the downstream process of spray drying by affecting the properties of the nanoparticle agglomerates produced.

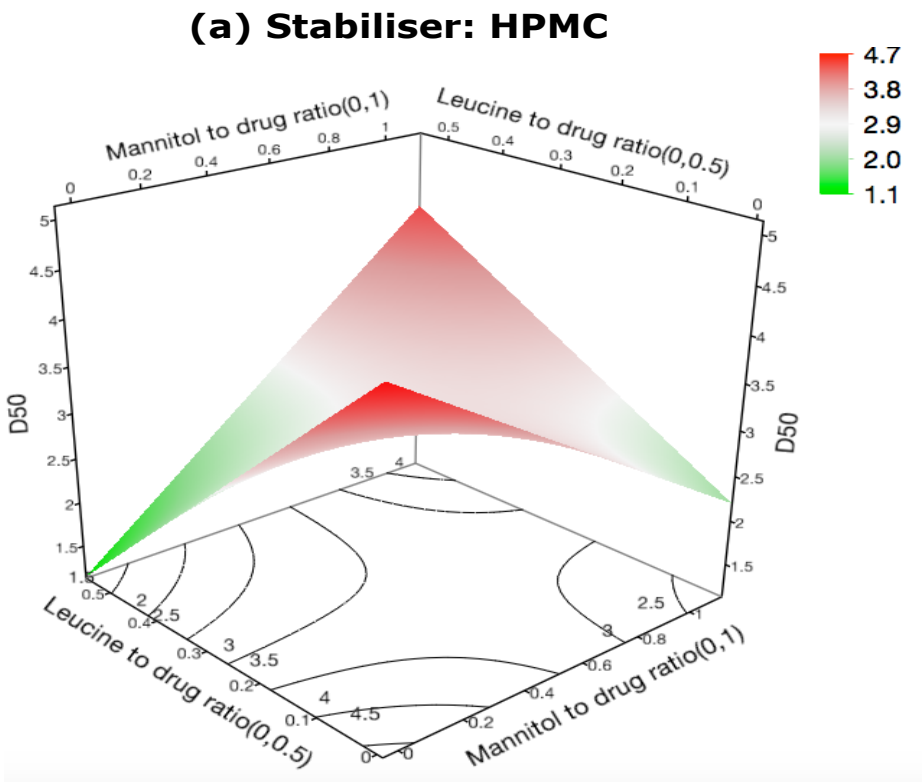

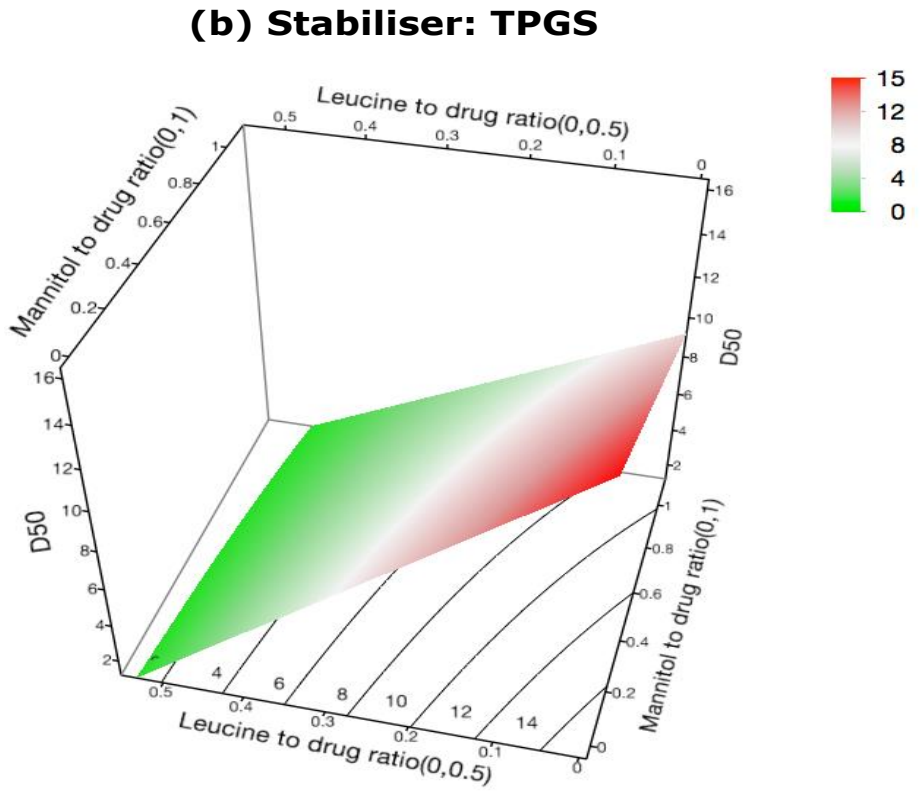

Figure 3.11 Response surface plots showing the influence of the independent formulation variables mannitol to drug ratio and leucine to drug ratio on the quality attribute D_{50} particle size of nanoparticle agglomerates of ibuprofen. The stabiliser is (a) HPMC and (b) TPGS.

3.4.4.2. Redispersibility

Redispersibility is an important quality attribute of nanoparticle agglomerates as it is a prerequisite for the reformation of nanoparticles upon rehydration and potential enhancement of therapeutic efficacy. Particularly, for nanoparticles of low melting point drugs such as ibuprofen, thermal stresses during spray drying may lead to phase and composition changes of formulations causing irreversible aggregation and loss of the advantages of nanoformulations (Chaubal and Popescu, 2008). An RDI% value close to 100% means that the nanoparticle agglomerates reformed nanoparticles with z-average size close to the z-average size of the nanosuspensions prior to the solidification step. For the experimental conditions applied the redispersibility index (RDI%) ranged from 148% to 938% (Table 3.3). The results were analysed in the experimental design performing ANOVA for particle size focusing on the RDI% value and the model was found significant ($p < 0.05$, Fig.3.12).

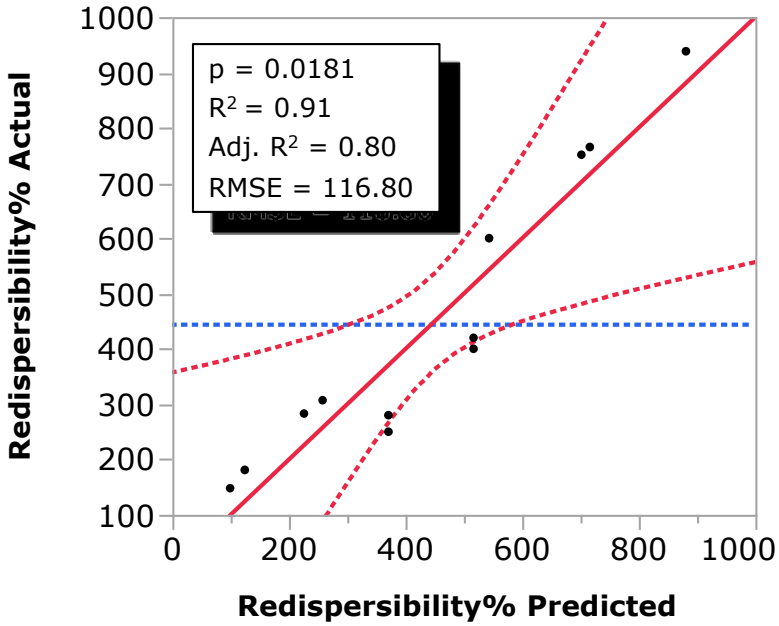

Figure 3.12 Actual vs predicted redispersibility index (RDI%) of the nanoparticle agglomerates of ibuprofen.

The mannitol to drug ratio was identified as the only significant factor affecting redispersibility (p value < 0.05, Table 3.6) with higher mannitol to drug ratio leading to RDI% values closer to 100%. The role of mannitol can be explained by the formation of a continuous matrix around the nanocrystals during the spray-drying step preventing their irreversible

aggregation. Upon rehydration, mannitol as a hydrophilic excipient dissolves and the nanocrystals are reconstituted. Zuo et al. (2015) reported similar results highlighting that a high mannitol to drug ratio is important for the redispersibility of nanoparticle agglomerates of fenofibrate.

Table 3.6 Sorted parameter estimates of effects and two-way interactions on the redispersibility index (RDI%) of the nanoparticle agglomerates of ibuprofen.

Term	t-ratio	prob > |t|
Mannitol to drug ratio (0,1)	-6.46	0.0013 *
Type of stabiliser [HPMC]	2.16	0.0830 *
Leucine to drug ratio (0,0.5)	-1.24	0.2708 *
Mannitol to drug ratio * Leucine to drug ratio	0.89	0.4129
Type of stabiliser [HPMC] * Mannitol to drug ratio	-0.19	0.8561
Type of stabiliser [HPMC] * Leucine to drug ratio	-0.04	0.9699

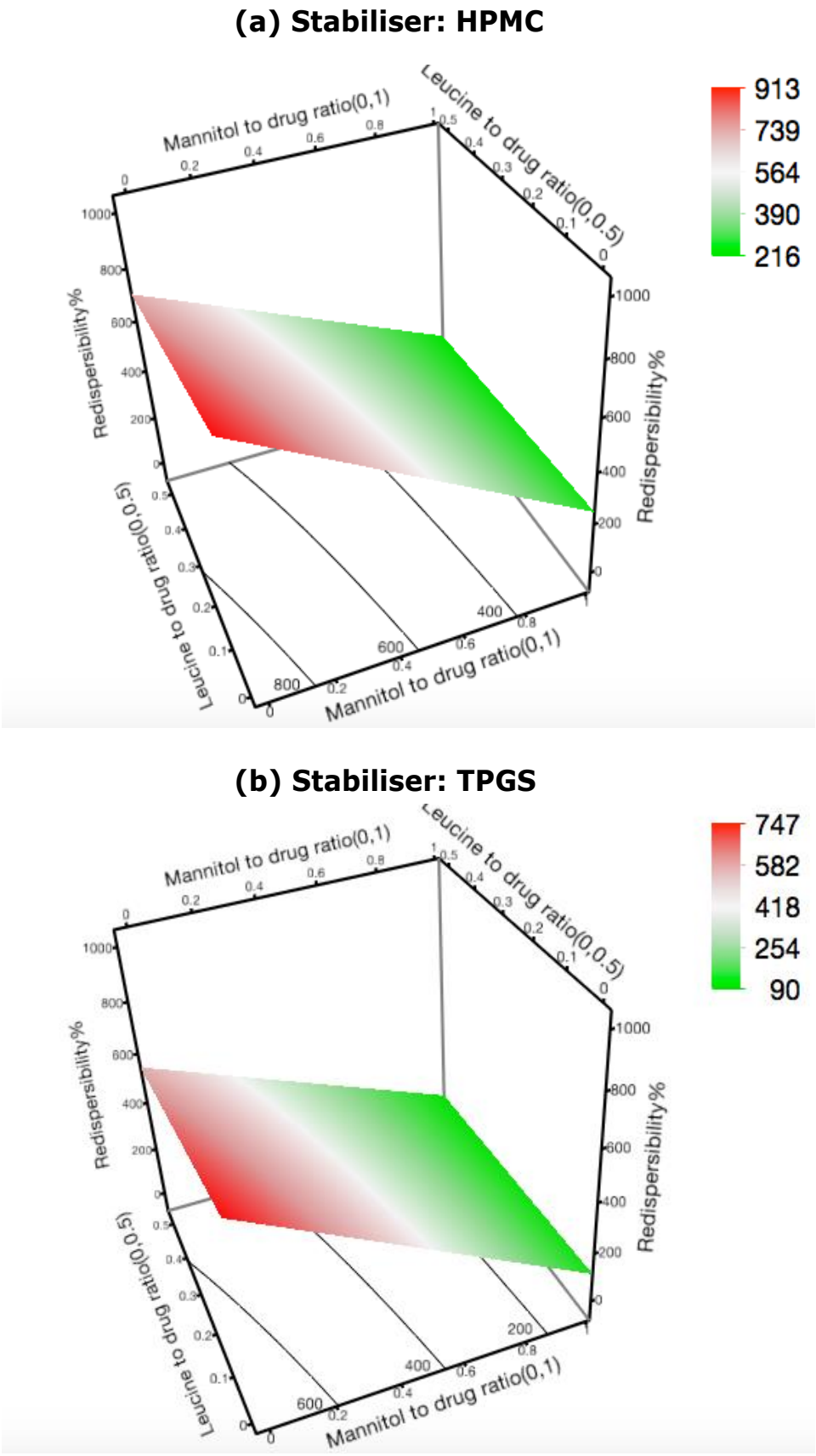

Figure 3.13 Response surface plots showing the influence of the independent formulation variables mannitol to drug ratio and leucine to drug ratio on redispersibility index of the nanoparticle agglomerates of ibuprofen. The stabiliser is (a) HPMC and (b) TPGS.

As shown in the response surface plot (Fig. 3.13), nanoparticle agglomerates of ibuprofen with enhanced redispersibility (RDI% value closer to 100%) are obtained only when high mannitol to drug ratios are present in the formulations prior to the spray-drying step.

3.4.4.3. Drug loading

The results of assayed ibuprofen content in the nanoparticle agglomerates are given in Table 3.7. Spray drying of nanosuspensions without matrix formers appeared to have lower drug loading than the nominal. This may be attributed to the melting of TPGS or ibuprofen during spray drying that led to drug loss due to deposition on the walls of the drying chamber and cyclone. For the spray-dried nanosuspensions containing mannitol and/or L-leucine the assayed ibuprofen content is close to the nominal content indicating that the addition of these excipients prevented ibuprofen loss or powder segregation during the production process.

Table 3.7 Nominal content and assayed ibuprofen content (% w/w) of nanoparticle agglomerates together with calculated drug loading efficiency (%) (mean ± SD, n=3).

Pattern	**Content (% w/w)**					**Drug Loading Efficiency (%)**
	Nominal				Assayed IBU	
	IBU	STAB	MAN	LEU		
100	54.05	5.41	27.03	13.51	50.8 ± 1.3	94.0 ± 2.4
200	54.05	5.41	27.03	13.51	51.8 ± 1.7	95.9 ± 3.2
1++	38.46	3.85	38.46	19.23	36.7 ± 0.2	95.4 ± 0.5
100	54.05	5.41	27.03	13.51	49.2 ± 1.3	91.0 ± 2.6
2+−	47.6	4.76	47.6	-	44.4 ± 0.8	93.2 ± 1.7
1−+	62.5	6.25	-	31.25	59.4 ± 1.2	95.0 ± 1.8
2−−	91	9	-	-	77.4 ± 1.4	85.1 ± 1.6
2−+	62.5	6.25	-	31.25	58.3 ± 1.1	93.3 ± 2.1
1+−	47.6	4.76	47.6	-	42.1 ± 2.1	88.5 ± 3.6
2++	38.46	3.85	38.46	19.23	35.4 ± 0.7	92.0 ± 1.9
200	54.05	5.41	27.03	13.51	50.4 ± 2.1	93.2 ± 3.5
1−−	91	9	-	-	80.3 ± 1.9	88.2 ± 2.6

Statistically significant differences ($p < 0.05$) between the drug loading efficiency (%) of the nanoparticle agglomerates of ibuprofen include 2-- and 100, 2-- and 200, 2-- and 1++, 2-- and 2+-, 2-- and 1-+, 2-- and 2-+, 2-- and 200, 200 and 1+-, 200 and 1-- and 1++ and 1--.

3.4.4.4. Solid state characterisation

The XRPD patterns of the starting materials are shown in Fig. 3.14. Raw ibuprofen exhibited sharp peaks in the range of 2theta: 15-25 ^{o} that are characteristic of the drug. The peaks are in agreement with detailed studies on the ibuprofen peak assignment and location, which already are already reported in the literature (Kayrak et al., 2003, Plakkot et al., 2011). Mannitol starting material exhibited characteristic peaks of the β- form (2 theta: 10.6^{o}, 14.7^{o}, 16.9^{o}, 21.2^{o}, 23.9^{o}, 29.5^{o}) (Hulse et al., 2009) while the diffractogram of L-leucine indicated a highly crystalline structure (2 theta:6^{o}, 12^{o}, 24^{o}, 31^{o}, 37^{o}) (Raula et al., 2007).

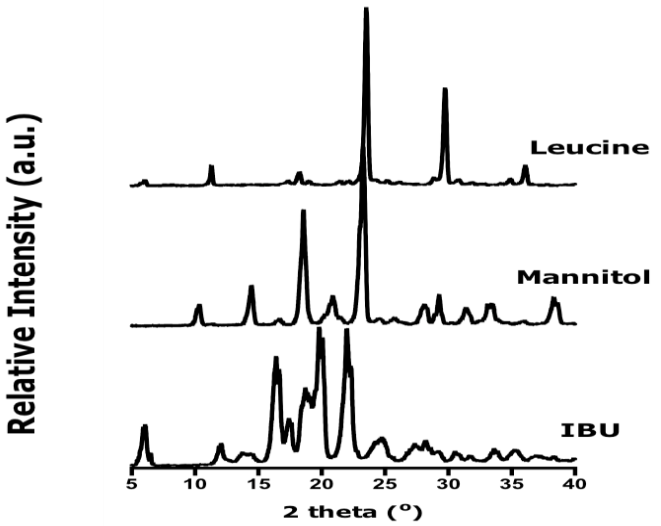

Figure 3.14 XRPD patterns of starting materials.

The diffractograms of all runs prepared according to the DoE are shown in Fig.3.15. The diffractograms of patterns *1*-- and *2*-- (without matrix formers) showed peaks at similar 2 theta positions to those of the raw ibuprofen. For the nanoparticle agglomerates of ibuprofen containing matrix formers the diffractograms were a summation of the patterns of their components. No new peaks or halo could be detected in the XRPD patterns indicating the absence of generation of amorphous content during the process.

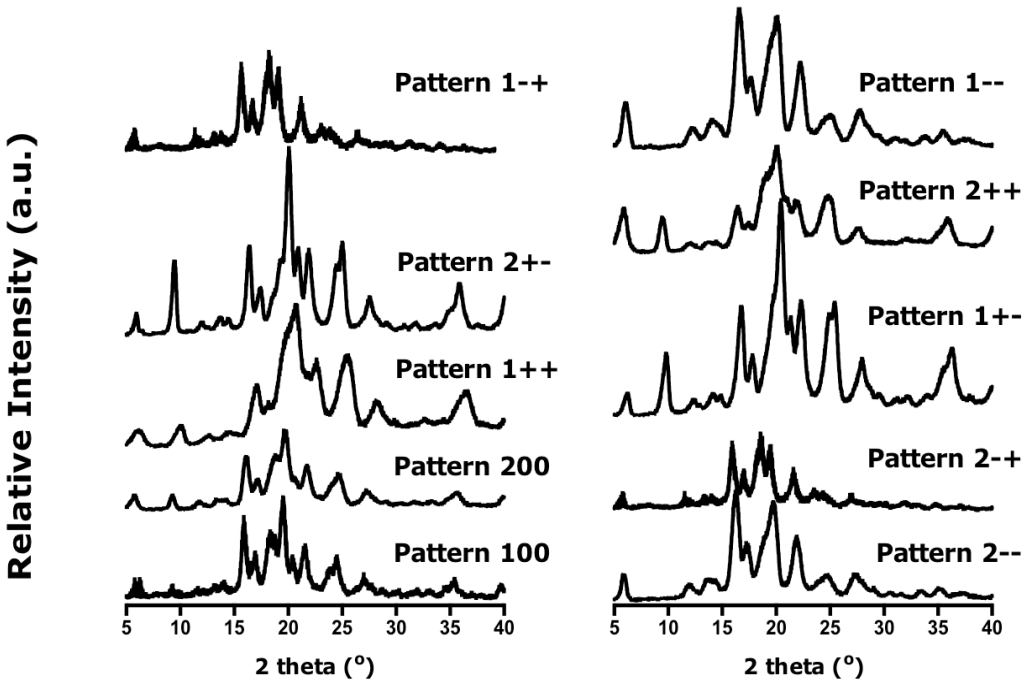

Figure 3.15 XRPD diffractograms of nanoparticle agglomerates of ibuprofen included in the full factorial design

The DSC was used to assess the thermal behaviour of the starting materials and nanoparticle agglomerates of ibuprofen (Fig. 3.16). The DSC thermogram of ibuprofen showed an endothermic peak at 76 °C corresponding to the melting of the drug. The nanoparticle agglomerates of ibuprofen without mannitol and leucine exhibited the same endothermic peak shifted to slightly lower temperature (Fig. 3.16a) while those containing mannitol exhibited thermal behaviour depending on the stabiliser.

More specifically, the nanoparticle agglomerates of ibuprofen containing mannitol and stabilised with TPGS exhibited two endothermic peaks (patterns 2++, 2+-, Fig.3.16b) as expected: the melting peak at around 70 ° C, which relates to the melting of the drug and a sharp endothermic peak at 168 ° C, which relates to the melting of mannitol (Pearlitol 160C). For the

nanoparticle agglomerates of ibuprofen containing mannitol and stabilised with HPMC, apart from the melting of ibuprofen, an endothermic peak at 150 °C was followed by an exothermic event and then an endothermic melting at 168 °C (patterns 1++, 1+-, Fig. 3.16b). Mannitol exists in three polymorphic forms; alpha (α), beta (β) and delta (δ) (Walter-Levi, 1968). Differing findings have been reported regarding the stability of D-mannitol polymorphs. According to Kim et al. (1998) both α and β forms are considered stable, while in a later study by Willart et al. (2007) it was found that form β is the most stable polymorph, δ is the least stable and form α exhibits an intermediate stability between the two. The thermal events observed in the DSC of patterns 1++ and 1+- could be attributed to the formation of the metastable δ-form of mannitol (mp: 150-158 °C) that is followed by crystallisation to the α- or/and β-form and the melting of the respective crystal form (Burger et al., 2000). Both α- and δ-form of mannitol were found to be chemically and physically stable for at least 5 years when stored at 25 °C and 43% relative humidity (Burger et al., 2000). Recently, co-spray drying of an aqueous solution of mannitol with PVP in a ratio 4:1 was reported to produce the δ-form of mannitol (Vanhoorne et al., 2016). At this point, it should be noted that the presence of the δ-form of mannitol could not be observed by XRPD but this may be explained by the small difference between the characteristic peaks of the β-form (10.6 °) and δ-form (9.6 °), while a method such as Raman spectroscopy may be more suitable to analyse the polymorphic mannitol composition.

Based on various studies, L-leucine sublimes and then to decomposes. The temperatures reported for the sublimation of L-leucine vary from 145 °C to 295 °C while decomposition occurs at around 300 °C (Lähde et al., 2009; Li et al., 2006). However, as ibuprofen decomposes at temperatures higher than 200 °C, a heating range from 30 °C to 200 °C was selected so as to carry out the DSC of the nanoparticle agglomerates in order to avoid decomposition of samples in the DSC cells. Thus, the thermal behaviour of L-leucine was left out of the scope of our study.

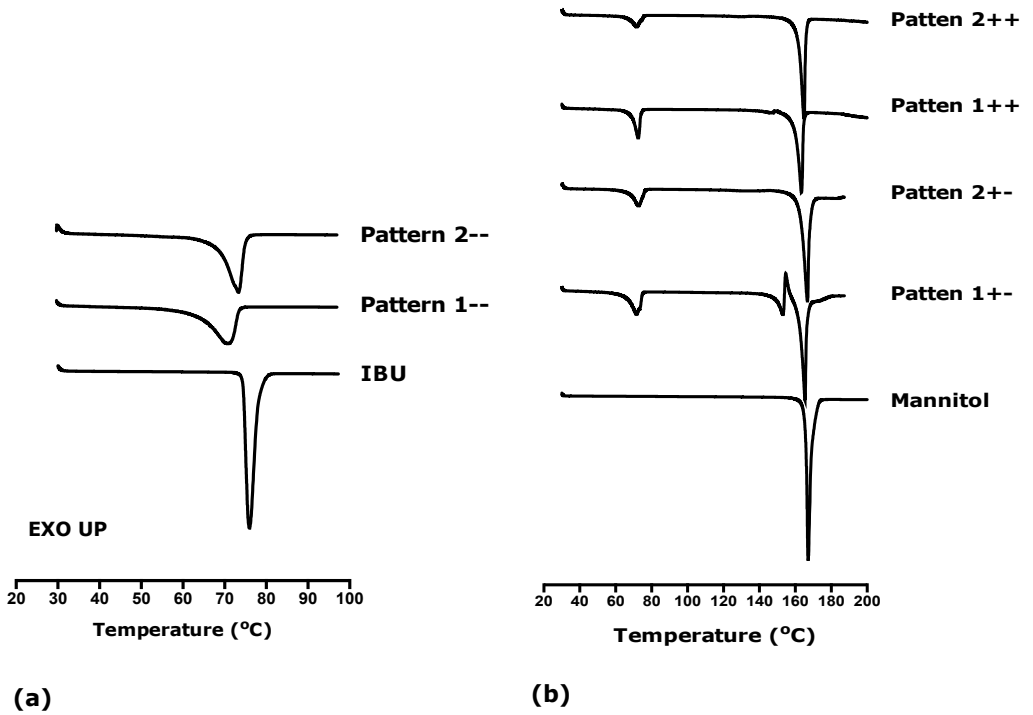

Figure 3.16 DSC thermograms of ibuprofen and mannitol starting materials and nanoparticle agglomerates included in the full factorial design.

Overall, the XRPD and DSC data suggest that the engineered nanoparticle agglomerates retain their crystallinity during wet bead milling followed by spray drying. The preservation of the crystalline state is advantageous, ensuring the long-term physical stability of the formulations during storage.

3.4.4.5. *In-vitro* dissolution tests

Dissolution studies of ibuprofen and nanoparticle agglomerates were performed in deionised water as it was found to be discriminatory as a dissolution media compared to phosphate buffer (pH: 7.2). This may be explained by the lower saturation solubility of ibuprofen in water (318.98 μg mL^{-1}) compared to phosphate buffer pH:7.2 (1234.09 μg mL^{-1}) (Attari et al., 2015). The dissolution profiles of the nanoparticle agglomerates prepared according to the matrix of the full factorial design are shown in Fig. 3.17. Nanoparticle agglomerates stabilised with either HPMC or TPGS exhibited enhanced dissolution profiles compared to ibuprofen. In the case of the raw ibuprofen, less than 40% was released in the first 20 min, while the nanoparticle agglomerates achieved complete dissolution in less than 5 min. The exception to this were the spray-dried nanosuspensions of ibuprofen without matrix former (patterns 1-- and 2--) which exhibited a higher

dissolution rate compared to ibuprofen but slower than the nanoparticle agglomerates containing mannitol and/or leucine. In the case of TPGS, this may be associated with the formation of large aggregates with size around 50 μm and poor redispersibility. Thus, the selection of suitable process and formulation parameters is of paramount importance in order to ensure that the dissolution benefit of nanoparticles is retained after the spray- drying process.

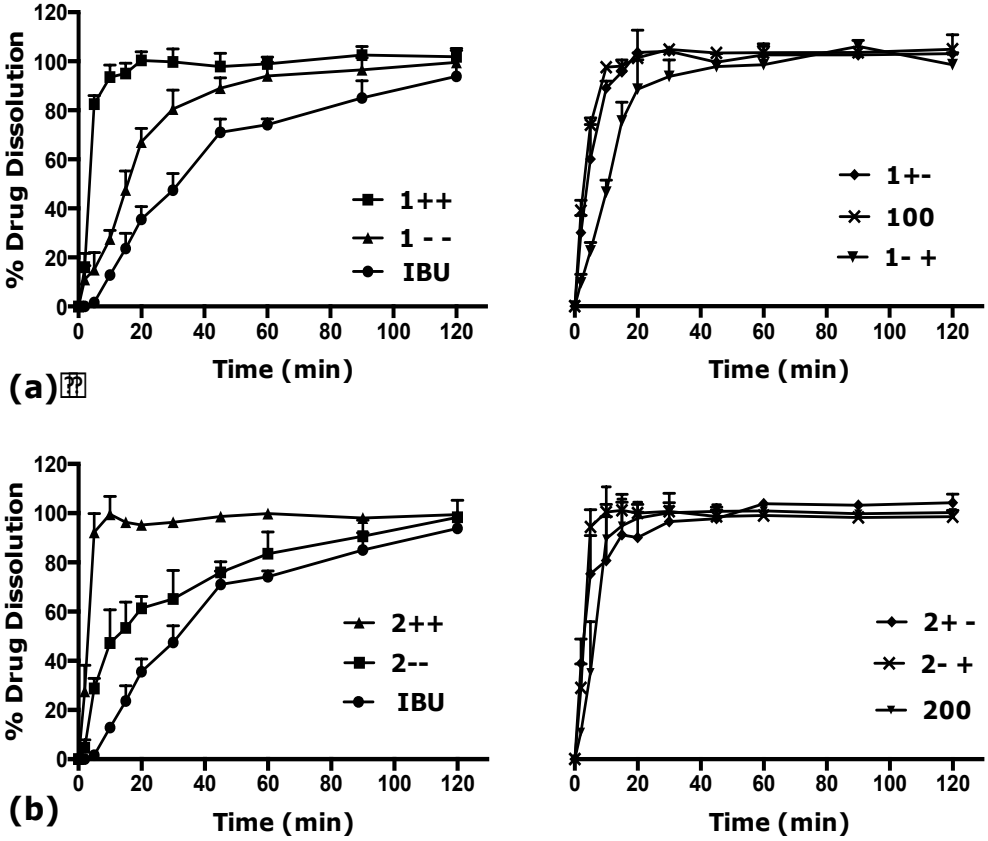

Figure 3.17 Dissolution profiles of ibuprofen starting material and nanoparticle agglomerates included in the full factorial design (mean + SD, n=3).

In this study no differences could be observed in the dissolution profiles of nanoparticle agglomerates containing different amounts of matrix formers. At this point, it should be noted that Yamasaki et al. (2011) using a flow-through setup found that increasing mannitol amounts enhanced the dissolution rate of ciclosporin A nanomatrix powders. Even if a comparison between the dissolution profiles of the two drugs is not feasible as they possess different physicochemical properties and different dissolution media were used, it should be highlighted that the dissolution testing method plays a significant role as well. A flow-through cell method was found to be

unequivocally the most robust method for nanoparticulate systems when compared with paddle, basket and dialysis method (Heng et al., 2008).

3.4.4.6.*In-vitro* aerosol performance

Fine particle fraction (FPF%) was selected as a quality attribute describing the aerodynamic performance of a dry powder for inhalation. The FPF% values of the nanoparticle agglomerates produced ranged from 5.84 to 68.55% (Table 3.3) and the model generated was found to be significant ($p < 0.05$, Fig.3.18).

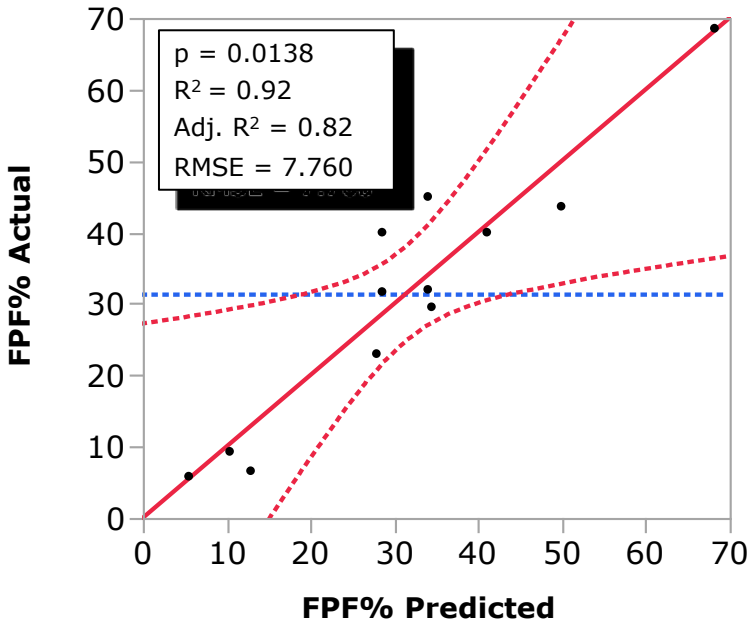

Figure 3.18 Actual vs predicted fine particle fraction (FPF%) of the nanoparticle agglomerates of ibuprofen.

Leucine to drug ratio and mannitol to drug ratio were identified as the most significant factors on the FPF% (Table 3.8.). The positive effect of leucine can be linked with its properties as an aerosolisation enhancer. According to Sou et al. (2013), the addition of leucine facilitates the formation of spray-dried particles. More specifically, addition of leucine (≈10% w/w) was found to increase the aerosolisation performance of particles by accumulating on their surface resulting in the formation of individual spherical particles. When leucine was used in higher amounts (≈20% w/w), it was found to produce particles of wrinkled morphology. The corrugated surface of the particles

increases their dispersibility from the inhalation device by reducing the contact points between particles and cohesiveness of the powdered nanoparticle agglomerates.

The positive effect of mannitol to drug ratio may be attributed to the good spray-drying properties of mannitol which facilitates the formation of spherical particles with narrow and unimodal particle size distribution (Li et al., 2014). As illustrated in the response surface plot (Fig. 3.19), both leucine and mannitol to drug ratio had a significant effect on the aerodynamic performance of the nanoparticle agglomerates resulting in large FPF% increase from 10% to 50%. Therefore, combination of high leucine and mannitol to drug ratios is required in order to maximise the FPF% of the nanoparticle agglomerates of the low melting point and ductile ibuprofen.

Table 3.8 Sorted parameter estimates of effects and two-way interactions on the fine particle fraction (FPF%) of the nanoparticle agglomerates of ibuprofen.

Term	t-ratio	prob > |t|
Leucine to drug ratio (0,0.5)	4.93	0.0044*
Mannitol to drug ratio (0,1)	3.01	0.0298 *
Type of stabiliser [HPMC] * Mannitol to drug ratio (0,1)	2.50	0.0543
Type of stabiliser [HPMC]	1.06	0.3366
Mannitol to drug ratio * Leucine to drug ratio	0.90	0.4071
Type of stabiliser [HPMC] * Leucine to drug ratio	-0.46	0.6649

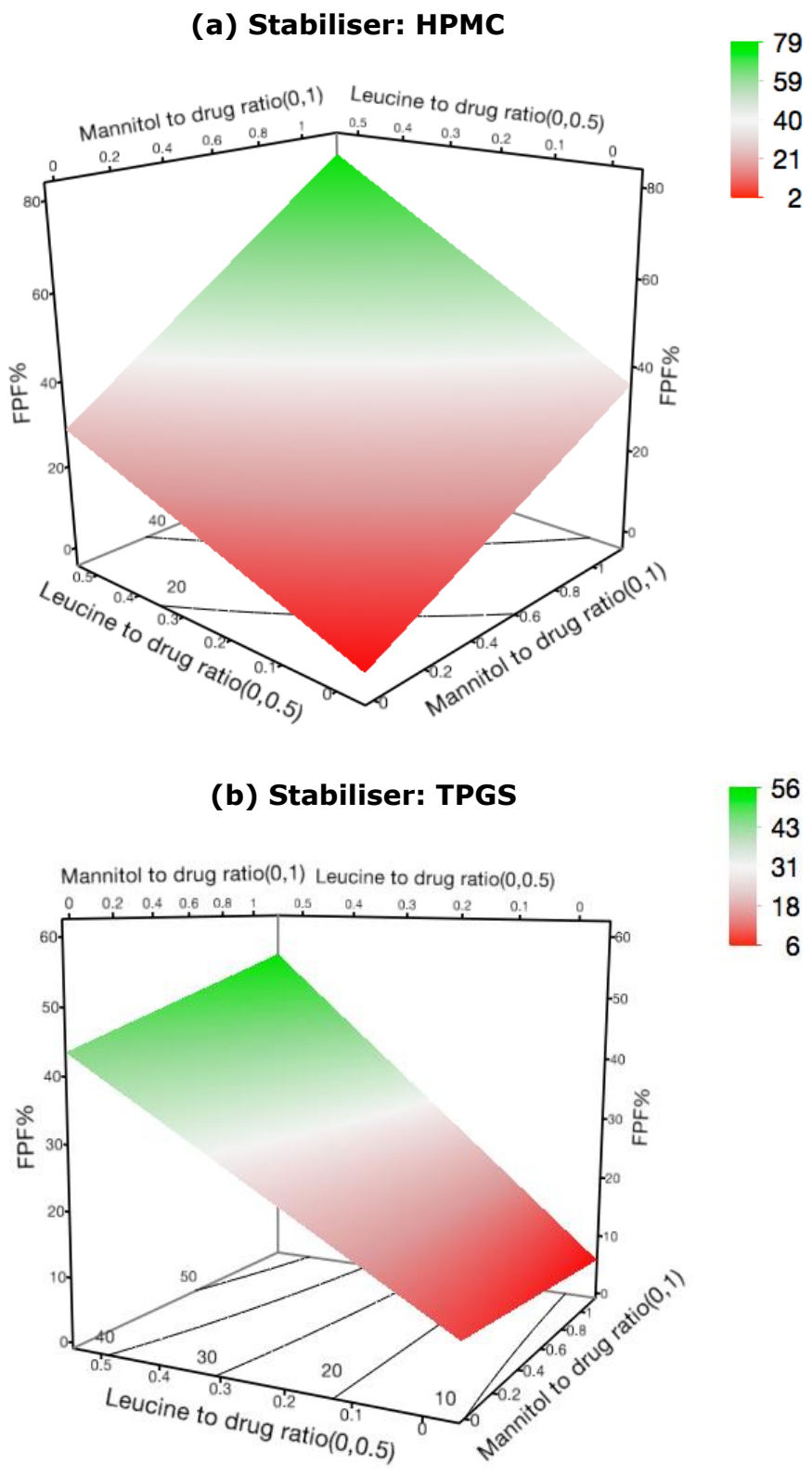

Figure 3.19 Response surface plots showing the influence of the independent formulation variables mannitol to drug ratio and leucine to drug ratio on the quality attribute fine particle fraction (FPF%) of the nanoparticle agglomerates of ibuprofen. The stabiliser is (a) HPMC and (b) TPGS.

3.5. Conclusions

Based on the aforementioned results presented in this chapter, it can be concluded that:

1. Nanosuspensions of the poorly water-soluble, low melting point and ductile drug ibuprofen stabilised with HPMC and TPGS were successfully produced and were further spray dried with or without the addition of matrix formers (mannitol and/or L-leucine) employing a full factorial design.
2. Design of experiments is a useful approach in order to gain insight and understanding on the formation of inhalable nanoparticle agglomerates using wet milling followed by spray drying.
3. Leucine to drug ratio, mannitol to drug ratio and the type of stabiliser were found to be significant ($p < 0.05$) factors affecting the yield of the particles obtained by combining wet milling and spray drying. The particle size response was mainly dependent on the leucine to drug ratio and the type of stabiliser ($p < 0.05$). Mannitol to drug ratio was found as the only critical parameter affecting redispersibility of nanoparticle agglomerates ($p < 0.05$) and both leucine to drug ratio and mannitol to drug ratio were found as significant factors affecting FPF% ($p < 0.05$).
4. The nanoparticle agglomerates were found to be crystalline and exhibit enhanced dissolution compared to the ibuprofen starting material.
5. High leucine and mannitol to drug ratio should be incorporated in ibuprofen nanosuspensions prior to spray drying in order to increase the yield of the process and produce nanoparticle agglomerates with enhanced redispersibility and aerosolisation efficiency.

CHAPTER 4

MICROCOMPOSITE PARTICLES OF THEOPHYLINE

4. MICROCOMPOSITE PARTICLES OF THEOPHYLLINE

4.1. INTRODUCTION

As described in the previous chapters, preparation of nanosuspensions by a wet size reduction technique (e.g. wet milling, high pressure homogenisation, antisolvent precipitation) followed by solidification, using spray drying, has been suggested as a preparation platform for inhalable micrometer-sized composites of nanocrystals with enhanced dissolution and aerosolisation efficiency (Bosch et al., 1999; Pilcer et al., 2009; Yamasaki et al., 2011).

The majority of such reported applications (nano-in-micro particle engineering approach) has focused on poorly water-soluble drugs and thus the size reduction step can take place in aqueous media where the drug is dispersed but not dissolved (Duret et al., 2012; Pomázi et al., 2013). However, some drugs used for the treatment of respiratory diseases are moderately or very water-soluble, such as salbutamol sulfate (albuterol sulfate) and terbutaline sulfate, or are prone to hydrate formation, e.g. nedocromil sodium. Therefore, water cannot be used as the wet milling medium, in the preparation of nanosuspensions for such drugs nor as the solvent during the spray-drying step as for poorly water-soluble drugs. Instead, an appropriate organic solvent has to be selected, in which the drug exhibits a solubility lower than 10 mg mL^{-1} and ideally lower than 5 mg mL^{-1} (Hong and Oort, 2011), to eliminate the possibility of crystallinity changes (e.g. amorphisation) during milling and spray drying.

Theophylline has been chosen as the model compound in this study as it has a long history of use within respiratory medicine, and its solid-state properties have been extensively investigated. More specifically, anhydrous theophylline is a challenging molecule with respect to wet milling and spray drying due to the following physicochemical properties:

(i) It is moderately water-soluble (7.36 mg mL^{-1}, at 25 ^{o}C, Yalkowsky et al., 2010).

(ii) Its needle-like crystal morphology can affect its fracture/breakage behaviour, as reported for other organic crystalline materials (Ho et al., 2012).

(iii) It is prone to process-induced solid-state transformations as it exists in four polymorphic forms (forms I-IV) along with a

monohydrate form (Fucke et al., 2012). Form II is the stable polymorph at room temperature while the monohydrate is the stable form in water and at high relative humidity environment.

Theophylline is a widely available and inexpensive methylxanthine that has been used in the treatment of airways diseases such as asthma and COPD for more than 90 years (Barnes, 2013).

The use of theophylline has been limited by its narrow therapeutic index (TI) and the marked inter-subject variability of its clearance. A therapeutic plasma concentration of 10 - 20 mg L^{-1} is required for theophylline to achieve bronchodilation comparable with β_2-agonists, while side effects (e.g. nausea, vomiting, heartburn, diarrhea) become an issue at concentrations above 20 mg L^{-1} (Barnes, 2013). Due to its narrow TI, it is administered as oral sustained-release (SR) preparations.

There is increasing evidence that theophylline at low doses (plasma concentrations < 7 mg L^{-1}) exhibits immunomodulatory properties in the pathophysiology of both asthma and COPD (Barnes, 2013). Moreover, it has been reported that theophylline has the potential to enhance the anti-inflammatory effect of corticosteroids and to reverse steroid resistance that is common in COPD patients (Hirano et al., 2006; Tilley, 2011). These observations may lead to the reevaluation of this old drug in the future, once clinical trials of low-dose theophylline therapy are completed (Barnes, 2008; 2003).

Theophylline applied intratracheally as a dry powder formulation to the airways of anaesthetised guinea pigs exhibited smooth muscle relaxant and anti-inflammatory properties at very low doses that would be predicted to have no systemic toxicity (Raeburn and Woodman, 1994). Thus, developing inhalable formulations for theophylline may offer advantages over oral administration for the treatment of inflammation in asthma and COPD, enhancing the local efficacy of the drug while minimising systemic side effects (Raeburn and Woodman, 1994; Zhu et al., 2015a).

There are few published studies on engineering inhalable theophylline particles. A low-dose pMDI formulation of theophylline (Zhu et al., 2015a) and formulations for DPIs (polymeric composite particles, microspheres, co-

crystals and nanosized rods agglomerates) have been produced and characterised (Alhalaweh et al., 2013; Kadota et al., 2015; Momeni and Mohammadi, 2009; Salem et al., 2011; Zhang et al., 2009; Zhu et al., 2015b). Blends of theophylline microparticles (63-90 μm) with inhalable budesonide and terbutaline particles (< 5 μm) were proposed as a formulation approach for concurrent oral and pulmonary drug delivery with theophylline acting as a carrier (Salama et al., 2014).

The aim of this chapter is to produce inhalable dry powder formulations of theophylline, by coupling wet bead milling in an organic solvent with spray drying of the milled suspension. The effect of mannitol addition during the wet milling of theophylline on the micromeritic, solid state and aerosol performance of the produced spray-dried particles will be investigated. The experimental data of this study are complemented with a computational study of the interaction between theophylline and mannitol (i.e. crystal morphology modelling and lattice matching calculations) in order to elucidate the role of mannitol as a co-milling agent.

4.2. MATERIALS

Theophylline (THEO), 3,7-dihydro-1,3-dimethyl-1H-purine-2,6-dione (LKT Laboratories, USA), was used as the drug under investigation. D-mannitol (MAN, Pearlitol 160C®, Roquette Freres, France) was used as co-milling agent and matrix former of the microcomposites (Fig. 4.1 and Table 4.1). Isopropanol (IPA, Thermo Scientific, UK) was used as the milling medium for the preparation of suspensions. Methanol and water both from Fisher Scientific UK, and trifluoroacetic acid (TFA, Sigma-Aldrich Co., USA) were used for the HPLC analysis. All the solvents used were of analytical grade.

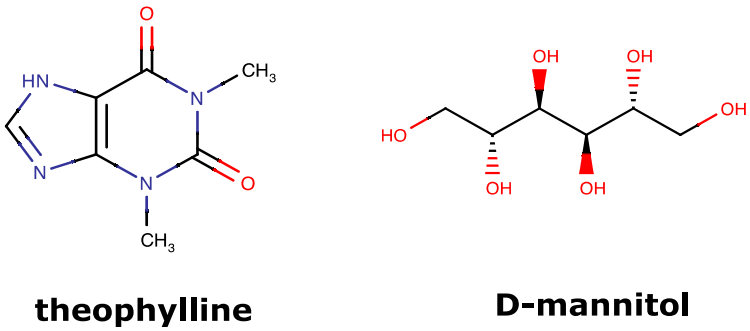

Figure 4.1 Chemical structures of theophylline and D-mannitol.

Table 4.1 Physicochemical properties of theophylline and mannitol.

Compound	Molecular weight (g mol^{-1})	Melting point (°C)	Solubility (mg mL^{-1}) at 25 °C	
			water	isopropanol
Theophylline	180.16	271-274	7.36[a]	2.45[b]
Mannitol	182.17	166-168	Soluble[c]	0.01[c]

[a] Yalkowsky et al., 2010; [b] Krasnov, 2011; [c] Rowe et al., 2012

4.3. METHODS

4.3.1. Preparation of suspensions

Suspensions were prepared by wet bead milling using a laboratory planetary mill (Pulverisette 5, Fritsch Co., Germany). 1.0 g of solids (THEO and MAN) and 10 g of milling beads (0.5 mm diameter aluminum borosilicate glass grinding beads, Gerhardt Ltd, UK) were weighed into a glass vial of 14 mL capacity and suspended in 10 mL IPA, as the dispersing medium. The total concentration of solids (THEO and MAN) in suspension was kept constant (10% w/v) and different THEO to MAN mass ratios (i.e. 25:75, 50:50 and 75:25) were employed (Table 4.2). The vials were placed into a stainless steel milling pot with a maximum loading capacity of 8 pots. Rotation speed (300 rpm) and milling duration (6 cycles of altered bowl rotation direction) were selected based on preliminary experiments. Each milling cycle comprised 60 min rotation followed by a 20 min pause to cool down the milling vessels and to prevent overheating of the instrument's rotors. The suspensions were left to cool to room temperature and collected by withdrawal with a pipette to separate from the milling beads.

4.3.2. Preparation of spray-dried microcomposite particles

The suspensions were diluted 1 in 2 with IPA, before spray drying, to obtain suspensions with an overall solid concentration 5% w/v in IPA. Spray drying was performed with a Gea Niro Spray Dryer SD Micro™ (Gea Process Engineering, Denmark, Fig.4.2) operated with nitrogen as the drying gas. An inlet temperature of 80 ± 3 ^{o}C was selected, and the atomiser gas flow and chamber inlet flow were set at 2.5 and 25 kg h^{-1}, respectively. The nozzle pressure was set at 1.5 bar and the bag filter pressure at 2.1 bar. The outlet temperature control was set at 20%, resulting in an outlet temperature of 60 ± 5 ^{o}C.

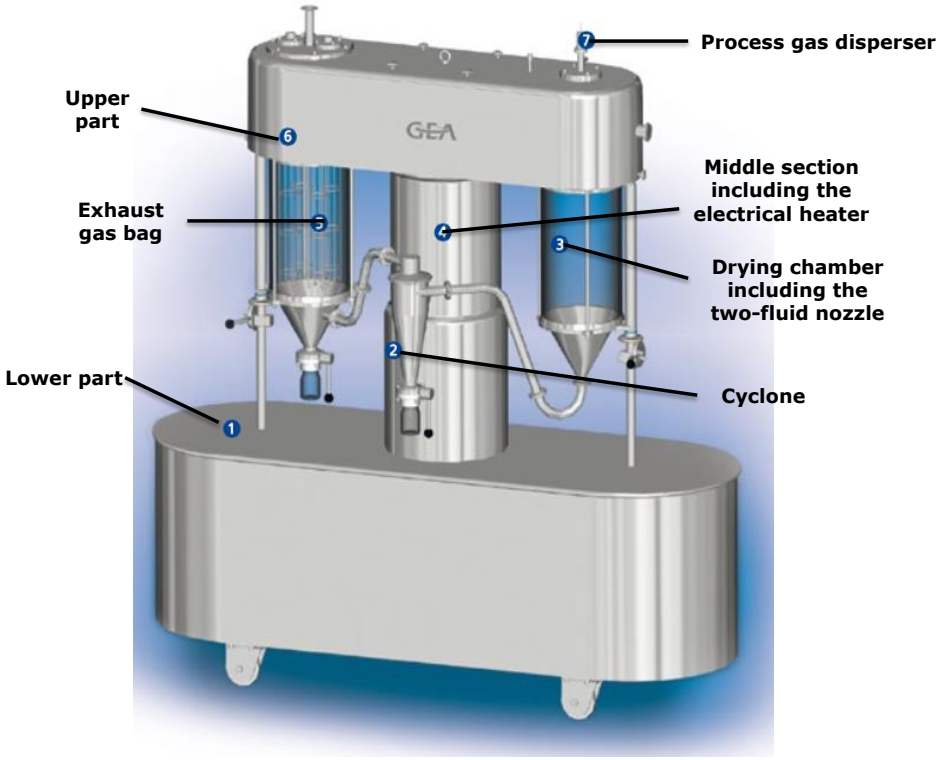

Figure 4.2 Gea Niro Spray Dryer SD Micro™. Adapted from Gea Process Engineering, 2013

4.3.3. Characterisation of spray-dried microcomposite particles

In this chapter, no further characterisation of the produced suspensions was carried out due to limitations of the available instrumentation. Regarding transmission electron microscopy (TEM), negative staining protocols treat the sample with aqueous solution of 1% uranyl acetate. This sample pre-treatment leads to dissolution of the theophylline and mannitol fine crystals.

The spray-dried powders were characterised for: particle surface morphology and shape by scanning electron microscopy (SEM) and image analysis of the SEM images; particle size distribution (PSD) by laser diffractometry; specific surface area by the Brunauer-Emmett-Teller (BET) method; solid state by X-ray powder diffraction (XRPD), Fourier transform infrared spectroscopy (FT-IR) and differential scanning calorimetry (DSC); drug loading by HPLC analysis of theophylline content and in-vitro aerosol performance using the next generation impactor (NGI).

The SEM, laser diffraction, XRPD and DSC methods applied have been described in previous chapters (sections 2.3.5.1-2.3.5.4).

4.3.3.1. Image Analysis

SEM images were processed with the open source image processing software FIJI/Image J (Schindelin et al., 2012) to determine the number-based aspect ratio of the particles. The major and minor axis (i.e. primary and secondary axis of the best fitting ellipse) of a minimum of 100 particles was measured for each spray-dried powder and for the starting materials, and the aspect ratio was calculated as the ratio of the minor to the major axis.

4.3.3.2. Specific surface area and porosity

The specific surface area was measured using the nitrogen adsorption Brunauer-Emmett-Teller (BET) method with a Quantachrome Nova 4200e multi-station gas sorption surface area analyser (Quantachrome Ltd, UK) Approximately 0.1 g of each powder was placed in each sample cell, and the outgassing process was conducted at 105 ^{o}C over 2 h. The total pore volume and the average pore radius were calculated following the t-plot method which was introduced by de Boer et al. (1966) and compares comparing the isotherm of a microporous material with a standard Type II isotherm. Each formulation was tested in triplicate (n=3).

4.3.3.3. Fourier transform infrared spectroscopy (FT-IR)

Spectra of the starting materials, their physical mixtures and the microcomposites were recorded using a Spectrum^{100} FT-IR spectrometer (PerkinElmer, Inc., USA) equipped with the attenuated total reflection sampling accessory. Samples were scanned at room temperature, at the transmission mode, over a wavenumber range of 4000-650 cm^{-1}, 16 accumulations and 1 cm^{-1} resolution. Before each measurement, a background spectrum of air was acquired under the same instrumental conditions. The acquired spectra were processed using the PerkinElmer Spectrum Express software.

4.3.3.4. Drug loading

5 mg of each spray-dried formulation were dissolved in 25 mL water and theophylline concentration determined using an HPLC system (Agilent 1100 Series, Agilent Technologies, Germany) following the method described by Alhalaweh et al. (2013). More specifically, the stationary phase was a Luna® (150 x 4.60 mm, 5 micron) column (Phenomenex Co., California, USA) kept at 40 ^{o} C. The mobile phase was composed of aqueous trifluoroacetic acid

solution (0.1% v/v) and methanol at 75/25 volumetric ratio. The mobile phase flow rate was 1 mL min^{-1}, the injection volume was 10 μL and the detection wavelength 273 nm. The retention time for theophylline was 4.8 min. The correlation coefficient of the calibration curve was R^2: 0.9997 for a concentration range of 5-400 μg mL^{-1}, indicating acceptable linearity. Each formulation was tested in triplicate (n=3).

4.3.3.5. In-vitro aerosol performance

Deposition profiles were determined with Ph. Eur. Apparatus E (Next Generation Impactor, NGI, Copley Instruments Ltd, UK) fitted with a stainless steel 90^O induction port (IP) and a pre-separator (PS) operated as specified in European Pharmacopoeia (Ph. Eur. 8^{th} edition, monograph 2.9.18) and connected to a high-capacity vacuum pump (Model HCP5, Copley Instruments Ltd, UK). Prior to use, the impaction cups in each of the seven stages were coated with 1% w/v silicone oil solution in hexane, and allowed to dry for 1 h, in order to minimise 'particle bounce' and entrainment of particles between the stages. The final stage of the impactor, known as micro-orifice collector (MOC), was fitted with a fiberglass filter (nylon 0.45 μm, Millipore, UK). The flow rate was measured using a flow meter (Flow Meter Model DFM 2000, Copley Instruments Ltd, UK) prior to each run, to ensure that a flow of 60 L min^{-1} was achieved. Gelatin capsules (size 3) were filled with accurately weighed amounts of product corresponding to about 10 mg of THEO. Following filling, capsules were stored in a desiccator over silica gel for 24 h prior to performing the deposition study. Storage for 24h allowed relaxation of any electrical charge without influencing the brittleness of the capsules as their water content in preliminary studies was found to comply with the normal moisture specification limits (13-16% for gelatin). The inhaler device (Cyclohaler®) was connected to the impactor via an airtight rubber mouthpiece adaptor and tested at 60 L min^{-1} for an actuation time of 4 s. The capsules were discharged into the NGI, and after dispersion the powder deposited on the capsules, mouthpiece, inhaler and each NGI component was collected by exhaustively washing with water (HPLC grade), transferred into volumetric flasks and assayed. The HPLC conditions for the assay were the same to those for drug content determination (section 4.3.3.4). To characterise the aerosol performance the following parameters were determined: the emitted fraction (EF %) was calculated as the ratio of

the drug mass depositing in the mouthpiece, induction port, pre-separator, and impactor stages (1 to MOC) to the cumulative mass of drug collected following actuation (total drug deposited in the capsule, inhaler, mouthpiece, throat, pre-separator and stages). The fine particle fraction (FPF %) of each dose was the ratio of the drug mass depositing on stages 2 to MOC over the recovered dose. The fine particle dose (FPD) was calculated as the ratio of mass deposited on stage 2 to MOC, to the number of doses (n=3). Stage 2 had a cut-off diameter of 4.46 μm. The mass median aerodynamic diameter (MMAD) defined as the median particle diameter of the formulation deposited within the NGI, and the geometric standard deviation (GSD) determined as the square root of the ratio of the particle size at 84.13th percentile to that of 15.87th percentile. Both MMAD and GSD were determined from the linear region in the plot of the cumulative mass distribution versus the logarithm of aerodynamic diameters. Each formulation was tested in triplicate (n=3).

4.3.4. Statistical data analysis

An analysis of variance (one-way ANOVA) with Tukey's multiple comparison test was carried out to evaluate differences between the mean values using Prism 6 (GraphPad Software, Inc., USA). Probability values less than 0.05 were considered as indicative of statistically significant differences.

4.3.5. Computational study of the interaction between the crystals of theophylline and mannitol

In order to gain insight into the intermolecular interactions that influence the mechanical properties of theophylline and mannitol, the energetic and structural aspects of their crystals were investigated following a combination of approaches, namely: crystal morphology modelling, semi-classical density sums (SCDS-Pixel) and lattice matching calculations. Crystal structure coordinates for theophylline form II (CSD-REFCODE BAPLOT01, Ebisuzaki et al., 1997) and D-mannitol form β (CSD-REFCODE DMANTL07, Kaminsky and Glazer, 1997) were taken from the Cambridge Structural Database (Allen, 2002).

4.3.5.1. Crystal morphology modeling

The minimisation of the energy of the crystal lattice was performed using the General Utility Lattice Program (GULP v.4.3) (Gale and Rohl, 2003). The

Dreiding 2.21 force field parameters (Mayo et al., 1990) were used in combination with high-quality electrostatic potential-derived atomic point charges calculated at the 6-31G**/MP2 level of theory. For the determination of the atomic charges the Firefly quantum chemistry package was used (A. Granovsky, http://classic.chem.msu.su/gran/gamess/index.html), which is partially based on the GAMESS (US) source code (Schmidt et al., 1993). Crystal morphologies based on Bravais-Friedel-Donnay-Harker (BFDH) theory (which assumes that the slowest growing faces are those with the greatest interplanar spacing, d_{hkl}) were constructed in order to identify faces more likely to occur in the crystal. For the morphology calculations the GDIS program was utilized, serving as a graphical front end to the GULP software program (Fleming and Rohl, 2005).

4.3.5.2. Semi-classical density sums (SCDS-Pixel) calculations

The crystal structures were analysed using the PIXEL approach developed by Gavezzotti (Gavezzotti, 2005). This method provides quantitative determination of crystal lattice energies and pairwise intermolecular interactions, with a breakdown of these energies into coulombic, polarisation, dispersion and repulsion terms. For the derivation of PIXEL energies, the electron density of theophylline and mannitol were calculated at the 6-31G**/MP2 level of theory using the Firefly quantum chemistry package. Finally, energy vector diagrams were constructed according to Shishkin et al. (2012) using the processPIXEL package and the results were visualised using the Mercury software program (Bond, 2014; Macrae et al., 2008; Shishkin et al., 2012).

4.3.5.3. Computational lattice matching calculations

Possible interactions between crystal faces of theophylline and mannitol were probed applying a computational lattice matching approach, using the Geometric Real-space Analysis of Crystal Epitaxy (GRACE) software (Mitchell et al., 2011). Cut-off distances of dc = 0.5 Å and d0 = 0.3 Å were selected. The value of θ was varied in the range of −90° to 90° with increments of 0.5°, and a search area of 400 × 400 Å and a range of overlayer *hkl* planes from $-3 \leq h, k, l \leq +3$ were employed. The epitaxy score, E, was calculated using the Gaussian function. The chemical complementarity at the

geometrically matching crystal faces was evaluated by visual inspection of the crystal structures using the Mercury software program (Macrae et al., 2008).

4.4. RESULTS AND DISCUSSION

4.4.1. Preparation of microcomposite particles

Isopropanol (IPA) was selected as the wet milling medium based on preliminary solubility measurements. The lower solubility of anhydrous theophylline in IPA (2.81 ± 0.18 mg mL^{-1}, at 25 ^{o}C for 24h) compared to its aqueous solubility (7.36 mg mL^{-1}, at 25 ^{o}C, Yalkowsky and He, 2003) ensured the formation of nanocrystals that will be suspended in the liquid medium. Also, it may limit the risk of solution-mediated phase transformation that can give rise to increased amounts of amorphous form. Moreover, anhydrous theophylline is transformed to monohydrate when processed in water, while such hydration transition is not expected to occur in IPA.

Wet bead milling of anhydrous theophylline, in IPA, did not result in the production of nanosized particles, even after 6 h milling. By contrast, wet milling of mannitol in IPA resulted in submicron-sized particles. The minor axis and major axis of the primary mannitol nanocrystals based on image analysis of SEM images were 405.44 ± 58.72 nm and 724.24 ± 113.46 nm, respectively. Therefore, use of isopropanol as the wet milling medium and mannitol as co-milling agent were selected.

The use of mannitol (MAN) as a co-grinding agent, enhancing the size reduction of drug particles and even leading to an increase in their bioavailability, has been reported previously (Kubo et al., 1996; Takahata et al., 1992). However, in these earlier studies dry grinding techniques were used and the authors mainly focused on bioavailability studies in animals rather than on the mechanism underlying size reduction of drug particles in the presence of mannitol.

Mannitol is a commonly used matrix former during the solidification of aqueous nanosuspensions, for both oral and pulmonary drug delivery. It is usually incorporated prior to spray drying due to its high aqueous solubility, and forms a continuous matrix around the drug nanocrystals enhancing their

redispresibility on rehydration (Chaubal and Popescu, 2008; Yue et al., 2013). It should be noted that in this study mannitol is not dissolved prior to spray drying but rather is added before the wet milling of anhydrous theophylline, i.e. both substances are in suspended form due to their marginal solubility in IPA. The total concentration of solids (THEO and MAN) in suspension was kept constant (5% w/v) and different THEO to MAN mass ratios (i.e. 25:75, 50:50 and 75:25) were employed (Table 4.2) in order to elucidate the potential effect on the particle size reduction of theophylline, and also on the micromeritic, solid state and aerosolisation properties of the microcomposite particles produced.

Table 4.2 Nominal composition and assayed theophylline content (% w/w) of microcomposite particles together with the calculated drug loading efficiency (%) (mean ± SD, n=3).

Formulation	Content (% w/w)			Drug loading efficiency (%)
	Nominal		Assayed	
	THEO	Mannitol	THEO	
SD susp. THEO	100	-	n/a	n/a
SD susp. THEO:MAN 75:25	75	25	76.2 ± 0.1	101.6 ± 0.1
SD susp. THEO:MAN 50:50	50	50	53.3 ± 0.1	106.7 ± 0.1
SD susp. THEO:MAN 25:75	25	75	28.7 ± 0.2	114.1 ± 1.0
SD susp. MAN	-	100	n/a	n/a

4.4.2. Characterisation of microcomposite particles

4.4.2.1. Micromeritic properties

The SEM images of starting materials are presented in Fig. 4.3. Anhydrous theophylline (THEO) particles consisted of primary crystallites bound together to form needle–shaped particles with a D_{50} of 124.12 ± 18.33 μm. Mannitol particles also exhibited an elongated morphology, with a D_{50} of 68.07 ± 1.36 μm (Table 4.3).

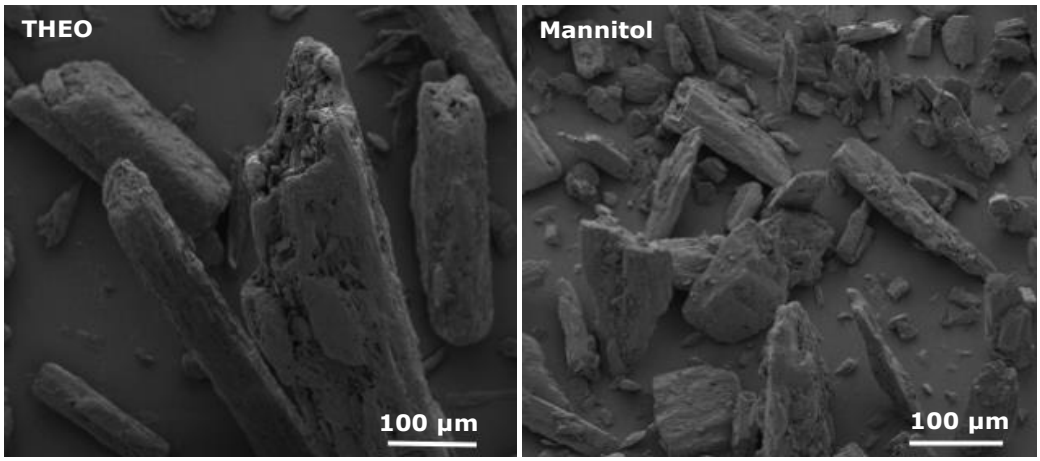

Figure 4.3 SEM images of theophylline and mannitol starting materials.

SEM images of the microcomposites produced by wet milling and spray drying are shown in Fig. 4.4. Wet milling of theophylline in the absence of mannitol followed by spray drying resulted in particles with smaller size compared to the raw drug, exhibiting a D_{50} of 4.64 ± 0.87 μm and an aspect ratio of 0.41 ± 0.14, with values closer to 1 indicating a more spherical shape (Table 4.3).

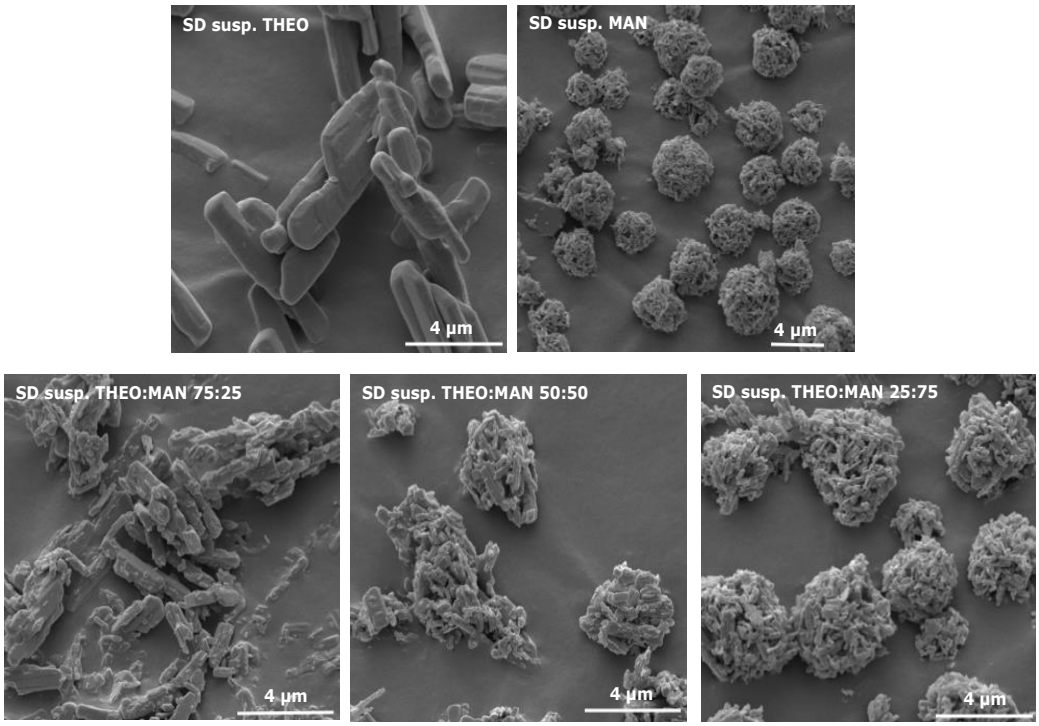

Figure 4.4 SEM images of microcomposite formulations containing theophylline and mannitol wet milled alone and in different mass ratios.

Simultaneous wet milling of theophylline and mannitol in isopropanol followed by spray drying resulted in microcomposite particles, which consisted of theophylline and mannitol crystals assembled together (Fig. 4.4). They exhibited D_{50} values ranging from 3.5 to 2 µm, with size decreasing as mannitol content increased, and D_{90} values less than 10 µm, making them potentially suitable for pulmonary drug delivery (Table 4.3).

Table 4.3 Particle size distribution data and aspect ratio values of the starting materials and microcomposite formulations containing different theophylline to mannitol ratios (mean ± SD, n=3).

Formulation	Size distribution: D_{10}, D_{50}, D_{90}			Image analysis
	D_{10} (μm)	D_{50} (μm)	D_{90} (μm)	Aspect ratio
THEO	29.90 ± 1.76	124.12 ± 18.33	352.27 ± 54.75	0.33 ± 0.18
Mannitol	12.23 ± 0.34	68.07 ± 1.36	208.13 ± 3.96	0.58 ± 0.21
SD susp. THEO	1.17 ± 0.31	4.64 ± 0.87	13.80 ± 4.60	0.41 ± 0.14
SD susp. THEO:MAN 75:25	0.97 ± 0.06	3.52 ± 0.68	9.72 ± 2.40	0.55 ± 0.15
SD susp. THEO:MAN 50:50	0.82 ± 0.05	2.95 ± 0.64	7.91 ± 1.95	0.68 ± 0.19
SD susp. THEO:MAN 25:75	0.61 ± 0.08	2.18 ± 0.30	5.11 ± 1.22	0.71 ± 0.12
SD susp. MAN	0.58 ± 0.03	2.86 ± 0.12	6.39 ± 0.50	0.85 ± 0.09

Inclusion of increasing amounts of mannitol resulted in production of particles with increased sphericity and porosity, demonstrated by aspect ratios closer to 1 and higher specific surface area and pore volume values, respectively (Table 4.3 and 4.4). Thus, addition of mannitol during wet milling in isopropanol facilitated the size reduction of theophylline crystals and their assembly in microcomposites by forming porous and spherical agglomerates of mannitol nanocrystals in which submicron theophylline particles are embedded.

Table 4.4 Specific surface area, total pore volume and average pore radius of the starting materials and microcomposite formulations containing different theophylline to mannitol ratios (mean, n=3)*.

Formulation	BET Surface area (m^2 g^{-1})	Total pore volume (cc g^{-1}) x10^3	Average pore radius (Å)
THEO	0.80	2.31	24.11
Mannitol	0.36	1.26	11.39
SD susp. THEO	5.23	8.63	21.82
SD susp. THEO:MAN 75:25	8.97	14.71	32.79
SD susp. THEO:MAN 50:50	9.64	20.14	41.77
SD susp. THEO:MAN 25:75	11.57	25.99	44.93
SD susp. MAN	19.73	39.13	39.67

* Relative standard deviation <4%

4.4.2.2. Solid state characterisation

The solid state of both theophylline and mannitol in the microcomposite formulations may change during either milling or spray drying. This was examined as different solid forms exhibit different physicochemical and mechanical properties, which may influence processability during product manufacturing and may also impact drug stability, solubility, dissolution and ultimately therapeutic efficacy (Adeyeye et al., 1995; Raw et al., 2004).

Mannitol is known to be highly crystalline even during milling and spray drying. It exists in three polymorphic forms; alpha (α), beta (β) and delta (δ) (Fronczek et al., 2003). The β-form is the stable form of mannitol, however both α- and δ-forms were found to be chemically and physically stable for at least 5 years when stored at 25 ^{o}C and 43% relative humidity (Burger et al., 2000). Preparation of mannitol particles by different methods (e.g. freeze drying, spray drying, jet milling or antisolvent crystallisation) as well as process parameters during spray drying (i.e. outlet temperature) have been reported to influence the solid form of D-mannitol (Kaialy and Nokhodchi, 2013; Maas et al., 2011; Tang et al., 2009).

XRPD is a fast and straightforward method for determining basic information regarding the solid state of a powdered material with a limit of crystallinity detection in amorphous drug compositions around 5-10% (Stephenson et al., 2001). According to the XRPD diffractograms of the starting materials (Fig. 4.5), the diffraction peaks of anhydrous theophylline are characteristic of form II (2 theta: 7.2 ^{o}, 12.6 ^{o}, 14.5 ^{o}) while for mannitol they are characteristic of the β form (2 theta: 14.7 ^{o}, 18.8 ^{o}, 23.6 ^{o}, 29.5 ^{o}). Similar results regarding the solid state of Pearlitol 160C®, the commercial type of mannitol used in our study, have been reported in other studies (Cares-Pacheco et al., 2015; Hulse et al., 2009).

The XRPD diffractograms of the spray-dried microcomposites of THEO wet milled alone (SD susp. THEO) exhibited the same characteristic peaks as the starting material, indicating that both processes (i.e. wet milling coupled with spray drying) did not alter the polymorphic form of anhydrous theophylline (Fig. 4.5). Similarly, the spray-dried microcomposite of mannitol wet milled alone (SD susp. MAN) was in the same form as the raw material (β-form) (Fig. 4.5).

For the microcomposites containing both THEO and MAN wet milled together in different mass ratios, the diffraction patterns shown in Fig. 4.5, were essentially summations of the patterns of the starting materials. In all cases, reduction in the intensities and broadening of the peaks, compared to the patterns of the starting materials, can be attributed to the smaller size of the primary crystals in the microcomposite formulations and strain caused by the milling process (Hecq et al., 2005).

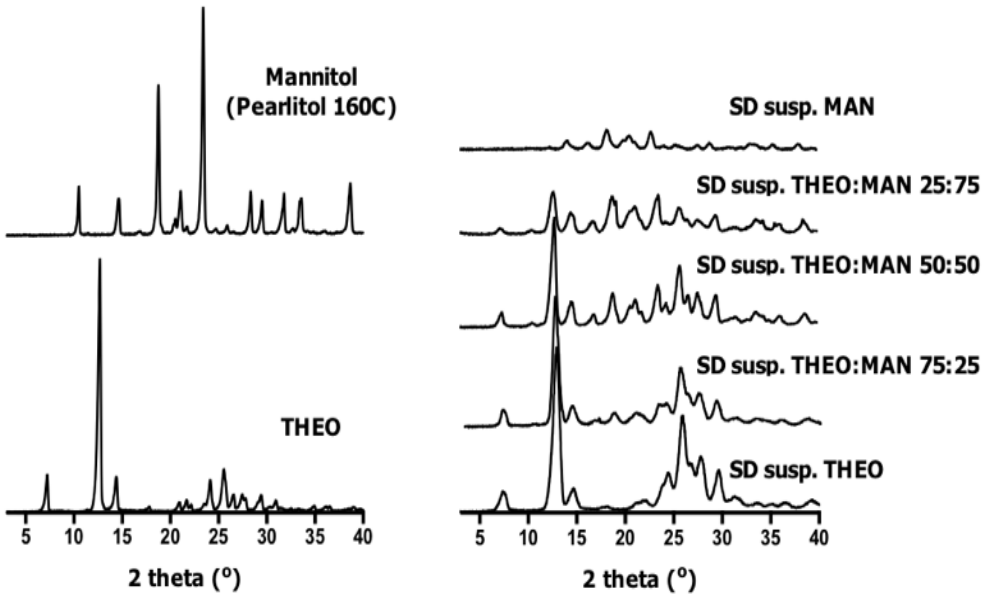

Figure 4.5 XRPD diffractograms of starting materials and microcomposite formulations containing different theophylline to mannitol ratios.

DSC was used to assess the thermal behaviour of the starting materials and the microcomposite formulations (Fig. 4.6). The DSC curve of the raw THEO showed an endothermic melting peak at 273 °C. The same thermal transition was observed for the SD susp. THEO formulation. The DSC of mannitol starting material (Pearlitol 160C®) and the SD susp. MAN showed one sharp endothermic peak at 167 °C that relates to the melting of mannitol crystals. Regarding the DSC curves of the microcomposite particles containing both THEO and MAN, instead of the expected two endothermic events corresponding to the melting of the two components, a change in the thermal behaviour of theophylline was observed in the presence of mannitol. More specifically, after the melting of mannitol at around 165 °C, theophylline appeared to dissolve completely in the melted mannitol when a drug load of up to 50 %w/w was used, and partially at higher drug loads leading to the broadening of the melting peak of theophylline and a shift

towards lower temperature (around 255 °C) compared to the raw THEO material.

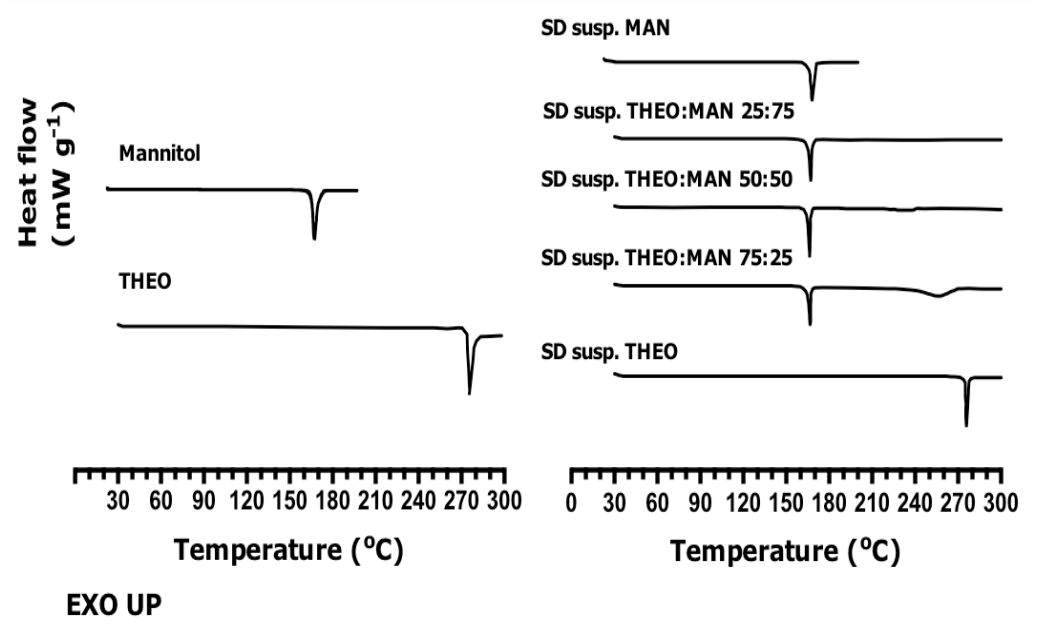

Figure 4.6 DSC thermograms of starting materials and microcomposite formulations containing different theophylline to mannitol ratios.

As the FT-IR spectra of the physical mixtures and spray-dried suspensions of THEO and MAN presented the same bands as the raw materials (Fig. 4.7), it can be assumed that the interaction between theophylline and mannitol is limited to temperatures above the melting point of mannitol (166 ± 2°C). Similar results have been reported for the interaction of mannitol with other drugs (e.g. carbamazepine and promethazine hydrochloride) indicating that DSC should not be used alone to detect any inherent incompatibility between substances, but it should be combined with other non-thermal techniques, such as XRPD and FT-IR (Flicker et al., 2011; Joshi et al., 2002; Thumma and Repka, 2009).

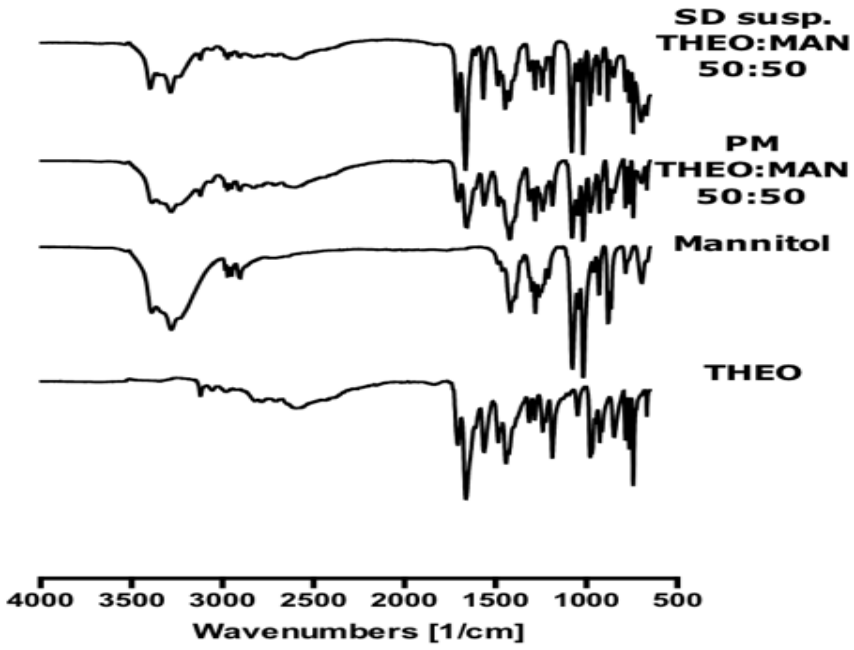

Figure 4.7 FT-IR spectra of starting materials, physical mixture (PM) of theophylline and mannitol (mass ratio 50:50) and SD susp. THEO:MAN 50:50.

Overall, the XRPD data suggest that the engineered microcomposite formulations retain their crystallinity during wet bead milling followed by spray drying. The preservation of the crystalline state is advantageous, ensuring the long-term physical stability of the formulations during storage. At this point, it should be highlighted, that dry milling techniques (e.g. air jet milling and ball milling) can induce crystal defects and even cause surface amorphisation of the particles (Ward and Schultz, 1995). These phenomena seem to be avoided during wet bead milling, as the liquid medium ensures rapid recrystallisation of potentially formed amorphous regions (Kayaert and Van den Mooter, 2012). Another suggested mechanism is that the liquid media allows fast cooling during particle breakage, which can minimise formation of local hot spots on particle surfaces and thus reduce the extent of surface amorphisation (Monteiro et al., 2012).

4.4.2.3. Drug loading

The value for THEO content in microcomposites are given in Table 4.2. The assayed THEO content was close to the nominal value, indicating no significant loss or powder segregation during the production processes. The small deviation of the assayed THEO amount compared to the theoretical value may be attributed to the suspension collection method employed at the

end of the milling process. Separation by pipetting cannot achieve total suspension recovery with small amounts remaining among the beads. In industrial settings this is unlikely to be an issue as mills with separate holding and receiving tanks equipped with paddle mixers are used (Monteiro et al., 2012). In this way, enhanced suspension homogeneity and recovery are ensured leading to the production of formulations with consistent drug loading.

4.4.2.4. In-vitro aerosol performance

The drug deposition profiles of the formulations produced are shown in Fig. 4.8, while parameters of their aerosol performance are given in Table 4.5. The SD susp. THEO exhibited a significantly lower emitted fraction (EF%) of 65.6 ± 0.8 compared to the formulations containing mannitol ($p<0.05$), which may be attributed to the needle-shaped morphology. Elongated particles, despite their ability to travel further in the lung airway, were found to have poor dispersion from inhaler when administered as dry powders for inhalation as they are subject to strong attractive forces when in contact along their axis (Crowder et al., 2002). For the formulations containing mannitol, reduced capsule and device retention was observed, leading to EF% of around 80% for all the various theophylline to mannitol (THEO:MAN) ratios examined in this study (Table 4.5). This may be attributed to their more spherical size that allows them to leave the capsule and device by the additional mechanism of rolling.

Wet milling of theophylline in the presence of mannitol followed by spray drying resulted in particles with enhanced aerosol performance as demonstrated by the higher fine particle fraction (FPF%) and fine particle doses (FPD) achieved compared to the SD susp. THEO. More specifically, the SD susp. THEO achieved a FPF of 26.1 ± 7.1 % and a mass median aerodynamic diameter (MMAD) of 4.5 ± 1.1 μm while incorporation of mannitol resulted in approximately 2- fold increase in FPF% ($p<0.05$), depending on the drug to mannitol ratio, and in MMADs close to 3 μm for the respective formulations (Table 4.5). Increasing the concentration of mannitol from 25% to 50% w/w or 75% w/w resulted in slightly higher FPF% however the increase was not found statistically significant ($p>0.05$). Moreover, increasing mannitol concentration shifted drug deposition from stages 2 and 3 to lower stages of the impactor (i.e. stages 4 to 6) (Fig. 4.8).

It is known, that the aerodynamic diameter, which is a function of the geometric size and particle density, governs the behaviour of a particle in the airstream. Thus, the improved aerosolisation efficiency of the formulations containing mannitol may be attributed to their smaller particle size and increased porosity compared to SD susp. THEO (Table 4.3 and 4.4).

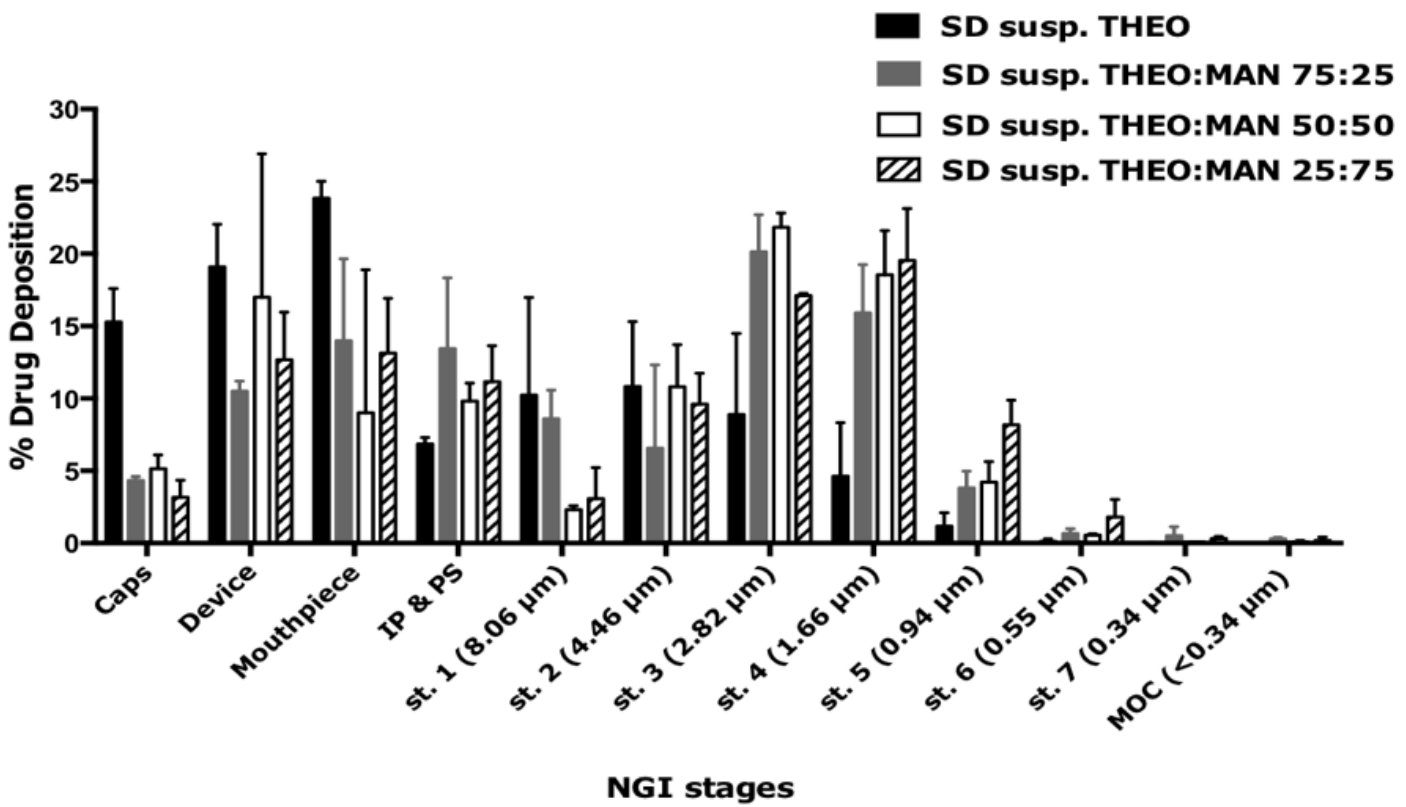

Figure 4.8 Drug deposition profiles of microcomposites containing different theophylline to mannitol ratios delivered using the Cyclohaler® at 60 L min^{-1} (mean + SD, n=3). St.1-St.7 denote stages 1-7 of the NGI, the aerodynamic cut-off diameter of each stage is given in parenthesis.

Table 4.5 Aerodynamic parameters of microcomposite formulations containing different theophylline to mannitol ratios delivered using the Cyclohaler® at 60L min^{-1} (mean ± SD, n=3).

Formulation	Emitted fraction (EF %)	Fine particle fraction (FPF %)	Fine particle dose (FPD, mg)	Mass median aerodynamic diameter (MMAD, μm)	Geometric Standard Deviation (GSD)
SD susp. THEO	65.6 ± 0.8	26.1 ± 7.1	2.6 ± 0.6	4.5 ± 1.1	1.7 ± 0.1
SD susp. THEO:MAN 75:25	84.0 ± 0.4	47.9 ± 2.3	4.8 ± 0.2	3.1 ± 0.2	1.6 ± 0.1
SD susp. THEO:MAN 50:50	78.9 ± 12.9	56.1 ± 0.8	5.6 ± 0.1	3.2 ± 0.3	1.6 ± 0.0
SD susp. THEO:MAN 25:75	84.1 ± 4.6	56.8 ± 8.7	5.7 ± 0.9	2.9 ± 0.1	1.7 ± 0.1

Previously, when mannitol was added as a matrix former in aqueous nanosuspensions prior to spray-drying, it was found to have no significant influence on the surface roughness and aerosol performance of the nano-matrix powders produced (Yamasaki et al., 2011). This result, which at first sight seems contradictory to the conclusions of this study, can be explained by the fact that in the former study mannitol was dissolved in the aqueous drug nanosuspensions and during spray drying it formed a continuous matrix around the drug nanocrystals. In the current study, mannitol nanocrystals were suspended in isopropanol prior to the spray-drying step, and after solvent evaporation they formed porous agglomerates wherein theophylline particles were embedded.

4.4.3. Computational study of the interactions between theophylline and mannitol

Results of PIXEL calculations for theophylline form II and mannitol form β are given in Table 4.6. Results for the mechanical properties of the crystals, calculated by molecular mechanics force field methods are presented in Table 4.7. Regarding the energy decomposition results for theophylline (Table 4.6), only the repulsive component is destabilising with all the other energy terms to contribute to the crystal lattice stabilisation. More specifically, the dispersion and coulombic components have almost equal contributions regarding the stabilisation. These results are in agreement with previously published data (Dunitz and Gavezzotti, 2005). In the case of mannitol, the coulombic component is by far the most important stabilising interaction, reflecting the significance of the hydrogen bonds in the stabilisation of the crystal structure.

Table 4.6 Lattice energy (kJ/mol) decomposition according to the PIXEL scheme, for theophylline form II and mannitol form β. E_{COUL}: coulombic; E_{POL}: polarisation; E_{DISP}: dispersion; E_{REP}: repulsion and E_{TOTAL}: total intermolecular interaction energy.

Substance	E_{COUL}	E_{POL}	E_{DISP}	E_{REP}	E_{TOTAL}	ΔH_{SUB}
THEO	-95.5	-47.5	-109.0	123.2	-128.9	135.0*
Mannitol	-312.7	-139.7	-132.2	356.7	-227.8	202.0*

*Sublimation enthalpies (ΔH_{SUB}) were taken from http://webbook.nist.gov/chemistry

Table 4.7 Calculated mechanical properties of theophylline form II and D-mannitol β-form.

	THEO	Mannitol
Bulk modulus (GPa)	14.81	10.85
Shear modulus (GPa)	4.59	4.15
Compressibility (GPa^{-1})	0.0675	0.0922
Young modulus (GPa)		
E_x	18.6	75.6
E_y	15.5	15.1
E_z	22.0	20.5

The crystal morphologies of theophylline and mannitol, determined according to the BFDH theory and energy vector diagrams are shown in Fig. 4.9. From Fig. 4.9c, it is seen that, as already described by Dunitz and Gavezzotti (2005), theophylline forms stacked dimers, but those do not form layers in the crystal structure, and there are strings of N-H···N hydrogen bonds between non-coplanar molecules. The direction of (stabilising) coulombic and polarisation, as well as the (destabilising) exchange repulsion interaction forces, coincides with the hydrogen bonding motif. On the other hand, the (stabilising) dispersion interaction forces extend mainly between adjacent coplanar purine rings, normal to the plane defined by the N-H···N hydrogen bond strings.

The spatial arrangement of the interaction forces in the lattice of theophylline defines the (200) plane as the most probable slip direction since no significant interaction forces act along or intersect this plane. However, as it becomes evident from the calculated crystal morphology in order to cause shearing of the crystal along the (200) plane, a force has to act on the much smaller (110) or (201) faces (Fig. 4.9a). The small relative surface area of these crystal faces, which is expected to get gradually smaller as milling proceeds, together with the rather high stiffness of its crystal structure (relatively high values of Young's modulus, (Table 4.7)) is probably the cause of the difficulty to break theophylline crystals by milling.

Mannitol exhibits a needle-like habit, with elongation along the a crystallographic axis, which is adequately represented by the BFDH morphology model, Fig. 4.9b. As demonstrated by the energy vector diagram of mannitol (Fig. 4.9d), intermolecular interaction forces extend parallel to the c crystallographic axis, clearly defining a slip direction along the (020) plane, in agreement with literature data (Al-Khattawi et al., 2015; Ho et al., 2012). Moreover it has been reported that mannitol crystals also fracture along the (011) plane (Ho et al. 2012). According to the energy vector diagram of mannitol, strong stabilising forces act along this plane, therefore fracture should not be very likely. However, when the elongated habit of the crystals is taken into account, it becomes evident that mechanical forces normal to the elongation axis eventually prevail and cause fracture.

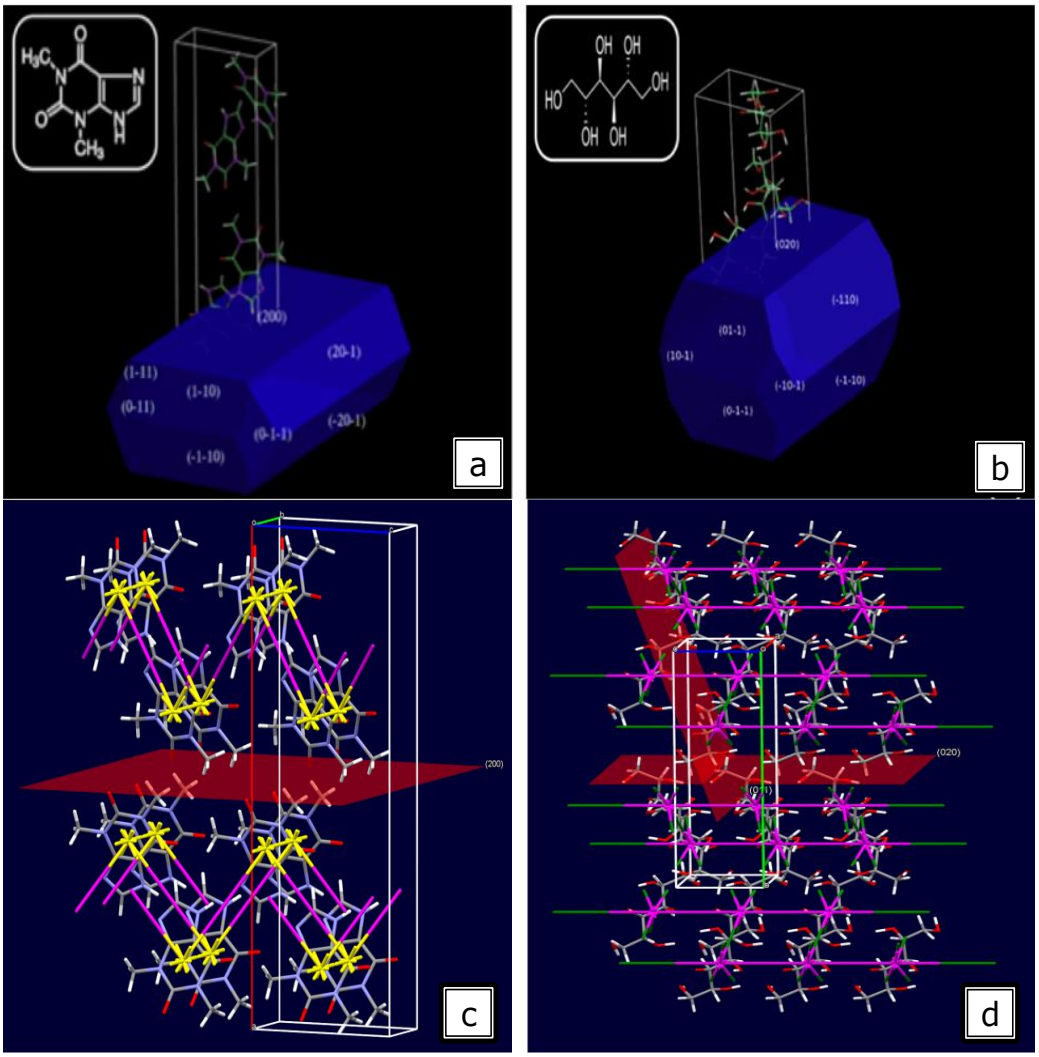

Figure 4.9 Chemical structures and crystal morphologies of (a) theophylline anhydrous form II and (b) D-mannitol β form. Crystal morphologies are calculated according to the BFDH theory showing the orientation of the unit cell in the bulk crystal. Energy vector diagrams of (c) theophylline form II showing the direction of coulombic and polarisation (pink) and dispersion (yellow) interactions, and of (d) D-mannitol β form, showing the direction of combined stabilising (pink) and destabilising repulsive (green) interactions. Red surfaces indicate the most probable slip planes.

Regarding the mechanism by which mannitol facilitates the size reduction of theophylline, this may be attributed to the interaction between certain crystal faces of the two substances, leading to subsequent adsorption-induced reduction of strength of a solid (AIRS); a phenomenon of physicochemical mechanics also known as the Rehbinder effect (Rehbinder and Shchukin, 1972). According to Rehbinder, adsorption of additives on the surface of the particles can make crack propagation easier by way of a reduction in surface energy (Andrade et al., 1950).

In order to investigate potential interactions between crystal faces of theophylline and mannitol, geometric lattice matching calculations were employed. It should be noted that geometric lattice matching calculations are developed to study epitaxial growth (i.e. growth of one crystal (overlayer) on the surface of another crystal (the substrate), on which the growth of the overlayer is oriented by the lattice structure of the substrate) (Datta and Grant, 2004). However, as the epitaxy score relates to the density and precision of lattice coincidence within a predefined search area and the higher its value, the larger the area a substrate and an overlayer can maintain a favourable low energy interaction, the use of these calculations has been extended in this case (Lee et al., 2010).

No significant geometric matching was found between the (200) plane of theophylline and (020) plane of mannitol. On the contrary, a high E value, the epitaxy score, indicates good matching between the (200) plane of theophylline and the (011) plane of mannitol. The value of the best matching theta, the angle between the (200) plane of theophylline and the (011) plane of mannitol is -79.5 ^{o} with an E value of 5.4895 (Fig. 4.10a). A one-dimension Moiré plot shows a high degree of superimposed patterns for theophylline's (200) and mannitol's (011) crystal plane, which is typical of registry between the two crystal lattices (Fig. 4.10b).

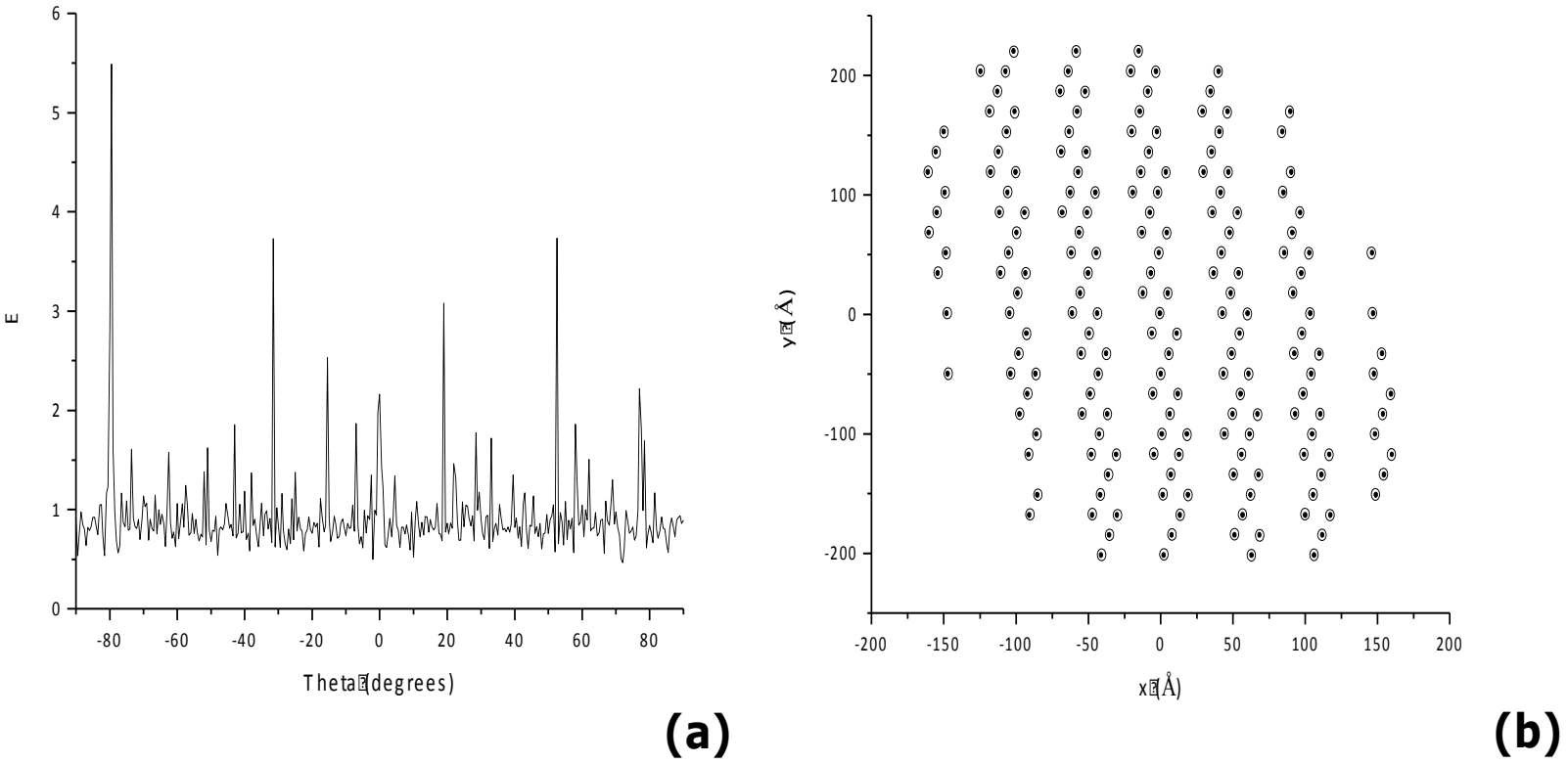

Figure 4.10 (a) Epitaxy score vs rotation angle and (b) Moiré patterns for the geometric matching of the crystal plane of theophylline (100) on that of mannitol (011).

The geometric matching of the lattice planes provides an indication of favourable interactions that could also lead to attachment of one crystal on the other, initiating processes involved in the adsorption-induced reduction of strength of theophylline particles. These results, together with the different physicomechanical properties of the compounds may shed light on the mechanisms behind the enhancement of theophylline's particle size reduction by mannitol during wet milling.

4.5. CONCLUSIONS

Based on the aforementioned results presented in this chapter, it can be concluded that:

1. Inhalable-sized particles of theophylline with various amounts of mannitol were successfully prepared by wet milling in isopropanol followed by spray drying.
2. The addition of mannitol as a co-milling agent facilitated the size reduction of theophylline's needle-like crystals and resulted in microcomposite particles which consisted of theophylline and mannitol submicron crystals assembled together. Increasing the proportion of mannitol was found to result in the production of smaller, more spherical and porous particles with enhanced aerosol performance.
3. Crystal morphology modelling and geometric lattice calculations were useful tools providing an insight into the intermolecular interactions that may influence the mechanical properties of theophylline and mannitol and the role of the latter as a co-milling agent.
4. Overall, wet milling of drugs in an organic solvent in the presence of mannitol, followed by spray drying, can be used a formulation approach for the production of respirable particles of water-soluble drugs or drugs that are prone to crystal transformation in an aqueous environment (i.e. formation of hydrates). Preservation of the solid phase makes this approach preferable to micronisation by dry milling techniques, which is associated with limitations, such as drug amorphisation and performance variability.

CHAPTER 5

GENERAL CONCLUSIONS AND FUTURE WORK

5. GENERAL CONCLUSIONS AND FUTURE WORK

5.1. INTRODUCTION

Pulmonary delivery is an attractive route of drug administration for the treatment of respiratory diseases such as asthma, COPD and cystic fibrosis. DPIs constitute one of the main types of inhalation devices for drug delivery to the lungs. The inherent stability of the dry powders, the ability to administer high doses, the absence of propellants and the easier use compared to pMDIs as they are breath-actuated can explain the increasing popularity of DPIs (in patients ≥ 5 years old and with adequate inspiratory flow), especially in Europe and North America (Geller, 2005). The application of inhaled dry powders has started to expand in new therapeutic areas as many drugs have shown to be suitable for lung delivery using DPIs including antibiotics, nucleic acids, peptides and vaccines (Yang et al., 2014).

Research on drug delivery to the lungs using DPIs has mainly focused on the devices (e.g. fabrication of novel inhaler devices with enhanced efficiency) and particle-engineering approaches in order to improve the properties of the formulation. Regarding the latter approach, the main goal of particle engineering is to produce particles with desirable attributes such as narrow particle size distribution, enhanced dispersibility and drug stability, optimised bioavailability and specific targeting at clinically relevant regions, taking into account the specifics of the device design and the drug delivery requirements (Chow et al., 2007).

The classical formulation approach for drug delivery to the lungs using DPIs is micronising the API and then mixing with a suitable coarse carrier (e.g. lactose). Micronisation (e.g. by ball or air-jet milling for particle size reduction) is a destructive, high-energy technique and may generate highly cohesive particles which suffer from poor physical and chemical stability, electrostatic charge and amorphous domains. More specifically, the amorphous state tends to revert back to a lower energy and more stable crystalline state upon storage that may adversely influence the product performance as it affects critical particle properties such as morphology, particle size distribution, dissolution and aerosolisation (Brodka-Pfeiffer et al., 2003; Chow et al., 2007). Moreover, engineered blends of micronised drug with coarse carrier particles do not exist as simple ordered mixtures. For example, micronised drug particles may adhere to coarse carrier

particles, to fine lactose particles or form large agglomerates indicating the complexity and heterogeneity of these formulations that have been described by Stewart et al. (2005) as as "multi-particulate nightmares".

Currently, many particle-engineering techniques have been developed (e.g. spray drying, sonocrystallisation, supercritical fluid technology) that offer a significant level of control over the key micromeritic and physicochemical properties of the particles produced. At the Drug Delivery to the Lungs 25 Conference, Stewart (2014) highlighted that such engineering techniques that produce more homogeneous particles, compared to micronisation, should be an integral part of the future research and development of drug delivery using DPIs. Among these particle-engineering techniques, spray drying is a well-established technique for pulmonary drug delivery due to its simplicity, flexibility and scalability making it an enduring technology.

5.2. SUMMARY

The work presented in this thesis has focused on engineering nanoparticle agglomerates (i.e. microparticles consisting of nanoparticles) as dry powders with tailored properties for pulmonary drug delivery. A combined approach comprising two steps was employed: wet milling of drug to produce nanosuspensions followed by the spray drying of such suspensions in order to produce nanoparticle agglomerates suitable for inhalation.

In this thesis, the process of wet milling followed by spray drying as a particle-engineering strategy was carried out using three model drugs, each drug exhibiting different physicochemical properties and thus posing different challenges to the formation of nanoparticle agglomerates. The particles produced for each drug were characterised in terms of their particle size distribution and morphology, solid state, redispersibility, dissolution and in-vitro aerosolisation performance.

More specifically, in Chapter 2, indometacin was selected as a poorly water-soluble drug, which is prone to polymorphic transformations and amorphisation upon processing (e.g. dry milling, spray drying). In order to elucidate the effect of stabiliser characteristics (e.g. total molecular weight, hydrophilic/hydrophobic ratio) on the formation of nanosuspensions, three members of the Pluronic® family as well as TPGS were used as stabilisers

during wet milling of indometacin. Pluronic® F127 and F68 as well as TPGS managed to stabilise the nanosuspensions of indometacin, which after 180 min of wet milling exhibited a mean hydrodynamic diameter in the range of 200-300 nm and narrow polydispersity. Based on particle size reduction kinetics data, it was found that the molecular weight of the stabilisers used influenced the rate but not the limit (steady state) of particle size reduction, which was probably determined by the physico-mechanical properties of the drug. The nanosuspensions of indometacin were spray dried either immediately after preparation without any further pre-treatment or after the addition of matrix formers (i.e. mannitol and L-leucine). Incorporation of the matrix-formers markedly improved the redispersibility of the nanoparticle agglomerates (i.e. their ability to reform nanoparticles after rehydration) and their dissolution rate. Regarding the aerosolisation performance, the nanoparticle agglomerates containing matrix formers were found to outperform those without matrix formers (FPF: 48.9 - 61.9%, compared to 34.9 - 43.2%) as determined by in-vitro aerosol testing.

Chapter 3 builds on the knowledge gained in Chapter 2. In this chapter, ibuprofen was selected as a poorly water-soluble drug, which is problematic during size reduction due to its low melting point and high mechanical ductility. A full factorial design was employed as a systematic approach to understand the critical formulation parameters, as well as any interactions between them, involved in the combined wet milling and spray drying process. In particular, the critical formulation parameters investigated were: type of stabiliser (HPMC, TPGS), mannitol to drug ratio and leucine to drug ratio. The responses investigated were: the yield of the process, the particle size distribution, the redispersibility and the FPF of the nanoparticle agglomerates. Both HPMC and TPGS were effective stabilisers. Ibuprofen nanosuspensions stabilised by HPMC exhibited a mean hydrodynamic diameter of 533 ± 28 nm, while those stabilised by TPGS had a mean of 663 ± 12 nm. By applying Partial Least Squares to the results of the full factorial design (significance level $\alpha=0.05$), leucine to drug ratio, mannitol to drug ratio and the type of stabiliser were found to be significant factors affecting the yield of the combination of wet milling and spray drying. The particle size was mainly dependent on the leucine to drug ratio and the type of stabiliser. Mannitol to drug ratio was found as the only critical parameter affecting redispersibility of nanoparticle agglomerates and both leucine to drug ratio and mannitol to drug ratio were found as significant factors affecting FPF%.

In Chapter 4 the approach of coupling wet milling with spray drying as a particle-engineering method for inhalable composite particles was expanded to drugs that cannot be milled in aqueous media. Theophylline, which has a long history in respiratory medicine, was selected as it is a moderately water-soluble drug, which transforms to its hydrate form when processed in water. Moreover, the crystals of theophylline exhibit a needle-like shape and thus it can be used as a model for compounds with strongly anisotropic morphology that are known to be more difficult to process, but which nevertheless are increasingly commonly encountered during discovery and early development. In this chapter, theophylline was milled in isopropanol in the presence of various amounts of mannitol, and the suspensions prepared were solidified by spray drying. Addition of mannitol as a co-milling agent facilitated size reduction of the elongated crystals of theophylline, and microcomposite particles consisting of theophylline and mannitol submicron crystals assembled together were obtained after spray drying. It was found that increasing the ratio of mannitol to theophylline resulted in smaller, more spherical microcomposites with enhanced aerosolisation performance.

Solid-state characterisation demonstrated that the inhalable particles prepared using the methodology outlined in this thesis retained the crystallinity of the starting materials and that was a common finding for all the drugs used. More specifically, in the nanoparticle agglomerates obtained, indometacin was in the stable γ-form, ibuprofren was in the same crystalline state as the raw drug and theophylline was in the form II (stable form at room temperature) while no solvate formation was observed. The fact that by carefully selecting the milling solvent and by fine-tuning the process parameters, the crystallinity of the particles can be retained is beneficial as it ensures the long-term physical stability of these formulations.

5.3. CONCLUSIONS

In this thesis, it was demonstrated that preparation of nanosuspensions by wet milling and then spray drying such suspensions could be used as an industrially feasible approach to produce composite microparticles of poorly water-soluble drug with properties suitable for inhaler formulation.

The selection of the suitable stabiliser is a key step for the successful formation of nanosuspensions. Monitoring the particle size of the suspensions at various intervals during wet milling provided information on the particle size reduction kinetics of the drug. For both indometacin and ibuprofen, breakage rate was high initially but with further milling the size continued to decrease but at markedly slower rate. These results corroborate the observation that breakage rate kinetics of a drug can be described by a first-order exponential decay function (Afolabi et al., 2014). For a certain milling speed, the duration of milling should be equal to the amount of time required for the steady state size to be achieved (plateau region). Milling speed is another parameter that should be adjusted especially when wet milling equipment without temperature control is used. This was found to be particularly important in the case of the low-melting point drug ibuprofen, where a milling speed of 200 rpm had to be selected in order to prevent melting of the drug nanocrystals. It should be noted that in this thesis, two different planetary mills were used for the preparation of suspensions. In the case of indometacin, nanosuspensions were produced by a planetary micro mill Pulverisette 7 which can reach a maximum of 1100 rpm while for ibuprofen and theophylline, wet milling was carried out using a planetary mill Pulverisette 5 which can reach a maximum of 300 rpm. In this latter case, a replacement of the common milling pot by a stainless steel pot whereby 8 glass vials could be fitted, allowed the reduction of the amount of time and material required for each milling experiment. Therefore, wet milling is a versatile technique for the production of nanocrystals that can be applied from early development (e.g. pre-formulation stage) when small amounts of a compound are available through commercial-scale manufacturing using wet milling equipment operating in a recirculation mode.

Nanosuspensions were converted to nanoparticle agglomerates by spray drying. The formation of the nanoparticle agglomerates can be explained by the one-droplet-to-one-particle (ODOP) principle. More specifically, at high

atomisation gas flow, two-fluid nozzles generate droplets with a size of 4-7 μm, which after drying result in particles around 2-3 μm (Kemp et al., 2013). Therefore, during the spray drying of the nanosuspensions, a droplet contained many nanocrystals, which after drying formed a composite microparticle.

In the case of indometacin and ibuprofen, the matrix formers were dissolved in the aqueous nanosuspensions. Based on SEM images and previously published studies, it is assumed that in the spray-dried particles, mannitol formed a continuous matrix around the nanocrystals while L-leucine preferentially accumulated on the surface of the particles (Vehring, 2008). The addition of matrix formers enhanced the redispersibility, the dissolution rate and the aerosolisation behaviour of the nanoparticle agglomerates. The full factorial design employed in the case of ibuprofen provided a systematic basis in order to understand the effect of the amounts of both mannitol and L-leucine on the production and *in-vitro* performance of the nanoparticle agglomerates. Analysis of the full factorial design results showed that high mannitol and L-leucine to drug ratio should be incorporated in the nanosuspensions prior to spray drying, with mannitol having a significant effect on the redispersibility of the nanoparticle agglomerates, while L-leucine acted as an aerosolisation enhancer. Moreover, addition of high amounts of mannitol and leucine improved the yield of the process, which was attributed to the formation of a matrix around the nanocrystals, which prevented them from melting. At this point, it should be highlighted that while the results of the full factorial design may guide the selection of formulation parameters regarding the formation of nanoparticle agglomerates, they should not be generalised to other drugs without further testing.

The use of wet milling followed by spray drying as a particle-engineering approach was extended to the formation of microcomposite particles of (moderately) water-soluble drugs, with theophylline as a model drug. Prior to the extension of the process, suitable modifications had to be implemented including the selection of the milling solvent and the stage at which mannitol was incorporated.

In the case of theophylline, the selection of isopropanol as the milling solvent was governed by the drug solubility. A rule of thumb is that a milling solvent

in which a drug exhibits low solubility should be selected in order to avoid the presence of the drug in both a solution and a suspended phase. Having the drug partly dissolved and partly suspended in the milling solvent may result in the formation of partially amorphous particles during spray drying. Using an organic solvent instead of water during wet milling called for a further modification of the process, as mannitol cannot be incorporated in the suspension before spray drying, due to its limited solubility in isopropanol. Instead, incorporation of mannitol during the wet-milling step of theophylline resulted in suspensions containing fine particles of both compounds. Spray drying of these suspensions resulted in respirable microcomposite particles where submicron theophylline were embedded in a porous network of mannitol nanocrystals. Increasing the proportion of mannitol was found to facilitate the size reduction of theophylline crystals and smaller, more spherical and porous microcomposite particles with enhanced aerosolisation performance were produced after spray drying. Thus, when wet milling takes place in an organic solvent, mannitol can play a double role: matrix former and co-milling agent.

In conclusion, the main aim of the thesis was achieved as a drug delivery platform based on wet milling and spray drying for the engineering of nanoparticle agglomerates suitable for inhalation was developed. The rational selection of formulation and process parameters allows the application of this platform to a range of drugs with different physicochemical and mechanical properties (e.g. water-soluble, low-melting point and ductile drugs). In all cases, after the optimisation of the process, the particles produced demonstrated enhanced aerosolisation performance and they retained the crystalline form of the starting materials. Especially for poorly water-soluble drugs, the in-vitro performance of the nanoparticle agglomerates was complemented by an improved dissolution profile. The observation that the microcomposite particles produced by this platform tend to exhibit a rather uniform set of properties may indicate that their in-vitro performance is process-related. Furthermore, preservation of the solid state makes this approach preferable to micronisation by dry milling techniques, which is associated with limitations, such as drug amorphisation and performance variability. These conclusions support the hypothesis outlined in the beginning of this thesis that it is possible to engineer respirable particles with a tailored crystalline form for a range of drugs with different physicochemical properties, by preparing nanoparticles and spray drying them in the presence

of suitable excipients in order to produce inhalable microcomposite particles with predictable performance.

Finally, based on the findings of this thesis, an initial "road map" was developed to guide the selection of formulation and process parameters that should be considered in order to engineer inhalable nanoparticle agglomerates, by taking into account the physicochemical properties of the drug in question (Fig. 5.1). As it is depicted in the roadmap, the selection of the stabiliser during wet milling is one of the first decisions that should be taken. Despite a few studies focusing on this topic, the selection of the suitable stabiliser is an empirical decision and an open challenge for future research. However, the "road map" presented in this thesis may pave the way towards the development of a "universal" delivery system where input drugs with different physicochemical properties can be processed by wet milling and spray drying in the presence of suitable excipients in order to produce inhalable microcomposite particles with predictable performance.

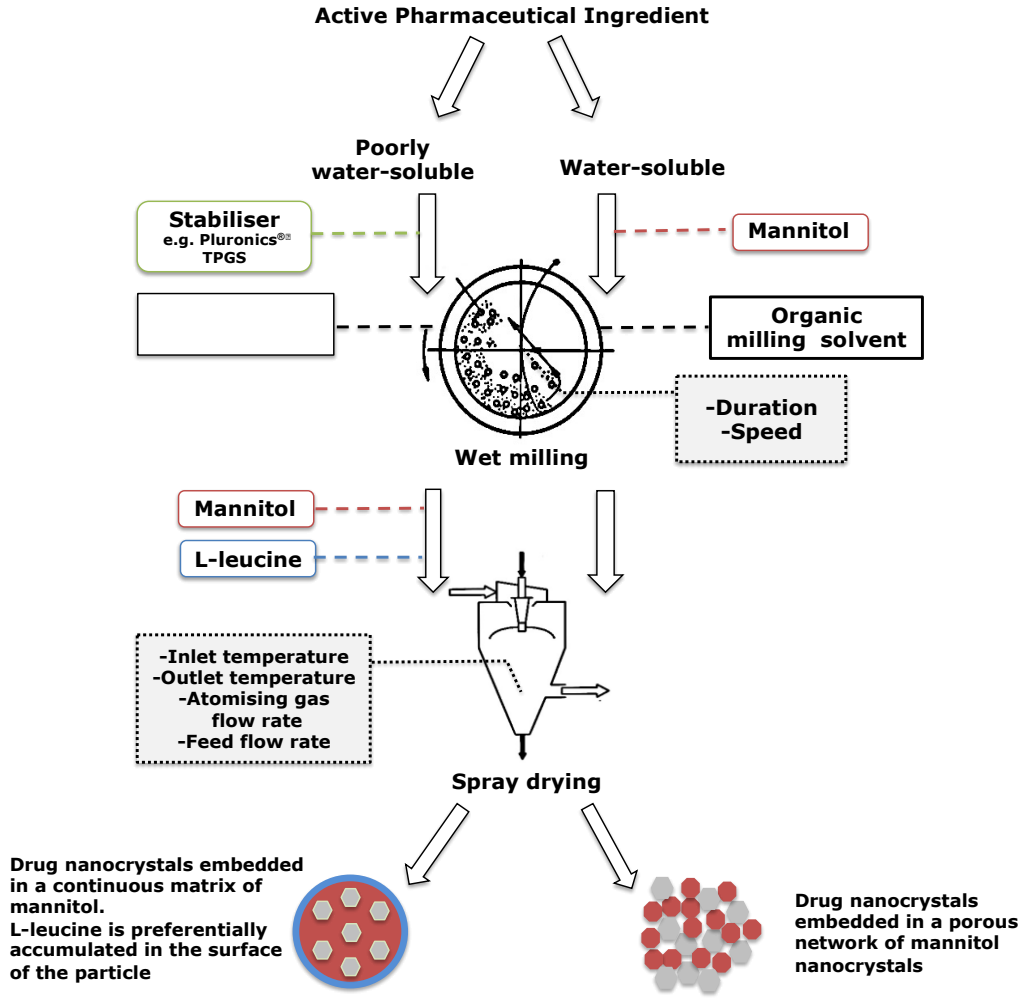

Figure 5.1 "Road map" developed in this thesis to guide the selection of formulation and process parameters that should be adjusted in order to engineer inhalable nanoparticle agglomerates, by taking into account the physicochemical properties of the drug in question.

5.4. FUTURE WORK

There are two main areas that future work could focus upon: i) the optimisation of the wet milling and spray drying as well as of the combination of these two processes as a particle-engineering approach and ii) the application of the approach in new areas inside the field of respiratory medicine.

One of the current limitations is the empirical nature of the stabiliser selection for the production of nanosuspensions. At present there is no systematic approach to guide the choice of stabiliser with respect to the active ingredient. Recently, many studies have focused on scaling-down the wet-milling process so as to allow the parallel screening of different

stabilisers (Juhnke et al., 2010; Romero et al., 2016). While these scaling-down approaches do not provide a first-principle-based predictive method towards the identification of a suitable drug stabiliser, they manage to reduce the time, effort and materials required for the development of drug nanosuspensions (Li et al., 2016). Focus should be given to approaches such as molecular modeling and scanning probe microscopy that can provide valuable insight into the way the stabiliser adsorbs to the surface of the crystal particles (Konkel and Myerson, 2009; Verma et al., 2009a). In this way, these two techniques may be able to prioritise and narrow-down the number of stabilisers that need to be screened. Measuring the adsorption of stabilisers on the drug surface and constructing adsorption isotherms can be a valuable tool for the rational selection of the type and concentration of polymeric stabilisers in formulation development (Goodwin et al., 2013). Moreover, potential within the areas of nanosuspension preparation and solidification can be accelerated with the implementation of the concept of quality by design (Verma et al., 2009b). In this way, the knowledge of the interplay between formulation, process, and quality attributes will facilitate rational design of nanocrystalline-based formulations.

Regarding pulmonary drug delivery, one of the distinct advantages of inhalable nanoparticle agglomerates is their enhanced aerosolisation performance even without the addition of carrier particles (e.g. lactose). In this way, high drug payloads can be administered to the lungs, which are difficult with the traditional approach of adhesive mixtures of carrier particles and micronised drug. This approach can revolutionise the administration of antibiotics to patients with chronic respiratory conditions (e.g. cystic fibrosis), as it enables local delivery of higher drug concentration at the lung tissue while concentrations elsewhere are kept at a minimum. In this way, maximum therapeutic effect can be achieved by administering lower inhaled doses compared to those required for systemic administration, and as a result side effects can be minimised.

Moreover, as asthma and COPD are multi-factorial diseases, the use of an inhaled corticosteroid (ICS) plus a long-acting β_2-agonist (LABA) has been reported to offer a more effective management in these respiratory diseases compared to monotherapy (Kankaanranta et al., 2004). In particular, the single inhaler for maintenance and relief therapy (SMART) approach, which advocates the administration of an ICS/LABA combination from a single

inhaler, is recognised as a simple, cost-effective approach which enhances patient adherence and provides more effective asthma and COPD control (Barnes, 2007). Currently, available inhalable combination products are produced by blending discrete micronised particles of both active compounds with a coarse carrier (e.g. lactose) and loading into an inhaler device. Apart from the limitations of dry micronisation techniques and adhesive mixtures that have been mentioned above, it is a challenge to maintain the ratio of micronised actives in the formulation by powder blending, especially taking into account that in ICS/LABA combinations, the ICS is present in a five to 30-fold mass excess (Parikh et al., 2012). Most importantly, the micronised particles of the two drugs can exhibit different particle size distributions, morphologies and surface characteristics resulting in differences in their aerodynamic performance. Thus, it is very challenging to ensure that both drugs are deposited at the correct ratio and within the same region of the lungs.

Combining both drugs in a single particle has been proposed as a particle engineering approach to achieve co-deposition in the same lung region, and thus to achieve synergy at the cellular/molecular level (Pitchayajittipong et al., 2009; Westmeier and Steckel, 2008). Following this direction, the concept of nano-in-micro can be tailored to the preparation of inhalable combination particles especially when the poor aqueous solubility of ICSs is taken into account. However, when designing inhalable particles containing a combination of two or more drugs, it is not always easy to identify a common solvent for the preparation of the nanosuspensions. Therefore, advanced spray-drying techniques (e.g. multiple-fluid nozzle) may be required in order to allow each drug to be milled in a different solvent and thus the final combination particle to contain crystalline nanoparticles of both drugs.

REFERENCES

REFERENCES

Adeyeye, C.M., Rowley, J., Madu, D., Javadi, M., Sabnis, S.S., 1995. Evaluation of crystallinity and drug release stability of directly compressed theophylline hydrophilic matrix tablets stored under varied moisture conditions. Int. J. Pharm. 116, 65–75.

Afolabi, A., Akinlabi, O., Bilgili, E., 2014. Impact of process parameters on the breakage kinetics of poorly water-soluble drugs during wet stirred media milling: A microhydrodynamic view. Eur. J. Pharm. Sci. 51, 75–86.

Al-Khattawi, A., Koner, J., Rue, P., Kirby, D., Perrie, Y., Rajabi-Siahboomi, A., Mohammed, A.R., 2015. A pragmatic approach for engineering porous mannitol and mechanistic evaluation of particle performance. Eur. J. Pharm. Biopharm. 94, 1–10.

Alhaddad, B., Smith, F.J., Robertson, T., Watman, G., Taylor, K.M.G., 2015. Patients' practices and experiences of using nebuliser therapy in the management of COPD at home. BMJ Open Respir. Res. 2, 1-9.

Alhalaweh, A., Kaialy, W., Buckton, G., Gill, H., Nokhodchi, A., Velaga, S., 2013. Theophylline Cocrystals Prepared by Spray Drying: Physicochemical Properties and Aerolisolization Performance. AAPS PharmSci Tech. 14, 265–276.

Allen, F.H., 2002. The Cambridge Structural Database: A quarter of a million crystal structures and rising. Acta Crystallogr. Sect. B Struct. Sci. 58, 380–388.

Anandharamakrishnan, C., Ishwarya, P.S., 2015. Spray Drying Techniques for Food Ingredient Encapsulation, first ed. Wiley-Blackwell, New Jersey.

Andrade, E.N.D.C., Randall, R.F.Y., Makin, M.J., 1950. The Rehbinder Effect. Proc. Phys. Soc. Sect. B 63, 990–995.

Arun, J.J., Lodha, R., Kabra, S.K., 2012. Bronchodilatory effect of inhaled budesonide/formoterol and budesonide/salbutamol in acute asthma: a double-blind, randomized controlled trial. BMC Pediatr. 12, 21-28.

Asgharian, B., Anjilvel, S., 1994. A Monte Carlo calculation of the deposition efficiency of inhaled particles in lower airways. J. Aerosol Sci. 25, 711–721.

Atkins, P.J., 2005. Dry powder inhalers: An overview. Respir. Care 50, 1304-1312.

Attari, Z., Kalvakuntia, S., Reddy, S., Deshpande, M., Mallikarjuna Rao, C., Koteshware, K.B., 2016. Formulation and characterisation of nanosuspensions of BCS Class II and IV drugs by combinative method. J. Exp. Nanosci. 4, 276-288.

Bahl, D., Bogner, R.H., 2008. Amorphization alone does not account for the enhancement of solubility of drug co-ground with silicate: the case of indomethacin. AAPS PharmSciTech. 9, 146-153.

Balakrishnan, A., Rege, B.D., Amidon, G.L., Polli, J.E., 2004. Surfactant-mediated dissolution: Contributions of solubility enhancement and relatively low micelle diffusivity. J. Pharm. Sci. 93, 2064-2075.

Barnes, P.J., 2003. Therapy of chronic obstructive pulmonary disease. Pharmacol. Ther. 97, 87–94.

Barnes, P.J., 2007. Scientific rationale for using a single inhaler for asthma control. Eur. Respir. J. 29, 587-595.

Barnes, P.J., 2008. Frontrunners in novel pharmacotherapy of COPD. Curr. Opin. Pharmacol. 8, 300–307.

Barnes, P.J., 2013. Theophylline. Am. J. Respir. Crit. Care Med. 188, 901–906.

Ben Zirar, S., Astier, A., Muchow, M., Gibaud, S., 2008. Comparison of nanosuspensions and hydroxypropyl-beta-cyclodextrin complex of melarsoprol: pharmacokinetics and tissue distribution in mice. Eur. J. Pharm. Biopharm. 70, 649–56.

Birchall, J.C. Jones, B.C., Morissey, A., 2008. A comparison of the puncturing properties of gelatin and hypromellose capsules for use in dry powder inhalers. Drug Dev. Ind. Pharm. 34, 870-876.

Benet, L.Z., 2007. Predicting DMPK of NMEs: what do we need in terms of science and tools? New England Drug Metabolism Discussion Group: Gerald Miwa Retirement Symposium.

Bond, A.D., 2014. processPIXEL: a program to generate energy-vector models from Gavezzotti's PIXEL calculations. J. Appl. Crystallogr. 47, 1777–1780.

Börgstrom, L., Derom, E., Ståhl, E., Wåhlin-Boll, E., Pauwels, R., 1996. The inhalation device influences lung deposition and bronchodilating effect of terbutaline. Am. J. Resp. Crit. Care Med. 153, 1636-1640.

Bosch, H.W., Ostrander, K.D., Cooper, E.R., 1999. Aerosols Comprising Nanoparticle Drugs. US Patent 20020102294 A1.

Britland, S., Finter, W., Chrystyn, H., Eagland, D., Abdelrahim, M.E., 2012. Droplet aerodynamics, cellular uptake, and efficacy of a nebulizable corticosteroid nanosuspension are superior to a micronized dosage form. Biotechnol. Prog. 28, 1152–1159.

Brockmeier, D., Voegele, D., Hattinger, H.M., 1983. In vitro- in vivo correlation, a time scaling problem? Basic techniques for testing equivalence. Arzeimittel- Forschung/ Drug Res. 33, 598–601.

Brodka-Pfeiffer, K., Langguth, P., Graβ, P., Häusler, H., 2003. Influence of mechanical activation on the physical stability of salbutamol sulphate. Eur. J. Pharm. Biopharm. 56, 393–400.

Brough, C., Williams, R.O., 2013. Amorphous solid dispersions and nano-crystal technologies for poorly water-soluble drug delivery. Int. J. Pharm. 453, 157–166.

Brunner, E., 1904. Reaktionsgeschwindigkeit in heterogenen systemen. Z. Phys. Chem. 43,56–102.

Büchi, 2010. Mini Spray Dryer B-290, http://www.buchi.com/gb-en/products/spray-drying-and-encapsulation/mini-spray-dryer-b-290 (accessed 22-07-2016).

Buckton, G., Beezer, A.E., 1992. The relationship between particle size and solubility. Int. J. Pharm. 82, 7–10.

Burger, A., Henck, J.O., Hetz, S., Rollinger, J.M., Weissnicht, A.A., Stöttner, H., 2000. Energy/temperature diagram and compression behaviour of the polymorphs of D-mannitol. J.Pharm. Sci. 89, 457-468.

Butler, J.M., Dressman, J.B., 2010. The developability classification system: application of biopharmaceutics concepts to formulation development. J. Pharm. Sci. 99, 4940–54.

Byron, P., 1986. Prediction of drug residence times in regions of the human respiratory tract folowing aerosol inhalation. J. Pharm. Sci. 75, 433–438.

Cares-Pacheco, M.G., Calvet, R., Vaca-Medina, G., Rouilly, A., Espitalier, F., 2015. Inverse gas chromatography a tool to follow physicochemical modifications of pharmaceutical solids: Crystal habit and particles size surface effects. Int. J. Pharm. 494, 113–126.

Carstensen, H., Müller, B.W., Müller, R.H., 1991. Adsorption of ethoxylated surfactants on nanoparticles. I. Characterization by hydrophobic interaction chromatography. Int. J. Pharm. 67, 29–37.

Cerdeira, A.M., Mazzotti, M., Gander, B., 2013. Formulation and drying of miconazole and itraconazole nanosuspensions. Int. J. Pharm. 443, 209-220.

Chaubal, M. V, Popescu, C., 2008. Conversion of nanosuspensions into dry powders by spray drying: a case study. Pharm. Res. 25, 2302–2308.

Chawla, A., Taylor, K.M.G., Newton, J.M., Johnson, M.C.R., 1994. Production of spray dried salbutamol sulphate for use in dry powder aerosol formulation. Int. J. Pharm. 108, 233–240.

Cheow, W.S., Ng, M.L.L., Kho, K., Hadinoto, K., 2011. Spray-freeze-drying production of thermally sensitive polymeric nanoparticle aggregates for inhaled drug delivery: effect of freeze-drying adjuvants. Int. J. Pharm. 404, 289–300.

Chiappetta, D.A., Sosnik, A., 2007. Poly(ethylene oxide)-poly(propylene oxide) block copolymer micelles as drug delivery agents: improved hydrosolubility, stability and bioavailability of drugs. Eur. J. Pharm. Biopharm. 66, 303–317.

Chingunpituk, J., 2007. Nanosuspension technology for drug delivery. Walailak J. Sci. Tech. 4, 139–153.

Chow, A.H.L., Tong, H.H.Y., Chattopadhyay, P., Shekunov, B.Y., 2007. Particle engineering for pulmonary drug delivery. Pharm. Res. 24, 411–437.

Chow, A.H.L., Tong, H.H.Y., Chattopadhyay, P., Shekunov, B.Y., 2007. Particle engineering for pulmonary drug delivery. Pharm. Res. 24, 411–437.

Chrystyn, H., 2006. Closer to an 'ideal inhaler' with the Easyhaler: An innovative dry powder inhaler. Clin. Drug Investig. 26, 175-183.

Chrystyn, H., 2007. The DiskusTM: A review of its position among dry powder inhaler devices. Int. J. Clin. Pract. 61, 1022-1036.

Chrystyn, H., Price, D., 2009. Not all asthma inhalers are the same: Factors to consider when prescribing an inhaler. Prim. Care Respir. J. 18, 243-249.

Clark, A.R., Hollingworth, A.M., 1993. The relationship between powder inhaler resistance and peak inspiratory conditions in healthy volunteers--implications for in vitro testing. J. Aeros. Med. 6, 99-110.

Coates, M.S., Fletcher, D.F., Chan, H.K., Raper, J. A, 2004. Effect of design on the performance of a dry powder inhaler using computational fluid dynamics. Part 1: Grid structure and mouthpiece length. J. Pharm. Sci. 93, 2863–2876.

Copley, M., 2007. Cascade impactors enter a new decade, http://www.copleyscientific.com/files/ww/articles/Manufacturing%20Chemist%20NGI%20Article%20_High%20Res_.pdf (accessed 22-07-2016).

Copley, M., Mitchell J.P., Svensson, M., Christopher, D., Quiroz, J., Daniels, G., Hamilton, M., Russell-Graham, D., 2013. Validating AIM-Based Instrumentation and Associated Measurement Techniques, in: Tougas, T.P., Mitchell, J.P., Lyapustina, S.A. (Eds), Good Cascade Impactor Practices, AIM and EDA for Orally Inhaled Products. Springer, New York, pp. 283-357.

Cristini, F., Delalonde, M., Joussot-Dubien, C., Battaille, B., 2003. Elaboration of ibuprofen microcomposites in supercritical CO2, in: Brunner, G., Kikic, I., Perrut, M. (Eds), Proceeding of the 6th International Symposium on Supercritical Fluids. ISASF. Valence, pp. 1917-1922.

Crowder, T.M., Louey, M.D., Sethuraman, V. V., Smyth, H.D.C., Hickey, A.J., 2001. 2001: An odyssey in inhaler formulation and design. Pharm. Technol. 25, 99–113.

Crowder, T.M., Rosati, J. A, Schroeter, J.D., Hickey, A.J., 2002. Fundamental effects of particle morphology on lung delivery : Predictions of Stoke's law and the particular relevance to dry powder inhaler formulation and development. Pharm. Res. 19,239-245.

Datta, S., Grant, D.J.W., 2004. Crystal structures of drugs: advances in determination, prediction and engineering. Nat. Rev. Drug Discov. 3, 42–57.

de Boer, J.H., Lippens, B.C., Linsen, B.G., Broekhoff, J.C.P., van den Heuvel, A., Osinga, J.T., 1966. T-curve method of multimolecular N_2-absorption. J. Colloid Interface Sci. 21, 405-414.

Demoly, P., Hagedoorn, P., de Boer, A.H., Frijlink, H.W., 2014. The clinical relevance of dry powder inhaler performance for drug delivery. Respir. Med. 108, 1195–1203.

Derjaguin, B., Landau, L., 1941. Theory of the stability of strongly charged lyophobic sols and of the adhesion of strongly charged particles in solution of electrolytes. Acta Physicochim. URSS 14, 633-662.

Despres-Gnis, F., Williams, G., 2010. Comparison of Next Generation Impactor and Fast Screening Impactor for determining Fine Particle Fraction of Dry Powder Inhalers. EPAG-Sponsored Workshop on Abbreviated Impactor Measurement (AIM) and Efficient Data Analysis (EDA) Concepts in Inhaler Testing: Overview of AIM-EDA.

Dhabale, S., 2014. World COPD and Asthma Devices Market Opportunities and Forecasts, 2013-2020, https://www.alliedmarketresearch.com/COPD-asthma-devices-market (accessed 22-07-2016).

Du, X. L., Zhu, Z., Fu, Q., Li, D.-K., Xu, W.-B., 2002. Pharmacokinetics and relative bioavailability of salbutamol metered-dose inhaler in healthy volunteers. Acta Pharmacol Sin. 23, 663–666.

Dunitz, J.D., Gavezzotti, A., 2005. Molecular recognition in organic crystals: Directed intermolecular bonds or nonlocalized bonding? Angew. Chemie 44, 1766–1787.

Duret, C., Wauthoz, N., Sebti, T., Vanderbist, F., Amighi, K., 2012. New inhalation-optimized itraconazole nanoparticle-based dry powders for the treatment of invasive pulmonary aspergillosis. Int. J. Nanomedicine 7, 5475–5489.

Ebisuzaki, Y., Boyle, P.D., Smith, J.A., 1997. Methylxanthines .1. Anhydrous theophylline. Acta Crystallogr. Sect. C - Cryst. Struct. Commun. 53, 777–779.

Edwards, D.A., Hanes, J., Caponetti, G., Hrkach, J., BenJebria, A., Eskew, M. Lou, Mintzes, J., Deaver, D., Lotan, N., Langer, R., 1997. Large Porous Particles for Pulmonary Drug Delivery. Science 276, 1868–1871.

Eerikäinen, H., Kauppinen, E.I., Kansikas, J., 2004. Polymeric Drug Nanoparticles Prepared by an Aerosol Flow Reactor Method. Pharm. Res. 21, 136–143.

El-Gendy, N., Gorman, E.M., Munson, E.J., Berkland, C., 2009. Budesonide nanoparticle agglomerates as dry powder aerosols with rapid dissolution. J. Pharm. Sci. 98, 2731–2746.

El-Gendy, N., Pornputtapitak, W., Berkland, C., 2011. Nanoparticle agglomerates of fluticasone propionate in combination with albuterol sulfate as dry powder aerosols. Eur. J. Pharm. Sci. 44, 522–33.

Elversson, S., Milliqvist-Fureby, A., 2005. Particle size and density in spray drying – effects of carbohydrate properties. J. Pharm. Sci. 94, 2049-2060.

Fink, J.B., Rubin, B.K., 2005. Problems with inhaler use: a call for improved clinician and patient education. Respir. Care 50, 1360–1365.

Fischer, E.W., 1958. Electron-microscopic investigation of suspension stability in macromolecular solutions. Kolloid Z. 160, 120-141.

Fleming, S., Rohl, A., 2005. GDIS: A visualization program for molecular and periodic systems. Zeitschrift fur Krist. 220, 580–584.

Flicker, F., Eberle, V.A., Betz, G., 2011. Variability in commercial carbamazepine samples - Impact on drug release. Int. J. Pharm. 410, 99–106.

Florence, A.T., Attwood, D., 2015. Physicochemical Principles of Pharmacy in Manufacture, Formulation and Clinical Use, sixth ed. Pharmaceutical Press, London.

Forbes, B., Richer, N.H., Buttini, F., 2015. Dissolution: A Critical Performance Characteristic of Inhaled Products?, in: Nokhodchi, A., Martin, G.P. (Eds), Pulmonary Drug Delivery: Advances and Challenges. John Wiley & Sons Ltd, Chichester, pp. 223-240.

Fritsch, 2007. Premium line planetary mills, http://www.fritsch-international.com/sample-preparation/milling/planetary-mills/details/product/pulverisette-7-premium-line/downloads (accessed 22-07-2016).

Fröhlich, E., Salar-Behzadi, S., 2014. Toxicological assessment of inhaled nanoparticles: Role of in vivo, ex vivo, in vitro, and in Silico Studies. Int. J. Mol. Sci. 12, 4795-4822.

Fronczek, F.R., Kamel, H.N., Slattery, M., 2003. Three polymorphs (alpha, beta, and delta) of D-mannitol at 100 K. Acta Crystallogr. C. 59, 567–570.

Fucke, K., McIntyre, G.J., Wilkinson, C., Henry, M., Howard, J.A.K., Steed, J.W., 2012. New Insights into an Old Molecule: Interaction Energies of Theophylline Crystal Forms. Cryst. Growth Des. 12, 1395–1401.

Fussell, A.L., Grasmeijer, F., Frijlink, H., W., de Boer, A.H., Offerhaus, H.L., 2014. CARS microscopy as a tool for studying the distribution of micronised drugs in adhesive mixtures for inhalation. J. Raman Spectrosc. 45, 495-500.

Gale, J.D., Rohl, A.L., 2003. The General Utility Lattice Program (GULP). Mol. Simul. 29, 291–341.

Gao, L., Liu, G., Wang, X., Liu, F., Xu, Y., Ma, J., 2011. Preparation of a chemically stable quercetin formulation using nanosuspension technology. Int. J. Pharm. 404, 231–237.

Gavezzotti, A, 2005. Calculations of lattice energies of organic crystals: the PIXEL integration method in comparison with more traditional methods. Zeitschrift fur Krist. 220, 499–510.

Gea Process Engineering, 2013. GEA Niro Spray Dryer SDMicroTM, http://www.gea.com/global/en/binaries/GEA%20Spray%20Dryer%20SDMicro_tcm11-24396.pdf (accessed 22-07-2016).

Geller, D.E., 2005. Comparing clinical features of the nebulizer, metered-dose inhaler, and dry powder inhaler. Respir. Care 50, 1313-1321.

George, M., Ghosh, I., 2013. Identifying the correlation between drug/stabilizer properties and critical quality attributes (CQAs) of nanosuspension formulation prepared by wet media milling technology. Eur. J. Pharm. Sci. 48, 142-152.

Ghosh, I., Schenck, D., Bose, S., Ruegger, C., 2012. Optimization of formulation and process parameters for the production of nanosuspension by wet media milling technique: effect of Vitamin E TPGS and nanocrystal particle size on oral absorption. Eur. J. Pharm. Sci. 47, 718–728.

Goodwin, D.J., Sepassi, S., King, S.M., Holland, S.M., Mantini, L.G., Lawrence, M.J., 2013. Characterization of polymer adsorption onto drug nanoparticles using depletion measurements and small-angle neutron scattering. Mol. Pharm. 10, 4146-4158.

Grasmeijer, F., Grasmeijer, N., Hagedoorn, P., Frijlink, H.W., de Boer, A.H., 2015. Recent Advances in the Fundamental Understanding of Adhesive Mixtures for Inhalation. Curr. Pharm. Des. 21, 5900-5914.

Guo, Y., Luo, J., Tan, S., Otieno, B.O., Zhang, Z., 2013. The applications of Vitamin E TPGS in drug delivery. Eur. J. Pharm. Sci. 49, 175–186.

Hafner, A., Lovrić, J., Lakoš, G.P., Pepić, I., 2014. Nanotherapeutics in the EU: an overview on current state and future directions. Int. J. Nanomedicine 9, 1005–1023.

Harris, D., 2016. Capsule dry powder inhalers- time to innovate? https://www.team-consulting.com/insights/capsule-dry-powder-inhalers-time-to-innovate (accessed 22-07-2016).

Healy, A.M., Amaro, M.I., Paluch, K.J., Tajber, L., 2014. Dry powders for oral inhalation free of lactose carrier particles. Adv. Drug Deliv. Rev. 75, 32-52.

Hecq, J., Deleers, M., Fanara, D., Vranckx, H., Amighi, K., 2005. Preparation and characterization of nanocrystals for solubility and dissolution rate enhancement of nifedipine. Int. J. Pharm. 299, 167–177.

Heinemann, L., 2008. The Failure of Exubera: Are We Beating a Dead Horse? J. Diabetes Sci. Technol. 2, 518–529.

Heng, D., Cutler, D.J., Chan, H.K., Yun, J., Raper, J.A., 2008. What is a suitable dissolution method for drug nanoparticles? Pharm. Res. 25, 1696–1701.

Heyder, J., 2004. Deposition of inhaled particles in the human respiratory tract and consequences for regional targeting in respiratory drug delivery. Proc. Am. Thorac. Soc. 1, 315–320.

Heyder, J., Gebhart, J., Rudolf, G., Schiller, C.F., Stahlhofen, W., 1986. Deposition of particles in the human respiratory tract in the size range 0.005–15 μm. J. Aerosol Sci. 17, 811–825.

Hirano, T., Yamagata, T., Gohda, M., Yamagata, Y., Ichikawa, T., Yanagisawa, S., Ueshima, K., Akamatsu, K., Nakanishi, M., Matsunaga, K., Minakata, Y., Ichinose, M., 2006. Inhibition of reactive nitrogen species production in COPD airways: comparison of inhaled corticosteroid and oral theophylline. Thorax 61, 761–766.

Ho, R., Naderi, M., Heng, J.Y.Y., Williams, D.R., Thielmann, F., Bouza, P., Keith, A.R., Thiele, G., Burnett, D.J., 2012. Effect of milling on particle shape and surface energy heterogeneity of needle-Shaped crystals. Pharm. Res. 29, 2806–2816.

Hong, J., Oort, M.M., 2011. Aggregate nanoparticulate medicament formulations, manufacture and use thereof. Patent WO2012051426 A2.

Hoppentocht, M., Hagedoorn, P., Frijlink, H.W., de Boer, A.H., 2014. Technological and practical challenges of dry powder inhalers and formulations. Adv. Drug Deliv. Rev. 75, 18-31.

Hulse, W.L., Forbes, R.T., Bonner, M.C., Getrost, M., 2009. The characterization and comparison of spray-dried mannitol samples. Drug Dev. Ind. Pharm. 35, 712–718.

Huttenrauch, R., Fricke, S., Zielke, P., 1985. Mechanical activation of pharmaceutical systems. Pharm. Res. 6, 302–306.

ICH, 2009. ICH Harmonised Tripartite Guideline: Pharmaceutical Development Q8 (R2). Interanational Conference on Harmonisation of Technical Requirements for Registration of Pharmaceuticals for Human Use, http://www.ich.org/fileadmin/Public_Web_Site/ICH_Products/Guidelines/Quality/Q8_R1/Step4/Q8_R2_Guideline.pdf (accessed 22-07-2016).

Illum, L., Jacobsen, L.O., Müller, R.H., Mak, E., Davis, S.S., 1987. Surface characteristics and the interaction of colloidal particles with mouse peritoneal macrophages. Biomaterials 8, 113–117.

Islam, N., Cleary, M.J., 2012. Developing an efficient and reliable dry powder inhaler for pulmonary drug delivery-a review for multidisciplinary researchers. Med. Eng. Phys. 34, 409–427.

Islam, N., Gladki, E., 2008. Dry powder inhalers (DPIs)-A review of device reliability and innovation. Int. J. Pharm. 360, 1-11.

Jacobs, C., Kayser, O., Müller, R.H., 2001. Production and characterisation of mucoadhesive nanosuspensions for the formulation of bupravaquone. Int. J. Pharm. 214, 3–7.

Johnson, D.L., Martonen, T.B., 1994. Predicted and observed behavior of platelet aerosols. Part. Sci. Technol. 12, 149–159.

Jones, B.E., 2003. Quali-V-I: a new key for dry powder inhalers. Drug Deliv. Technol. 3, 2-7.

Joshi, B. V, Patil, V.B., Pokharkar, V.B., 2002. Compatibility studies between carbamazepine and tablet excipients using thermal and non-thermal methods. Drug Dev. Ind. Pharm. 28, 687–694.

Junke, M., Berghausen, J., Timpe, C., 2010. Accelerated formulation development for nanomilled active pharmaceutical ingredients using a screening approach. Chem. Eng. Technol. 33, 1412-1418.

Kadota, K., Nishimura, T., Hotta, D., Tozuka, Y., 2015. Preparation of composite particles of hydrophilic or hydrophobic drugs with highly branched cyclic dextrin via spray drying for dry powder inhalers. Powder Technol. 283, 16–23.

Kaialy, W., Nokhodchi, A., 2013. Freeze-dried mannitol for superior pulmonary drug delivery via dry powder inhaler. Pharm. Res. 30, 458–477.

Kamin,W., Schwabe, A., Krämer, I., 2006. Inhalation solutions: Which one are allowed to be mixed? Physico-chemical compatibility of drug solution in nebulizers. J. Cyst. Fibr. 4, 205-213.

Kankaanranta, H., Lahdensuo, A., Moilanen, E., Barnes, P.J., 2004. Add-on therapy options in asthma not adequately controlled by inhaled corticosteroids: a comprehensive review. Respir. Res. 5, 17.

Karmwar, P., Graeser, K., Gordon, K.C., Strachan, C.J., Rades, T., 2012. Effect of different preparation methods on the dissolution behaviour of amorphous indomethacin. Eur. J. Pharm. Biopharm. 80, 459–64.

Kayaert, P., Van den Mooter, G., 2012. Is the amorphous fraction of a dried nanosuspension caused by milling or by drying? A case study with Naproxen and Cinnarizine. Eur. J. Pharm. Biopharm. 81, 650–656.

Kayrak, D., Akman, U., Hortaçsu, Ö., 2003. Micronization of Ibuprofen by RESS. J. Supercrit. Fluids 26, 17–31.

Kayser, O., 2001. A new approach for targeting to Cryptosporidium parvum using mucoadhesive nanosuspensions: research and applications. Int. J. Pharm. 214, 83–85.

Keck, C.M., Müller, R.H., 2006. Drug nanocrystals of poorly soluble drugs produced by high pressure homogenisation. Eur. J. Pharm. Biopharm. 62, 3–16.

Kemp, I.C., Wadley, R., Hartwig, T., Ugo, C., See-Toh, Y., Gorvinge, L., Fordham, K., Ricard, F., 2013. Experimental Study of Spray Drying and Atomization with a Two-Fluid Nozzle to Produce Inhalable Particles. Drying Technol. 31, 930-941.

Kesisoglou, F., Panmai, S., Wu, Y., 2007. Nanosizing--oral formulation development and biopharmaceutical evaluation. Adv. Drug Deliv. Rev. 59, 631–644.

Khan, K.A., 1975. The concept of dissolution efficiency. J. Pharm. Pharmacol. 25, 48–49.

Kim, A.I., Akers, M.J., Nail, S.L., 1998. The physical state of mannitol after freeze-drying: Effects of mannitol concentration, freezing rate, and a noncrystallizing cosolute. J. Pharm. Sci. 87, 931–935.

Kleinhans, S., Arpagaus, C., Schönenberger, G., 2007. The Laboratory Assistant, third ed. Büchi Labortechnik, Flawil.

Kleinstreuer, C., Zhang, Z., 2010. Airflow and Particle Transport in the Human Respiratory System. Annu. Rev. Fluid Mech. 42, 301–334.

Konkel, J.T., Myerson, A.S., Empirical molecular modeling of suspension stabilisation with Polysorbate 80. Mol. Simul. 34, 1353-1357.

Krasnov, A., 2011. Solubility and physical stability improvement of natural xanthine derivatives. University of Helsinki, Helsinki.

Kubo, H., Osawa, T., Takashima, K., Mizobe, M., 1996. Enhancement of oral bioavailability and pharmacological effect of 1-(3,4-dimethoxyphenyl)-2,3-bis(methoxycarbonyl)-4-hydroxy-6,7,8-trimethoxynaphthalene (TA-7552), a new hypocholesterolemic agent, by micronization in co-ground mixture with D-mannitol. Biol. Pharm. Bull. 19, 741–7.

Kumar, S., Gokhale, R., Burgess, D.J., 2014. Quality by Design approach to spray drying processing of crystalline nanosuspensions. Int. J. Pharm. 464, 234–42.

Labiris, N.R., Dolovich, M.B., 2003. Pulmonary drug delivery. Part II: the role of inhalant delivery devices and drug formulations in therapeutic effectiveness of aerosolized medications. Br. J. Clin. Pharmacol. 56, 600–12.

Lähde, A., Raula, J., Kauppinen, E.I., 2008. Simultaneous synthesis and coating of salbutamol sulphate nanoparticles with L-leucine in the gas phase. Int. J. Pharm. 358, 256-262.

Larsson, I., Kristensen, H., 2000. Comminution of a brittle/ductile material in a Micros Ring Mill. Powder Technol. 107, 175–178.

Leach, C.L., 2005. The CFC to HFA transition and its impact on pulmonary drug development. Respir. Care 50, 1201–1208.

Lebrun, P., Krier, F., Mantanus, J., Grohganz, H., Yang, M., Rozet, E., Boulanger, B., Evrard, B., Rantanen, J., Hubert, P., Design space approach in the optimization of the spray-drying process. Eur. J. Pharm. Biopharm. 80, 226-234.

Lechuga-Ballesteros, D., Charan, C., Stults, C.L., Stevenson, C.L., Miller, D.P., Vehring, R., Tep, V., Kuo, M.C., 2008. Trileucine improves aerosol performance and stability of spray-dried powders for inhalation. J. Pharm. Sci. 97, 287– 302.

Lee, E.H., Boerrigter, S.X.M., Byrn, S.R., 2010. Epitaxy of a structurally related compound on the (100) faces of flufenamic acid form I and III single crystals. Cryst. Growth Des. 10, 518–527.

Lee, J., 2003. Drug nano- and microparticles processed into solid dosage forms: Physical properties. J. Pharm. Sci. 92, 2057–2068.

Lee, J., Choi, J.Y., Park, C.H., 2008. Characteristics of polymers enabling nano-comminution of water-insoluble drugs. Int. J. Pharm. 355, 328–336.

Legendre, B., Feutelais, Y., 2004. Polymorphic and Thermodynamic Study of Indomethacin. J. Therm. Anal. Calorim. 76, 255–264.

Leuenberger, H., 1982. The compressibility and compactibility of powder systems. Int. J. Pharm. 12, 41–55.

Li, M., Azad, M., Davé, R., Bilgili, E., 2016. Nanomilling of drugs for bioavailability enhancement: a holistic formulation approach process perspective. Pharmaceutics, 8.

Li, X., Vogt, F.G., Hayes, D., Mansour, H.M., 2014. Design, characterization, and aerosol dispersion performance modeling of advanced co-spray dried antibiotics with mannitol as respirable microparticles/nanoparticles for targeted pulmonary delivery as dry powder inhalers. J. Pharm. Sci. 103, 2937–2949.

Lindfors, L., Skantze, P., Skantze, U., Westergren, J., Olsson, U., 2007. Amorphous drug nanosuspensions. 3. Particle dissolution and crystal growth. Langmuir 23, 9866–9874.

Lipinski, C., 2002. Poor aqueous solubility - an industry wide problem in drug discovery. Am. Pharm. Rev. 5, 82–85.

Liu, P., Rong, X., Laru, J., van Veen, B., Kiesvaara, J., Hirvonen, J., Laaksonen, T., Peltonen, L., 2011. Nanosuspensions of poorly soluble drugs: preparation and development by wet milling. Int. J. Pharm. 411, 215–222.

Maa, Y.F., Nguyen, P.A., Sweeney, T., Shire, S.J., Hsu, C., 1999. Protein inhalation powders: Spray drying vs spray freeze drying. Pharm. Res. 16, 249–254.

Maas, S.G., Schaldach, G., Littringer, E.M., Mescher, A., Griesser, U.J., Braun, D.E., Walzel, P.E., Urbanetz, N. a., 2011. The impact of spray drying outlet temperature on the particle morphology of mannitol. Powder Technol. 213, 27–35.

Macrae, C.F., Bruno, I.J., Chisholm, J. A., Edgington, P.R., McCabe, P., Pidcock, E., Rodriguez-Monge, L., Taylor, R., Van De Streek, J., Wood, P.A., 2008. Mercury CSD 2.0 - New features for the visualization and investigation of crystal structures. J. Appl. Crystallogr. 41, 466–470.

Maltensen, M.J., Bjerregaard, S., Hovgaard, L., Havelund, S., van de Weert, M., 2008. Quality by desing- Spray drying of insulin intended for inhalation. Eur. J. Pharm. Biopharm. 70, 823-838.

Mark, G.S., 2007. Pfizer dumps Exubera. Nature Biotechnol. 25, 1331-1332.

Martena, V., Censi, R., Hoti, E., Malaj, L., Di Martino, P., 2012. Indomethacin nanocrystals prepared by different laboratory scale methods: effect on crystalline form and dissolution behavior. J. Nanoparticle Res. 14, 1275–1279.

Masters, K., 1991. Spray drying handbook, fifth ed. Longman Scientific and Technical, Essex.

Maulidin, R., Möschwitzer, J., Müller, R., 2012. Fast dissolving ibuprofen nanocrystal-loaded solid dosage forms. Int. J. Pharm. Pharm. Sci. 4, 543-549.

Maury, M., Murphy, K., Kumar, S., Shi, L., Lee, G., 2005. Effects of process variables on the powder yield of spray-dried trehalose on a laboratory spray-dryer. Eur. J. Pharm. Biopharm. 59, 565–573.

Mayo, S.L., Olafson, B.D., Goddard, W.A., 1990. DREIDING: a generic force field for molecular simulations. J. Phys. Chem. 94, 8897–8909.

Melandri, C., Tarroni, G., Prodi, V., De Zaiacomo, T., Formignani, M., Lombardi, C.C., 1983. Deposition of charged particles in the human airways. J. Aerosol Sci. 14, 657–669.

Merisko-Liversidge, E., Liversidge, G.G., 2011. Nanosizing for oral and parenteral drug delivery: a perspective on formulating poorly-water soluble compounds using wet media milling technology. Adv. Drug Deliv. Rev. 63, 427–440.

Mitchell, J., Bauer, R., Lyapustina, S., Tougas, T., Glaab, V., 2011. Non-impactor-based methods for sizing of aerosols emitted from orally inhaled and nasal drug products (OINDPs). AAPS PharmSciTech. 12, 965–988.

Mitchell, J.P., Tougas, T.P., 2013. The AIM and EDA Concepts in: Why they are Needed and How They Fit Together, in: Tougas, T.P., Mitchell, J.P., Lyapustina, S.A. (Eds), Good Cascade Impactor Practices, AIM and EDA for Orally Inhaled Products. Springer, New York, pp. 119-133.

Momeni, A., Mohammadi, M.H., 2009. Respiratory delivery of theophylline by size-targeted starch microspheres for treatment of asthma. J. Microencapsul. 26, 701–710.

Monteiro, A., Afolabi, A., Bilgili, E., 2012. Continuous production of drug nanoparticle suspensions via wet stirred media milling: a fresh look at the Rehbinder effect. Drug Dev. Ind. Pharm. 39, 1–18.

Möschwitzer, J.P., 2013. Drug nanocrystals in the commercial pharmaceutical development process. Int. J. Pharm. 453, 142–156.

Müller, R.H., Gohla, S., Keck, C.M., 2011. State of the art of nanocrystals--special features, production, nanotoxicology aspects and intracellular delivery. Eur. J. Pharm. Biopharm. 78, 1–9.

Mumenthaler, M., Leuenberger, H., 1991. Atmospheric spray-freeze drying: a suitable alternative in freeze-drying technology. Int. J. Pharm. 72, 97–110.

Murnane, D., Hutter, V., Harang, M. 2014. Pharmaceutical Aerosols and Pulmonary Drug Delivery, in: Colbeck, I., Lazaridis, M. (Eds), Aerosol Science: Technology and Applications. John Wiley & Sons Ltd, Chichester, pp. 221-229.

Napper, D., 1977. Steric stabilization. J. Colloid Interface Sci. 58, 390–407.

Nernst, W., 1904. Theorie der reaktionsgeschwindigkeit in heterogenen systemen. Z. Phys. Chem. 43, 47-52.

Newman, S.P., 2005. Principles of metered-dose inhaler design. Respir. Care 50, 1177–1190.

Niwa, T., Miura, S., Danjo, K., 2011. Universal wet-milling technique to prepare oral nanosuspension focused on discovery and preclinical animal studies - Development of particle design method. Int. J. Pharm. 405, 218–227.

Palander, A., Mattila, T., Karhu, M., Muttonen, E., 2000. In vitro Comparison of Three Salbutamol-Containing Multidose Dry Powder Inhalers. Clin. Drug Investig. 20, 25-33.

Parikh, D., Burns, J., Hipkiss, D., Usmani, O., Price, R., 2012. Improved Localised Lung Delivery Using Smart Combination Respiratory Medicines. Eur. Resp. Dis. 8, 1-7.

Patton, J.S., Fishburn, C.S., Weers, J.G., 2004. The Lungs as a Portal of Entry for Systemic Drug Delivery. Proc. Am. Thorac. Soc. 1, 338–344.

Peltonen, L., Hirvonen, J., 2010. Pharmaceutical nanocrystals by nanomilling: critical process parameters, particle fracturing and stabilization methods. J. Pharm. Pharmacol. 62, 1569-1579.

Peltonen, L., Valo, H., Kolakovic, R., Laaksonen, T., Hirvonen, J., 2010. Electrospraying, spray drying and related techniques for production and formulation of drug nanoparticles. Expert Opin. Drug Deliv. 6, 705–719.

Peukert, W., Schwarzer, H.C., Götzinger, M., Günther, L., Stenger, F., 2003. Control of particle interfaces—the critical issue in nanoparticle technology. Adv. Powder Technol. 14, 411–426.

Pilcer, G., Amighi, K., 2010. Formulation strategy and use of excipients in pulmonary drug delivery. Int. J. Pharm. 392, 1–19.

Pilcer, G., Vanderbist, F., Amighi, K., 2009. Spray-dried carrier-free dry powder tobramycin formulations with improved dispersion properties. J. Pharm. Sci. 98, 1463–1475.

Pitchayajittipong, C., Shur, J., Price, R., 2009. Engineering of crystalline combination inhalation particles of a long-acting β2-agonist and a corticosteroid. Pharm. Res. 26, 2657–2666.

Plakkot, S., de Matas, M., York, P., Saunders, M., Sulaiman, B., 2011. Comminution of ibuprofen to produce nano-particles for rapid dissolution. Int. J. Pharm. 415, 307–314.

Plumley, C., Gorman, E.M., El-Gendy, N., Bybee, C.R., Munson, E.J., Berkland, C., 2009. Nifedipine nanoparticle agglomeration as a dry powder aerosol formulation strategy. Int. J. Pharm. 369, 136–43.

Pomázi, A., Buttini, F., Ambrus, R., Colombo, P., Szabó-Révész, P., 2013. Effect of polymers for aerolization properties of mannitol-based microcomposites containing meloxicam. Eur. Polym. J. 49, 2518–2527.

Rabbani, N.R., Seville, P.C., 2005. The influence of formulation components on the aerosolisation properties of spray-dried powders. J. Control. Release 110, 130-140.

Rabinow, B.E., 2004. Nanosuspensions in drug delivery. Nat. Rev. Drug Discov. 3, 785–796.

Rachmawati, H., Al Shaal, L., Müller, R.H., Keck, C.M., 2013. Development of curcumin nanocrystal: physical aspects. J. Pharm. Sci. 102, 204–214.

Raeburn, D., Woodman, V.R., 1994. Effect of Theophylline Administered Intratracheally as a Dry Powder Formulation on Bronchospasm and Airway Microvascular Leakage in the Anaesthetized Guinea-pig. Pulm. Pharmacol. 7, 243–249.

Rahimpour, Y., Kouhsoltani, M., Hamishehkar, H., 2014. Alternative carriers in dry powder inhaler formulations. Drug Discov. Today 19, 618–626.

Raula, J., Kuivanen, A., Lähde, A., Jiang, H., Antopolsky, M., Kansikas, J., Kauppinen, E.I., 2007. Synthesis of L-leucine nanoparticles via physical vapor deposition at varying saturation conditions. J. Aerosol Sci. 38, 1172–1184.

Raula, J., Rahikkala, A., Halkola, T., Pessi, J., Peltonen, L., Hirvonen, J., Järvinen, K., Laaksonen, T., Kauppinen, E.I., 2013. Coated particle assemblies for the concomitant pulmonary administration of budesonide and salbutamol sulphate. Int. J. Pharm. 441, 248–254.

Raula, J., Thielmann, F., Naderi, M., Lehto, V.P., Kauppinen, E.I., 2010. Investigations on particle surface characteristics vs. dispersion behaviour of l-leucine coated carrier-free inhalable powders. Int. J. Pharm. 385, 79–85.

Raw, A.S., Furness, M.S., Gill, D.S., Adams, R.C., Holcombe Jr., F.O., Yu, L.X., 2004. Regulatory considerations of pharmaceutical solid polymorphism in Abbreviated New Drug Applications (ANDAs). Adv. Drug Deliv. Rev. 56, 397–414.

Rehbinder, P.A., Shchukin, E.D., 1972. Surface phenomena in solids during deformation and fracture processes, in Davison, S.G. (Ed.), Progress in Surface Science, Pergamon, Oxford, pp. 97-188.

Rogueda, P., Morrical, B., Cheow, Y.D., 2010. FSI vs NGI: comparison and evaluation. EPAG-Sponsored Workshop on Abbreviated Impactor Measurement (AIM) and Efficient Data Analysis (EDA) Concepts in Inhaler Testing: Overview of AIM-EDA.

Rogueda, P., Traini, D., 2007. The nanoscale in pulmonary drug deliver. Part 1: deposition, fate, toxicology and effect. Expert Opin. Drug Deliv. 4, 595–606.

Romero, G.B., Keck, C.M., Müller, RH, 2016. Simple low-cost minituarization approach for pharmaceutical nanocrystals production. Int. J. Pharm. 501, 236-244.

Rowe, R.C., Sheskey, P.J., Cook, W.G., Fenton, M.E., 2012. Handbook of Pharmaceutical Excipients, seventh ed. Pharmaceutical Press, London.

Rundfeldt, C., Steckel, H., Scherliess, H., Wyska, E., Wlaź, P., 2013. Inhalable highly concentrated itraconazole nanosuspension for the treatment of bronchopulmonary aspergillosis. Eur. J. Pharm. Biopharm. 83, 44–53.

Salama, R.O., Young, P.M., Traini, D., 2014. Concurrent oral and inhalation drug delivery using a dual formulation system: the use of oral theophylline carrier with combined inhalable budesonide and terbutaline. Drug Deliv. Transl. Res. 4, 256–267.

Salem, H., Abdelrahim, M., Eid, K.A., Sharaf, M., 2011. Nanosized rods agglomerates as a new approach for formulation of a dry powder inhaler. Int. J. Nanomedicine 6, 311–320.

Schindelin, J., Arganda-Carreras, I., Frise, E., Kaynig, V., Longair, M., Pietzsch, T., Preibisch, S., Rueden, C., Saalfeld, S., Schmid, B., Tinevez, J.-Y., White, D.J., Hartenstein, V., Eliceiri, K., Tomancak, P., Cardona, A., 2012. Fiji: an open-source platform for biological-image analysis. Nat. Methods 9, 676–682.

Schmidt, M.W., Baldridge, K.K., Boatz, J. A, Elbert, S.T., Gordon, M.S., Jensen, J.H., Koseki, S., Matsunaga, N., Nguyen, K. a, Shyjun, S.U., Dupuis, M., Montgomery, J. A, 1993. General Atomic and Molecular Electronic Structure System. Building 14, 1347–1363.

Seton, L., Khamar, D., Bradshaw, I.J., Hutcheon, G. a., 2010. Solid state forms of theophylline: Presenting a new anhydrous polymorph. Cryst. Growth Des. 10, 3879–3886.

Seville, P., Learoyd, T.P., Li, H.Y., Williamson, I.J., Birchall, J.C., 2007. Amino acid-modified spray-dried powders with enhanced aerosolisation properties for pulmonary drug delivery. Powder Technol. 178, 40–50.

Sharma, P., Denny, W.A., Garg, S., 2009. Effect of wet milling process on the solid state of indomethacin and simvastatin. Int. J. Pharm. 380, 40–48.

Shegokar, R., Müller, R.H., 2010. Nanocrystals: industrially feasible multifunctional formulation technology for poorly soluble actives. Int. J. Pharm. 399, 129–139.

Shishkin, O., Medvediev, V., Zubatyuk, R., 2013. Supramolecular architecture of molecular crystals possessing shearing mechanical properties: columns versus layers. CrystEngComm. 15, 160–167.

Sou, T., Kaminskas, L.M., Nguyen, T.H., Carlberg, R., McIntosh, M.P., Morton, D.A. V, 2013. The effect of amino acid excipients on morphology and solid-state properties of multi-component spray-dried formulations for pulmonary delivery of biomacromolecules. Eur. J. Pharm. Biopharm. 83, 234–243.

Sou, T., Orlando, L., McIntosh, M.P., Kaminskas, L.M., Morton, D.A.V., 2011. Investigating the interactions of amino acid components on a mannitol-based spray-dried powder formulation for pulmonary delivery: A design of experiment approach. Int. J. Pharm. 421, 220–229.

Steckel, H., Bolzen, N., 2004. Alternative sugars as potential carriers for dry powder inhalations. Int. J. Pharm. 270, 297–306.

Stephenson, G. A., Forbes, R. A., Reutzel-Edens, S.M., 2001. Characterization of the solid state: Quantitative issues. Adv. Drug Deliv. Rev. 48, 67–90.

Stewart, P.J., 2014. Inhaled Drug Formulation- The Past, Present and Future. Proceedings of the International Conference of Drug Delivery to the Lungs 25. The Aerosol Society, Edinburgh, pp. 26-27

Stewart, P.J., Adi, H., Larson, I., 2005. Dry powder inhaler formulations: simple two component powder mixtures or a multi-particulate nightmare?

Proceedings of the International Conference of Drug Delivery to the Lungs 16. The Aerosol Society, Edinburgh, pp. 81-84.

Svedsater, H., Dale, P., Garrill, K., Walker, R., Woepse, M.W., 2013. Qualitative assessment of attributes and ease of use of the ELLIPTATM dry powder inhaler for delivery of maintenance therapy for asthma and COPD. BMC Pulm. Med. 13, 72-85.

Takahata, H., Nishioka, Y., Osawa, T., 1992. Micronization of poorly water soluble drug to submicron size by mixing grinding with low-molecular water-soluble crystalline. Funtai to Kogyo 24, 53–59.

Tang, P., Chan, H.K., Chiou, H., Ogawa, K., Jones, M.D., Adi, H., Buckton, G., Prud'homme, R.K., Raper, J. A., 2009. Characterisation and aerosolisation of mannitol particles produced via confined liquid impinging jets. Int. J. Pharm. 367, 51–57.

Tang, X., Pikal, M.J., 2004. Design of Freeze-Drying Processes for Pharmaceuticals: Practical Advice. Pharm. Res. 21, 191-200.

Taniguchi, N., 1974. Proceeding of the International Conference on Production Engineering. The Japan Society for Precision Engineering, Tokyo.

Taylor, G., Kellaway, I., 2001. Pulmonary drug delivery, in: Hillery, A.M., Lloyd, A.W., Swarbrick, J. (Eds), Drug Delivery and Targeting: For Pharmacists and Pharmaceutical Scientists. Taylor & Francis. London, pp. 244-273.

Taylor, K.M.G., 2013. Pulmonary drug delivery, in: Aulton, M.E., Taylor, K.M.G. (Eds), Aulton's Pharmaceutics: The Design and Manufacture of Medicines. Elsevier Health Sciences. London, pp. 638-656.

Thumma, S., Repka, M.A., 2009. Compatibility studies of promethazine hydrochloride with tablet excipients by means of thermal and non-thermal methods. Pharmazie 64, 183–189.

Tilley, S.L., 2011. Methylxanthines in Asthma, in: Fredholm, B.B. (Ed.), Methylxanthines, Handbook of Experimental Pharmacology 200. Springer, Berlin, pp. 439-456.

Tolman, J. A, Williams, R.O., 2010. Advances in the pulmonary delivery of poorly water-soluble drugs: influence of solubilization on pharmacokinetic properties. Drug Dev. Ind. Pharm. 36, 1–30.

Traini, D., Inhalation drug delivery, in: Colombo, P., Traini, D., Buttini, F. (Eds), Inhalation Drug Delivery: Techniques and Products. Wiley-Blackwell. Chichester, pp. 1-16.

Tsapis, N., Bennett, O., Jackson, B., Weitz, D., Edwards, D., 2002. Trojan particles: Large porous carriers of nanoparticles by drug delivery. Proc. Natl. Acad. Sci 99, 12001–12005.

US. Pharmaceutical Sales- Q4 2013, 2014. Top 100 Drugs for Q4 2013 by Sales, https://www.drugs.com/stats/top100/sales (accessed 22-07-2016).

Van Eerdenbrugh, B., Froyen, L., Van Humbeeck, J., Martens, J. A, Augustijns, P., Van Den Mooter, G., 2008a. Alternative matrix formers for nanosuspension solidification: Dissolution performance and X-ray microanalysis as an evaluation tool for powder dispersion. Eur. J. Pharm. Sci. 35, 344–353.

Van Eerdenbrugh, B., Van den Mooter, G., Augustijns, P., 2008b. Top-down production of drug nanocrystals: nanosuspension stabilization, miniaturization and transformation into solid products. Int. J. Pharm. 364, 64–75.

Van Oort, M., Sacchetti, M., 1996. Spray drying and Supercritical Fluid Particle Generation Techniques, in: Hickey, A. (Ed.), Inhalation Aerosols. Taylor & Francis, New York, pp. 307–346.

Vanhoorne, V., Van Bockstal, P.J., Van Snick, B., Peeters, E., Monteyne, T., Gomes, P., De Beer, T., Remon, J.P., Vervaet, C., 2016. Continuous manufacturing of delta mannitol by cospray drying with PVP. Int. J. Pharm. 501, 139–147. doi:10.1016/j.ijpharm.2016.02.001

Vehring, R., 2008. Pharmaceutical particle engineering via spray drying. Pharm. Res. 25, 999–1022.

Verhoff, F.H., Snow, R.A., Pace, G.W., 2003. Media milling. US Patent 6604698.

Verma, S., Huey, B.D., Burgess, D.J., 2009a. Scanning probe microscopy method for nanosuspension stabilizer selection. Langmuir 25, 12481–12487.

Verma, S., Lan, Y., Gokhale, R., Burgess, D.J., 2009b. Quality by design approach to understand the process of nanosuspension preparation. Int. J. Pharm. 377, 185–98.

Verwey, E.J.W., Overbeek, J.T.G., 1948. Theory of the stability of lyophobic colloids. Elsevier, Amsterdam.

Ward, G.H., Schultz, R.K., 1995. Process-induced crystallinity changes in albuterol sulfate and its effect on powder physical stability. Pharm. Res. 12, 773-779.

Watts, A.B., Williams III, R.B., 2011. Nanoparticles for Pulmonary Delivery, in: Smyth, H., Hickey, A. (Eds), Controlled Pulmonary Drug Delivery. Springer, New York, pp. 335–356.

Weibel, E.R., 1963. Morphometry of the human lung, first ed. Springer, New York.

Westmeier, R., Steckel, H., 2008. Combination particles containing salmeterol xinafoate and fluticasone propionate: Formulation and aerodynamic assessment. J. Pharm. Sci. 97, 2299–310.

Willart, J.F., Caron, V., Descamps, M., 2007. Transformations of crystalline sugars upon milling. J. Therm. Anal. Calorim. 90, 125–130.

Wong, J., Brugger, A., Khare, A., Chaubal, M., Papadopoulos, P., Rabinow, B., Kipp, J., Ning, J., 2008. Suspensions for intravenous (IV) injection: a review of development, preclinical and clinical aspects. Adv. Drug Deliv. Rev. 60, 939–954.

Wu, L., Zhang, J., Watanabe, W., 2011. Physical and chemical stability of drug nanoparticles. Adv. Drug Deliv. Rev. 63, 456–69.

Xu, E.Y., Guo, J., Xu, Y., Li, H.Y., Seville, P.C., 2014. Influence of excipients on spray-dried powders for inhalation. Powder Technol. 256, 217–223.

Yalkowsky, S.H., He, Y., Jain, P., 2010. Handbook of Aqueous Solubility Data, second ed. CRC press, Boca Raton.

Yamasaki, K., Kwok, P.C.L., Fukushige, K., Prud'homme, R.K., Chan, H. K., 2011. Enhanced dissolution of inhalable cyclosporine nano-matrix particles with mannitol as matrix former. Int. J. Pharm. 420, 34–42.

Yang, M.Y., Chan, J.K., Chan, H.K., 2014. Pulmonary drug delivery by dry powder aerosols. J. Control. Release 10, 228-240.

Yang, W., Tam, J., Miller, D.A., Zhou, J., McConville, J.T., Johnston, K.P., Williams, R.O., 2008. High bioavailability from nebulized itraconazole nanoparticle dispersions with biocompatible stabilizers. Int. J. Pharm. 361, 177–188.

Yue, P.F., Li, Y., Wan, J., Yang, M., Zhu, W.F., Wang, C.H., 2013. Study on formability of solid nanosuspensions during nanodispersion and solidification: I. Novel role of stabilizer/drug property. Int. J. Pharm. 454, 269–277.

Zeng, X.M., Martin, G.P., Marriott, C., 2001. Particulate interactions in dry powder formulations for inhalation, first ed. Taylor & Francis, London.

Zhang, J., Wu, L., Chan, H.K., Watanabe, W., 2011. Formation, characterization, and fate of inhaled drug nanoparticles. Adv. Drug Deliv. Rev. 63, 441–455.

Zhang, W., Zhou, H., Chen, X., Tang, S., Zhang, J., 2009. Biocompatibility study of theophylline/chitosan/β-cyclodextrin microspheres as pulmonary delivery carriers. J. Mater. Sci. Mater. Med. 20, 1321–1330.

Zhang, X., Guan, J., Ni, R., Li, L., Mao, 2014. Preparation and solidification of redispersible nanosuspensions. J. Pharm. Sci. 103, 2166–2176.

Zhu, B., Haghi, M., Goud, M., Young, P.M., Traini, D., 2015a. The formulation of a pressurized metered dose inhaler containing theophylline for inhalation. Eur. J. Pharm. Sci. 76, 68–72.

Zhu, B., Haghi, M., Nguyen, A., Goud, M., Yeung, S., Young, P.M., Traini, D., 2015b. Delivery of theophylline as dry powder for inhalation. Asian J. Pharm. Sci. 10, 520–527.

PUBLICATIONS AND PRESENTATIONS

Publications

Malamatari, M., Somavarapu, S., Kachrimanis, K., Bloxham, M., Taylor, K.M.G., Buckton, G., 2016. Preparation of theophylline inhalable microcomposite particles by wet milling and spray drying: the influence of mannitol as a co-milling agent. Int. J. Pharm. (In press).

Malamatari, M., Somavarapu, S., Taylor, K.M.G., Buckton, G., 2016. Solidification of nanosuspensions for the production of solid oral dosage forms and inhalable drug powders. Expert Opin. Drug Deliv. 13, 435-450.

Malamatari, M., 2016. Theophylline: Increasing scientific and clinical evidence gives this old drug a new lease of life. 2016 UKICRS Newsletter – *Bronze award in the 2016 UKICRS Essay Competition.*

Malamatari, M., Somavarapu, S., Bloxham, M., Buckton, G., 2015. Nanoparticle agglomerates of indomethacin: The role of poloxamers and matrix former on their dissolution and aerosolisation efficiency. Int. J. Pharm. 495, 516–526.

Oral presentation

Malamatari, M., Somavarapu, S., Bloxham, M., Taylor, K.M.G., Buckton G., Comparative study on the aerosolisation performance of theophylline microcomposite particles and adhesive mixtures with lactose carriers. 10th World Meeting on Pharmaceutics and Biopharmaceutics and Pharmaceutical Technology, Glasgow (UK), 4-7 April 2016

Poster presentation

Malamatari, M., Somavarapu, S., Taylor, K.M.G., Buckton G., 2016. Expanding the use of wet milling and spray drying for the preparation of nanoparticle agglomerates for thermolabile and ductile drugs: the case of ibuprofen. 10th World Meeting on Pharmaceutics and Biopharmaceutics and Pharmaceutical Technology, Glasgow (UK), 4-7 April 2016.

Toziopoulou, F., **Malamatari, M.**, Nikolakakis, I., Kachrimanis, K., 2016. Production of aprepitant nanocrystals by wet media milling. 10th World Meeting on Pharmaceutics and Biopharmaceutics and Pharmaceutical Technology, Glasgow (UK), 4-7 April 2016.

Malamatari, M., Somavarapu, S., Taylor, K.M.G., Buckton, G., 2016. Nanoparticle agglomerates for pulmonary drug delivery prepared by wet milling and spray drying: A quality by design approach. 4th QbD Symposium, De Montfort University School of Pharmacy, Leicester (UK), 16 March 2016.

Malamatari, M., Somavarapu, S., Bloxham, M., Buckton, G., 2015. Mannitol as a co-milling agent for the preparation of inhalable theophylline nanocrystal agglomerates. 4th World Conference on Physico Chemical Methods in Drug Discovery and Development, Red Island (Croatia), 21-24 September 2015.

Malamatari, M., Muwaffak-Hassan, M., Kanwal, H., Somavarapu, S., Buckton, G., 2015. Particle engineering of lactose agglomerates with potential for use as carriers for pulmonary drug delivery. ULLA Summer School 2015, Faculty of Pharmacy Paris Sud (France), 4-11 July 2015.

Malamatari, M., Bloxham, M., Somavarapu, S., Buckton, G., 2014. Conversion of nanosuspensions to dry powders by spray drying: a platform for the preparation of inhalation particles. Drug Delivery to the Lungs 25, Edinburgh (UK), 10-12 December 2014.